

University of Alberta

**Reduced-Complexity Transmission and Reception  
Strategies in Coordinated Multi-cell Wireless Networks**

by

**Saeed Kaviani**

A thesis submitted to the Faculty of Graduate Studies and Research  
in partial fulfillment of the requirements for the degree of

Doctor of Philosophy  
in  
Communications

Department of Electrical and Computer Engineering

©**Saeed Kaviani**  
Fall 2012  
Edmonton, Alberta

Permission is hereby granted to the University of Alberta Libraries to reproduce single copies of this thesis and to lend or sell such copies for private, scholarly or scientific research purposes only. Where the thesis is converted to, or otherwise made available in digital form, the University of Alberta will advise potential users of the thesis of these terms.

The author reserves all other publication and other rights in association with the copyright in the thesis and, except as herein before provided, neither the thesis nor any substantial portion thereof may be printed or otherwise reproduced in any material form whatsoever without the author's prior written permission.

*to my beloved wife, Niloofar Farboodi.*

*My infinite love to you is not describable in words. You are the most valuable achievement in my life. Thank you for being with me and to give me the opportunity to see how incredible a person can be.*

# Abstract

Interference is known as a major obstacle for the spectral efficiency increase promised by multiple-antenna techniques in cellular wireless communications. Recently, it has been shown that multi-cell coordination can mitigate interference and improve system performance dramatically. Hence, we concentrate on the downlink of multi-cell multiple-antenna (at both ends) wireless networks also known as *network multiple-input multiple-output (MIMO)* or *coordinated multi-point (CoMP)* transmission/reception systems. In multi-cell coordination, antennas from multiple base stations form a large MIMO system. Consequently, coordination comes with high signal processing overhead. In this dissertation we focus on reduced-complexity transmission and reception strategies in partially coordinated multi-cell systems, where the user data are partially shared between base stations. We first model partial coordination using MIMO interference channel with generalized linear constraints. Then, we investigate linear transmission strategies using this channel model. The contributions of this dissertation fall into the following categories of techniques: *(i)* Block diagonalization (multiple-antenna multi-user zero-forcing) transmit precoding under individual power constraints. *(ii)* Minimum mean square error (MMSE) linear precoding and equalization design; *(iii)* Worst-case robust precoding and equalization, where we consider imperfect channel state information available at the transmitter and receiver. Furthermore, our simulation setup accounts for realistic cellular parameters in evaluating the performance in multi-cell networks.

# Acknowledgements

I would like to start by thanking God for all the blessings in my life. Besides, there are definitely a few people I must surely thank for helping me to accomplish this success. First and foremost, I must thank my supervisor, Dr. Witold A. Krzymień, for his support, care, guidance and mentorship throughout my Ph.D. program. I would also like to give special thanks to our collaborators, Dr. Osvaldo Simeone from New Jersey Institute of Technology and Dr. Shlomo Shamai (Shitz) from the Technion-Israel Institute of Technology for the opportunity to work together and their valuable insights and comments into parts of my project. I would like to thank my dear committee members, Dr. Robert W. Heath Jr. from the University of Texas at Austin, Dr. Mike MacGregor, Dr. Chintha Tellambura, and Dr. Hai Jiang for their fundamental comments and feedback. I wish to extend my warmest thanks to my friends, graduate students, and the staff at the department of electrical and computer engineering at the Department of Electrical and Computer Engineering of the University of Alberta, and at TRILabs.

I would also like to gratefully acknowledge the funding and research environment provided by TRILabs. Generous funding for this work was also provided by the Natural Sciences and Engineering Research Council (NSERC) of Canada, Rohit Sharma Professorship, Alberta Innovates – Technology Futures, and the University of Alberta.

Last but not least, I thank my dear love, Niloofar Farboodi for the inspiration, support, and company. She is the main reason for all my achievements and I thank God everyday for having her.

# Contents

<b>1</b>	<b>Introduction</b>	<b>1</b>
1.1	Motivation . . . . .	1
1.2	Network MIMO (Multinode Cooperative Interference Management) . . . . .	4
1.2.1	Interference Coordination . . . . .	5
1.2.2	MIMO Coordination . . . . .	10
1.2.3	Partial Cooperation . . . . .	12
1.3	Linear Precoding Schemes . . . . .	13
1.4	Implementation Challenges . . . . .	14
1.4.1	Complexity . . . . .	14
1.4.2	Synchronization . . . . .	15
1.4.3	Channel estimation . . . . .	15
1.5	Contributions . . . . .	15
<b>2</b>	<b>System Model and Preliminaries</b>	<b>18</b>
2.1	Channel Model and Configurations . . . . .	18
2.2	Downlink Transmission . . . . .	20
2.2.1	Equivalence with MIMO-IFC-GC . . . . .	22
2.2.2	Capacity Region . . . . .	25
2.3	Problem Formulation . . . . .	27
2.4	Uplink-Downlink Duality . . . . .	29
2.5	Conclusions . . . . .	34
<b>3</b>	<b>Multi-cell Block Diagonalization</b>	<b>35</b>
3.1	Motivation . . . . .	35

3.2	Introduction . . . . .	36
3.3	Multi-cell Multiuser ZF . . . . .	37
3.3.1	Conventional BD . . . . .	39
3.3.2	Optimal Multi-Cell BD . . . . .	41
3.4	Simulation Setup . . . . .	44
3.4.1	User Selection . . . . .	45
3.5	Numerical Results . . . . .	47
3.5.1	Network MIMO Gains . . . . .	47
3.5.2	Multiple-Antenna Gains . . . . .	48
3.5.3	Multiuser Diversity . . . . .	49
3.5.4	Fairness Advantages . . . . .	50
3.5.5	Convergence . . . . .	51
3.6	Conclusions . . . . .	52
3.A	Proof of Theorem 3.1 . . . . .	53
<b>4</b>	<b>MMSE Precoding and Equalization</b>	<b>55</b>
4.1	Problem Definition and Preliminaries . . . . .	56
4.2	Known Techniques . . . . .	58
4.2.1	Soft Interference Nulling . . . . .	59
4.2.2	SDP Relaxation . . . . .	60
4.2.3	Polite Waterfilling . . . . .	61
4.2.4	Leakage Minimization . . . . .	63
4.2.5	Max-SINR . . . . .	64
4.3	MSE Minimization . . . . .	64
4.3.1	MMSE Interference Alignment . . . . .	64
4.3.2	Diagonalized MMSE . . . . .	66
4.4	Numerical Results . . . . .	75
4.5	Conclusions . . . . .	80
<b>5</b>	<b>Robust Precoding and Equalization</b>	<b>83</b>
5.1	System Model and Problem Formulation . . . . .	86
5.2	Single-user Case . . . . .	88

5.2.1	Perfect Knowledge of System Matrices . . . . .	89
5.2.2	Imperfect Knowledge of System Matrices . . . . .	90
5.2.3	Robust Transceiver Design . . . . .	94
5.3	Multiuser Case ( $K > 1$ ) . . . . .	97
5.3.1	Perfect Channel Knowledge . . . . .	97
5.3.2	Imperfect Channel Knowledge . . . . .	99
5.4	Numerical Results . . . . .	103
5.5	Conclusions . . . . .	107
5.A	Proof of Lemma 5.1 . . . . .	108
5.B	Proof of Lemma 5.2 . . . . .	111
5.C	Proof of Theorem 5.1 . . . . .	114
<b>6</b>	<b>Summary of Contributions and Future Work</b>	<b>117</b>
6.1	Summary of Contributions . . . . .	117
6.1.1	Block diagonalization (multiple-antenna user zero-forcing)	117
6.1.2	MMSE Linear Precoding and Equalization . . . . .	118
6.1.3	Network MIMO User Scheduling . . . . .	119
6.1.4	Semi-orthogonal User Selection Algorithm for Multiple- antenna Users . . . . .	119
6.1.5	Robust Linear Precoding and Equalization . . . . .	119
6.2	Future Work . . . . .	120
6.2.1	Decentralized solution to the optimization problems . .	120
6.2.2	Robust linear strategies . . . . .	120
6.2.3	Multi-cell user scheduling . . . . .	121
6.2.4	MMSE interference alignment . . . . .	121
6.2.5	Synchronization . . . . .	122
	<b>Appendices</b>	<b>123</b>
<b>A</b>	<b>Convex Optimization Theory</b>	<b>124</b>
A.1	Basic Optimization Concepts . . . . .	124
A.2	Lagrangian Duality . . . . .	126
A.3	Semidefinite Programming . . . . .	128

A.4 Gradient and Sub-gradient Algorithms . . . . .	129
A.5 Gauss-Seidel Algorithms . . . . .	130
A.6 Dual Decomposition . . . . .	131

# List of Figures

1.1	(a) Conventional cellular system: The BSs are not coordinated. Each BS intends to transmit to the users within its cell area. (b) Coordinated multi-cell system: Neighboring BSs are connected via a high capacity back-haul link to a central processing site, which manages the signaling of the system. Green arrows represent signals with intended message for the user (useful signals), while interference signals are in red. . . . .	3
1.2	(a) Interference coordination where each BS delivers message to the users within its cell area. (b) Interference channel model with $K$ transmitter/receiver pairs. Green arrows represent useful signal, while interference signals are in red. . . . .	6
1.3	(a) MIMO coordination: Each user receives its signal from all the BSs within the cluster. (b) MIMO broadcast channel where transmitters are cooperating in transmission to non-cooperating receivers. . . . .	10
1.4	Partial cooperation where the user data is shared partially. This may also include partial exchange of CSI. Each BS knows a subset of user messages in the cluster. . . . .	13
2.1	A downlink model with partial BS cooperation or equivalently partial message knowledge. . . . .	21
2.2	(a) A downlink model with partial BS cooperation or equivalently partial message knowledge, (b) The equivalent MIMO interference channel with generalized linear power constraints.	23
2.3	Duality for the MIMO-IFC-GC model. . . . .	30

3.1	Comparison of sum rates for conventional BD vs. the proposed optimal BD for $M = 1$ , $m_{t,k} = Mn_t = 6, 12$ , $d_k = n_r = 2$ using maximum sum rate scheduling. . . . .	41
3.2	The cellular layout of $M = 3$ and $M = 7$ clustered network MIMO joint processing. The borders of clusters are bold. Green colored cells represent the analyzed center cluster and the grey cells are causing inter-cell interference. For $M = 7$ , one tier of interfering clusters is considered, while for $M = 3$ two tiers of interfering cells are accounted for. . . . .	46
3.3	CDF of sum rate with different cluster sizes $M = 1, 3, 7$ , $n_t = 4$ , $n_r = 2$ and 10 users per cell (network MIMO joint processing).	48
3.4	Sum-rate increase with the number of antennas per base station. $n_r = 2$ . . . . .	49
3.5	Sum rate per cell achieved with the proposed optimal BD and the capacity limits of DPC for cluster sizes $M = 1, 3, 7$ ; $n_t = 4$ , $n_r = 2$ . . . . .	50
3.6	CDF of the mean rates in the clusters of sizes $M = 3, 7$ and comparison with $M = 1$ (no coordination) using the proposed optimal BD. . . . .	51
3.7	Convergence of the gradient descent method for the proposed optimal BD for $M = 3$ , $n_t = 4$ , $n_r = 2$ , and 8 users per cell. . .	52
4.1	Per-cell sum-rate for a MIMO-IFC-GC with $M = 3$ and $\kappa = 2$ .	77
4.2	Per-cell sum-rate for a MIMO-IFC-GC with $M = 5$ and $\kappa = 1, 2, 3, 5$ , $n_t = 4$ , $n_r = d_k = 2$ , and 2 users per cell. . . . .	78
4.3	Per-cell sum rate of the schemes that can support $d_k < \min(m_{t,k}, m_{r,k})$ for $d_k = 1$ , $n_t = 4$ , $n_r = 2$ , $M = 3$ and $\kappa = 2$ . .	79
4.4	Per-cell sum-rate of the proposed DMMSE scheme for cluster sizes $M = 1, 3, 7$ versus the cooperation factor, $\kappa$ , with $n_t = n_r = 2$ , SNR=20 dB, and single-user per cell. . . . .	80

4.5	CDF of the per-cell sum rates achieved by DMMSE for $S = 1, 3, 6$ sectors per cell, $M = 1, 3, 7$ coordinated clusters, and $\kappa = 1, 2, 3$ cooperation factors with $\gamma_0 = 20$ dB, $n_t = 6$ , and $n_r = 2$ . The circles represent the mean values of the per-cell sum-rates. . . . .	81
5.1	Comparison of performance of the proposed robust design, the non-robust design, and the transceiver design when system matrices are perfectly known (perfect CSI) for $n_t = n_r = 2$ . . .	104
5.2	Comparison of performance of different transceiver designs with respect to the size of uncertainty region $\bar{\varepsilon}$ for $n_t = n_r = 2$ . . .	105
5.3	Sum-MSE comparison of the proposed robust design, the non-robust design with $\bar{\varepsilon} = 0.01, 0.03, 0.05$ , and with perfect CSI in $K = 3$ interference channel. $n_t = n_r = 2$ . . . . .	106
5.4	Sum rate comparison of the proposed robust design, the non-robust design with $\bar{\varepsilon} = 0.01, 0.05$ , and with perfect CSI in $K = 3$ interference channel. $n_t = n_r = 2$ . . . . .	107
5.5	Sum rate comparison of the proposed robust design with the semi-definite relaxation based algorithm, with $\varepsilon_{H_{k,l}} = 0.1, \forall k, l$ in $K = 3$ interference channel. $n_t = n_r = 2$ . . . . .	108

# List of Symbols and Notation

$a$	scalar $a$
$\mathbf{a}$	vector $\mathbf{a}$
$\mathbf{A}$	matrix $\mathbf{A}$
$\text{vec}(\mathbf{A})$	operation stacks columns of $\mathbf{A}$ to one column vector
$\text{tr}(\mathbf{A})$	trace of matrix $\mathbf{A}$
$\mathbf{A} \succeq \mathbf{0}$	positive semidefinite condition
$(\cdot)^{\text{H}}$	conjugate (Hermitian) transpose
$\ \cdot\ $	vector Euclidean norm
$\ \cdot\ _{\text{F}}$	matrix Frobenius norm
$(\cdot)^*$	complex conjugate
$\mathbf{A}^{1/2}$	Hermitian square root of $\mathbf{A}$
$\mathcal{CN}(\mu, \sigma^2)$	circularly symmetric complex Gaussian variable with mean $\mu$ and variance $\sigma^2$
$\mathcal{N}(\mu, \sigma^2)$	Gaussian random variable with mean $\mu$ and variance $\sigma^2$
$\log_2(x)$	base-2 logarithm of $x$
$\log(x)$	natural logarithm of $x$
$\otimes$	Kronecker product
$\mathbb{C}^m$	$m$ -dimensional complex vector space
$\mathbb{C}^{m \times n}$	set of $m \times n$ complex matrices
$\mathcal{E}_y[\cdot]$	statistical expectation over $y$
$n_t$	number of transmit antennas
$n_r$	number of receive antennas
$M$	number of base stations in a cluster
$K$	number of users
$\mathbf{F}$	precoder matrix
$\mathbf{G}$	equalizer matrix
$\mathbf{H}$	MIMO channel matrix
$d_{k,j}$	distance between the base station $j$ and the user $k$
$\rho_{k,j}$	log-normal shadowing
$\mathbf{E}_k$	mean square error matrix for user $k$
$R$	data rate

$\mathbf{A}^\top$	transpose of matrix $\mathbf{A}$
$\mathcal{K}_m$	set of users assigned to base station $m$
$\mathcal{M}_k$	set of base stations serving user $k$
$\mathcal{L}$	Lagrangian function
$\lambda$	Lagrangian variable
$\Gamma$	reference signal to noise ratio
$\mathbf{A}^{-\frac{1}{2}}$	square root of the inverse of matrix $\mathbf{A}$
$\beta$	path-loss exponent
$[\cdot]^+$	minimum of zero and a value
$\text{Inf}$	infimum of a function

# Abbreviations

BC	Broadcast channel
BD	Block diagonalization
BS	Base station
CDF	Cumulative distribution function
CDMA	Code division multiple access
CoMP	Coordinated multipoint
CSI	Channel state information
DMMSE	Diagonalized minimum mean square error
DPC	Dirty paper coding
eMMSE-IA	extended minimum mean square error interference alignment
GPS	Global positioning system
INR	Interference to noise ratio
KKT	Karush-Kuhn-Tucker
LTE	Long-term evolution of 3rd generation cellular
MAC	Multiple access channel
MIMO	Multiple-input multiple-output
MIMO-IFC-GC	MIMO interference channel with generalized constraints
MMSE	Minimum mean square error
MMSE-IA	Minimum mean square error interference alignment
MRC	Maximal ratio combining
MS	Mobile station
MSE	Mean square error
OFDMA	Orthogonal frequency division multiple access
PWF	Polite waterfilling
SIN	Soft interference nulling
SC	Selection combining
SDP	Semidefinite programming
SINR	Signal to interference plus noise ratio

SNR	Signal to noise ratio
SR	sum rate
SRM	Sum rate maximization
SVD	Singular value decomposition
SM	Spatial multiplexing
WMMSE	Weighted sum of mean square error minimization
WSMSE	Weighted sum of mean square error
ZF	Zero-forcing

# Chapter 1

## Introduction

Mobile communications have received significant attention worldwide in the past few years due to introduction of user-friendly devices, which are capable of providing high-speed data access. The number of mobile phone users has exceeded 5.9 billion and currently these users demand cheap internet access as fast as their wired lines. This introduces increasing pressure on the mobile operators to provide the users with very high bit rates at high quality of service (which includes fairness), while dramatically reducing cost per bit/sec transmitted.

### 1.1 Motivation

Wireless Communication involves two fundamental challenges. First is related to the properties of the mobile radio channel that introduces small-scale *multipath fading*, distance-dependant path loss, and large-scale *shadow fading* caused by obstacles in the propagation path. *Diversity techniques* help combat fading in the wireless channel, and include time, frequency, and antenna diversity (also known as space diversity). Diversity makes possible reception of independently faded replicas of the same transmitted radio signal through multiple propagation paths (dimensions) and with suitable combining decreases the probability of failure in transmission. Deployment of multiple antennas at the transmitters and/or the receivers also referred to as *multiple-input multiple-output (MIMO)* provides even more potentials. In addition to diversity, MIMO systems achieve *spatial multiplexing (SM)*, which leads to

a linear capacity gain of the system (or *degrees of freedom*). In this case, the capacity of wireless system will be increased linearly with the minimum number of transmit and receive antennas when SM is employed [1, 2].

The second challenge in wireless communications (and especially in cellular systems) is the existence of *interference* when multiple users share a wireless channel to communicate. In the downlink of cellular systems, the interference may be from different signals transmitted from a transmission point (base station (BS)) to multiple users within a cell (i.e. *intra-cell interference*) or it can be from signals transmitted from the neighboring BSs intended for its own users (i.e. *inter-cell interference*). The potential capacity gains of MIMO techniques in point-to-point [1, 2] and single-cell multiuser [3] systems are significant, but in cellular environments the gains are severely degraded due to intra- and inter-cell interference [4, 5]. Traditionally, this problem has been handled by assigning separate orthogonal radio resources (e.g. time, frequency, code) to adjacent cells/users. Hence, the communication of each cell/user takes place in a separate channel than the other cells/users. This is at a price of decreasing the *spectral efficiency* of the system<sup>1</sup>. For example, full frequency reuse is used in *code division multiple access (CDMA)* systems, where different users' transmissions are separated by spreading codes rather than frequency. Due to full frequency reuse, CDMA systems have to manage the interference more efficiently. Hence, the main challenge is to handle interference while keeping the spectral efficiency high.

In cellular environments, the interference is more severe for the cell-edge users. These users receive degraded signals from their associated BS, but also receive significant amount of interference from the neighboring BSs. A very promising technique of mitigating inter-cell interference involves coordination (or cooperation) among BSs. The first attempts in this direction were based on the concept of *soft handoff* or *macro-diversity*. With soft handoff a mobile user at a cell boundary may receive its signal from more than one BS and perform maximal ratio combining (MRC) of several replicas of its signal.

---

<sup>1</sup>Spectral efficiency is the net information rate that can be transmitted within a specific bandwidth and it is measured in bit/s/Hz.

In the uplink a selection combining (SC) of user signals received by several BSs may occur under the control of the mobile switching center. More recently, the inter-cell interference management techniques evolved to include coordination of transmission from several BSs using high-capacity backhaul links. This is usually referred to as *network MIMO*, or *coordinated multi-point (CoMP)* transmission/reception, or *multi-cell coordination* (see [6] and references therein).

Multicell coordination is an efficient technique to improve the cell-edge and average data rates, so that it increases spectral efficiency (and

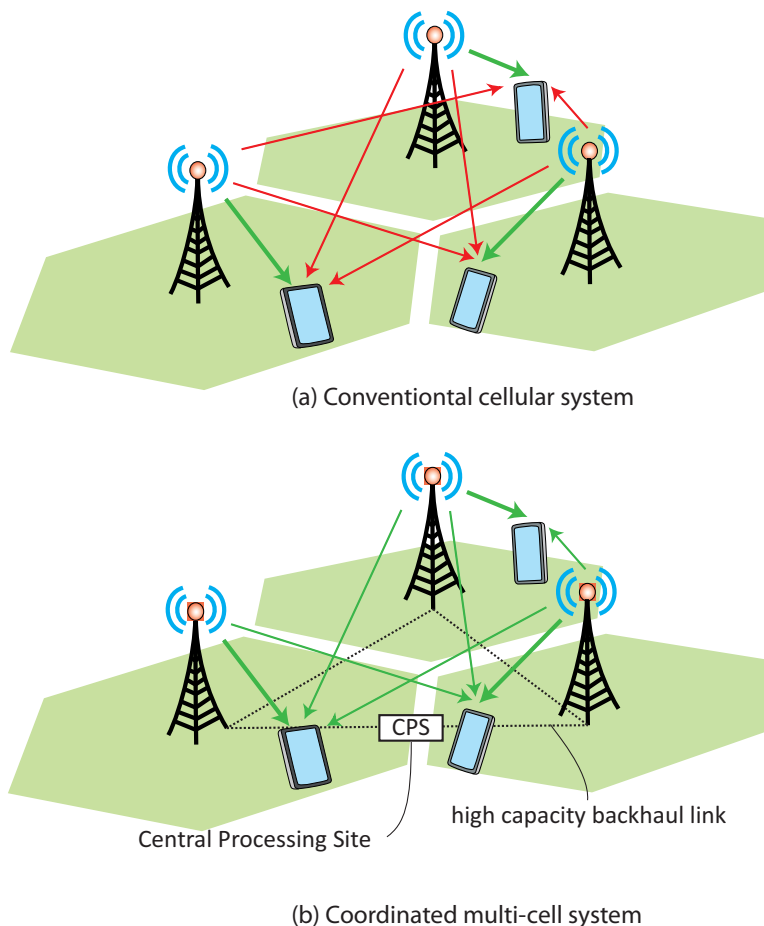


Figure 1.1: (a) Conventional cellular system: The BSs are not coordinated. Each BS intends to transmit to the users within its cell area. (b) Coordinated multi-cell system: Neighboring BSs are connected via a high capacity back-haul link to a central processing site, which manages the signaling of the system. Green arrows represent signals with intended message for the user (useful signals), while interference signals are in red.

capacity) especially for the dense networks such as in urban areas. Backhaul links between the BSs enable this cooperation. Recently developed wireless communication standards like long-term evolution (LTE) and LTE-Advanced require high-capacity backhaul (fibre or microwave) links and often the cost of the backhaul links increases less than linearly with the backhaul capacity. The backhaul links may be connected to a central processing site, which is able to jointly design downlink transmission using the channel information obtained via feedback and exchanged through the backhaul links.

Simply speaking, cellular downlink communication infrastructure consists of BS transmitters and mobile station (MS) receivers. The transmitters are typically static and lower in number, while the receivers are mobile and much larger in number. Hence, the transmitters can be connected and coordinated. This brings significant potential to maximize the net throughput of the system, while keeping the processing burden at the transmitter side.

Due to infeasibility of coordination between all BSs in the network, *clustering* in network MIMO has been proposed in [7–9]. In the clustered network MIMO, the neighboring cells are grouped together into clusters. Each cluster contains a number of cells. The BSs within each cluster are coordinated together in transmission to the users assigned to the cluster. The clustering also deals with the inter-cluster interference and if it is treated as noise, each cluster can be modeled separately. Unless otherwise stated, we concentrate on a cluster of coordinated BSs in this dissertation.

## 1.2 Network MIMO (Multinode Cooperative Interference Management)

Network MIMO is a network of multiple nodes (transmission points) each equipped with multiple antennas, which transmit to a number of multiple-antenna users. The transmission points are connected to each other and through this connection they can *(i)* share user data, *(ii)* exchange channel state information (CSI), and *(iii)* jointly process/optimize their transmission.

Hence, network MIMO can be categorized based on the level of coordination through this backhaul link.

If we consider full user data sharing and CSI exchange between the BSs, a well-known *MIMO broadcast channel (BC)* model emerges (fully cooperative transmitters broadcast to non-cooperative users). Therefore, most of the traditional multiuser MIMO transmission strategies can be extended in a straightforward fashion [5]. If we highlight particular characteristics of multi-cell systems, then these extensions can be nontrivial and novel. Nevertheless, the major difference between the multi-cell cooperation and a single-cell system lies in the type and amount of information exchanged via backhaul links. This defines the challenges in multi-cell coordination and vast research opportunities in the area. The coordination techniques can be classified as interference coordination, MIMO coordination, multi-cell cooperation with partial data sharing, and finally multi-cell cooperation with partial data sharing and partial CSI exchange (*partial cooperation*)<sup>2</sup>. Partial cooperation in multi-cell systems will be the main focus of this dissertation. We will review these coordination techniques in the following sections.

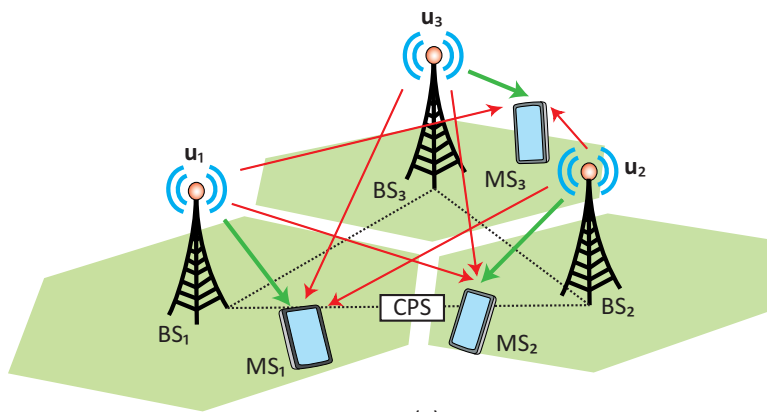
### 1.2.1 Interference Coordination

When the BSs are only aware of perfect CSI but they do not share their user data, multi-cell coordination is in a form of *interference coordination* to mitigate the interference in the system. The information theoretical channel model for this scenario is *interference channel* [12], in which cooperating transmitters transmit to their own users. This is illustrated in Figure 1.2. In this figure, the BS<sub>1</sub> knows the message of the user MS<sub>1</sub> and therefore the transmitted signal contains useful message, while the BS<sub>1</sub> is not aware of messages of the users outside its cell area (i.e. MS<sub>2</sub> and MS<sub>3</sub>). Hence, its transmitted signal contains interference only (depicted by a red line). However, the exchange of CSI between the BSs enables management of interference to improve the overall performance.

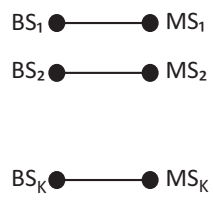
Several transmission and reception strategies have been discussed in the

---

<sup>2</sup>Different categories of multi-cell coordination is reviewed in [10, 11]



(a)



(b)

Figure 1.2: (a) Interference coordination where each BS delivers message to the users within its cell area. (b) Interference channel model with  $K$  transmitter/receiver pairs. Green arrows represent useful signal, while interference signals are in red.

literature for interference channels. In the following section, we review these techniques briefly.

### **Power Allocation**

A simple method of interference coordination involves joint power allocation across multiple BSs. Power allocation and scheduling in multi-cell systems has been investigated in [13–16]. Power control in the multiuser scenario, where the spectrum is commonly shared, is a topic of intensive research in signal processing (see [17] and its references). The power control problem is a non-convex problem and therefore the proposed (implementable) algorithms may be unable to converge globally and may converge to a poor spectrum allocation solution. In [18], it has been discussed that finding the global optimal solution for the power control problem is computationally intractable.

Viewing the power control problem as a non-cooperative game can lead to a competitive optimal solution [19–21]. Using this approach, a pricing algorithm is developed in [22, 23] where each user introduces a price paid by the other users as a form of interference. The total profit can be defined as the sum rate of the system. This method has been applied to multi-cell networks in [24].

### **Coordinated Beamforming**

When the BSs are equipped with multiple antennas, the power control problem must design the transmitting beams from each antenna. This is commonly called *transmit beamforming*. In the multi-cell scenario, the beamforming optimization can be performed jointly for coordinated BSs and is often referred to as *coordinated beamforming* [25–28].

Similar to the power control problem, the coordinated beamforming optimization problem is also non-convex. The problem of multi-cell transmit downlink beamforming was first considered in a classic work by Rashid-Farrokhi *et al.* [29], where the BSs employ multiple antennas and the users are single-antenna. The transmit beamforming optimization is formulated as the minimization of total transmit power while the signal to interference plus noise ratio (SINR) at each link satisfies a minimum target. Rashidi-

Farrokhi *et al.* proposed an iterative algorithm to achieve the optimal solution for this problem. This algorithm is based on establishing a virtual uplink network with transmitters and receivers reversed and the uplink channels equal to the Hermitian transpose of the downlink channels, but with the same achievable SINR target sets. The algorithm finds the optimal uplink receivers, which turned out to be minimum mean squared error (MMSE) receivers. These virtual uplink MMSE receivers define the transmitters for the downlink system. Next, the virtual uplink powers and correspondingly the downlink powers are updated. The algorithm iterates until convergence. Later, it was shown that this downlink-uplink duality concept may be unified under a Lagrangian duality in optimization theory [30]. Note that the formulation of the transmit beamforming problem as a minimization of the total power constraint enables global optimization of this problem. With this formulation, the SINR constraints can be transformed into a second-order-cone constraint [31] and therefore the problem can be solved via convex optimization<sup>3</sup>. Although the downlink-uplink duality can be extended to the systems with multiple-antenna users [32], the iterative transmit/receive beamforming and power update will not converge to the global optimal solution and only local optimal solution is guaranteed so far. This is due to the non-convex nature of joint transmit/receive beamforming optimization problem.

A competitive (noncooperative) approach based on game theory has been identified in [33] and further studied in [34, 35], where each link is a player competing against others by its power allocation (transmission strategy) in order to maximize its objective function (e.g. data rate). Although this noncooperative approach is not optimal, it achieves improvement over the distributed multi-cell networks. [36, 37] have shown that a linear combination of the altruistic approach (zero-forcing (ZF) transmit beamforming strategy) and the selfish approach (Nash equilibrium) achieves a Pareto-optimal rate region.

---

<sup>3</sup>A brief introduction to the convex optimization theory is given in Appendix A

## Successive Encoding

It is known that the capacity achieving transmission strategy in MIMO BC are based on a successive encoding, or so-called *dirty paper coding* (DPC) technique where the transmitter detects interference and subtracts it in the encoding process [38–40]. This is in contrast to the beamforming strategy where the interference is treated as noise (This is a result of averaging the interference and the use of law of large numbers). In information theory, the multi-cell scenario can be modeled as an interference channel.

In spite of intensive research on this subject over the past three decades, the capacity region of interference channels is still unknown (even for a small number of users). The largest known achievable rate region for the two-user case was obtained by Han and Kobayashi [41], who proposed common-private message splitting scheme. In this scheme, users' messages are divided into two parts: private message which is decoded by the intended receiver and common message, which is decoded by both receivers and it is intended for interference mitigation. Note that the beamforming strategies discussed so far only included private message. Recently, it has been shown that with this strategy and adjusting interference-to-noise-ratio (INR, which is the ratio of private message power at the opposite receiver to the noise power) larger or equal to one, one can approach within one bit (bits/sec/Hz) the interference channel capacity region [42]. This has been shown for only two-user single-antenna case. The extension of the common-private message splitting strategy to the multi-cell scenario is discussed in [43], where a numerical algorithm is proposed for out-of-cell user selection for common message decoding, rate splitting method and optimal beamforming to improve the overall network performance.

## Interference Alignment

Recently, it has been shown that in the interference channel with more than two users maximizing the overlap between interference signal subspaces (aligning the interference signals) maximizes the size of their null spaces, and this

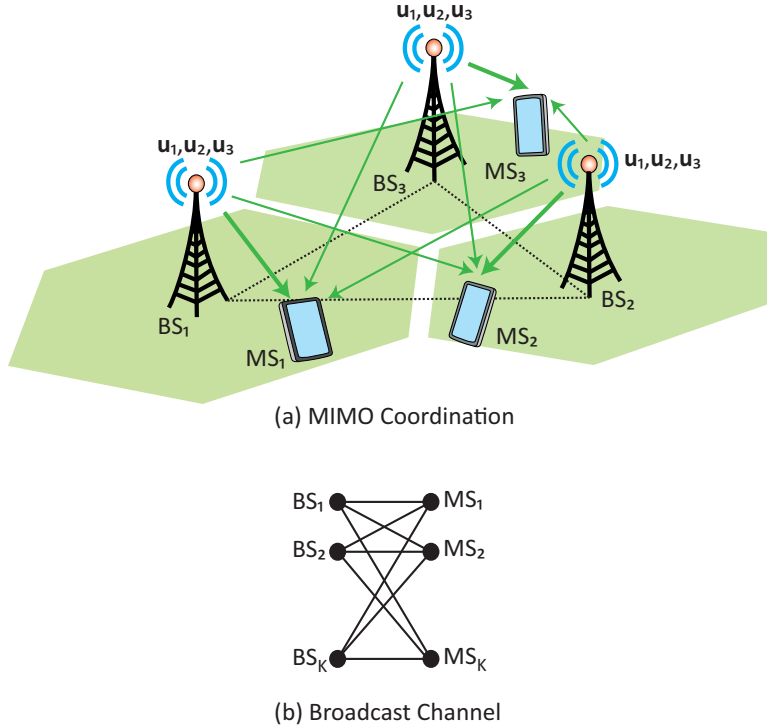


Figure 1.3: (a) MIMO coordination: Each user receives its signal from all the BSs within the cluster. (b) MIMO broadcast channel where transmitters are cooperating in transmission to non-cooperating receivers.

facilitates transmission in more interference-free dimensions, also known as degrees of freedom or multiplexing gains [44, 45]. This concept is known as *interference alignment*. These results have spurred an intensive research in this topic. However, without channel extensions, the computational complexity of numerically obtaining interference alignment is NP-hard [46].

### 1.2.2 MIMO Coordination

When the BSs are connected through high capacity backhaul network without any delay, then the BSs can share not only the channel state information but full user messages of the associated users. Availability of user messages at all BSs can improve the performance significantly over interference coordination. In this case, we have a large number of transmitting antennas coordinated in transmission to all the associated users and hence it is often referred to as *MIMO coordination*. MIMO coordination is illustrated in Figure 1.3.

The multi-cell downlink channel with full data sharing can be modeled as a MIMO BC with a single multiple-antenna transmitter and multiple receivers. Indeed, the number of transmit antennas are the total number of transmit antennas across the BSs within the cluster. To put it simply, this imitation of the giant antenna array produces the main gain in multi-cell scenario of this type.

The capacity region of a MIMO BC with sum power constraint has been previously discussed in [39, 47, 48]. The sum capacity of a Gaussian vector BC under per-antenna power constraint is the saddle-point of a minimax problem, where the maximization is over the set of transmit covariance matrices satisfying the power constraints and minimization is over the set of diagonal noise covariances [30, 49]. The dual minimax problem is convex-concave and consequently the original downlink optimization problem can be solved globally in the dual domain. By generalizing this result, we can transform the per-antenna transmitter optimization into an equivalent minimax optimization problem. An efficient algorithm has been proposed in [30] using Newton's method [50]. Particularly, [51, 52] use the simplistic Wyner channel model for the cellular system in these capacity results to show the benefits of MIMO coordination.

The capacity achieving strategy in MIMO BC is known to be the *dirty paper coding (DPC)* technique [53]. DPC is a non-linear technique based on pre-subtraction of interference at the transmitter [38, 39]. This requires the transmitted signals to be a result of successive encoding of information intended for the different users. Given an ordering of the users,  $\pi$ , at the time of encoding information for user  $\pi(j)$ , signals of users  $\pi(i < j)$  are known and can be taken into account in the encoding process to generate the signal for user  $\pi(j)$ . This means that the transmitter requires full non-causal knowledge of interfering signals for each user. Thus, perfect dirty paper coding implementation is infeasible. Moreover, finding the optimal ordering of users for successive encoding is a non-convex optimization problem. Furthermore, successive encoding to completely suppress interference requires adequate codes. The existence of such codes was proved in [40] and was extended

later [54]. However, these proofs use random codes that lack algebraic structure and detectors, and hence are very difficult to implement. Moreover, in the multi-cell scenario the burden of signal processing required for these schemes is even larger. Consequently, we are interested in reduced-complexity *linear precoding* schemes in this dissertation.

### 1.2.3 Partial Cooperation

When user messages are only available for a subset of all BSs in the cluster, then data sharing is *partial*. This method reduces the amount of information exchanged between the BSs. Note that full data sharing in multicell coordination requires all the data traffic routed to and from the central processing site which requires expensive infrastructure (and may not be available). Each user can receive the desired signal from the closest BSs and not necessarily all the BSs of the cluster to which it belongs. Furthermore, this enables studying distributed multi-cell coordination where the CSI is available partially. To obtain CSI, each BS transmits a training sequence. The size of the training sequence grows with the size of channel gains to be estimated. For multi-cell coordinated system with full cooperation, this size is prohibitive and limits the resources for the data transmission. Moreover, the estimation of the channel from the pilot sequence is usable within time coherence of the channel and it will be outdated after this time. We consider a multi-cell coordination with partial cooperation. In this case, each BS is aware of a subset of user messages and each user receives a signal from a subset of BSs within the cluster (partial data sharing). Therefore, the question is how to design a scheduling algorithm to benefit from gains of multi-cell coordination yet limit the data sharing. This problem has been addressed recently in [55, 56]. Furthermore, the CSI may also be shared partially. We refer to this type of multicell coordination as *partial cooperation*, which is illustrated in Figure 1.4. The channel model to study this type of coordination will be discussed in the next chapter. Particularly, this dissertation addresses this type of coordination.

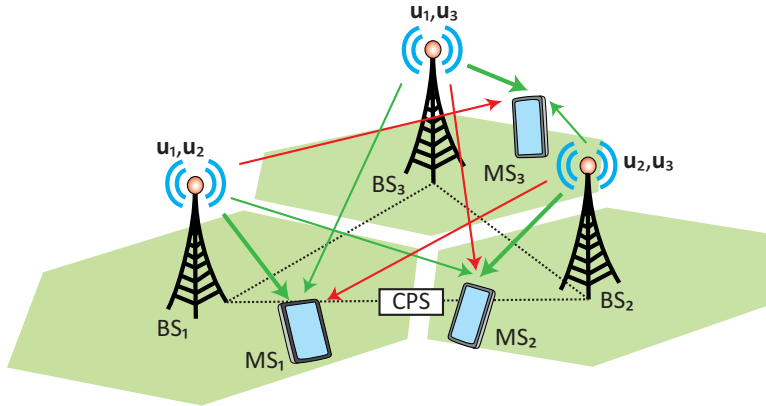


Figure 1.4: Partial cooperation where the user data is shared partially. This may also include partial exchange of CSI. Each BS knows a subset of user messages in the cluster.

### 1.3 Linear Precoding Schemes

Multicell coordination requires simple to implement and robust transmission strategies. Hence, in this dissertation we concentrate on linear precoding and equalization. A simple to implement linear precoding strategy involves complete cancelation of unwanted (intra-cluster) interference, which is referred to as *zero-forcing transmit precoding* technique [8, 28, 57–63]. For multiple-antenna users this must be in a form of block diagonalization (BD) technique [64]. The key idea of BD is linear precoding of data in such a way that transmission for each user lies within the null space of other users' transmissions. Therefore, the interference to other users is eliminated. Multi-cell BD has been employed explicitly for network MIMO coordinated systems in [8, 65–67]. However, they use specified structure for the BD (diagonal structure) which is designed for the sum power constraint. Although there were attempts in these papers to optimize the precoders to satisfy per-base-station and per-antenna power constraints, this structure of the precoders is no longer optimal for such power constraints and must be revised [65, 68, 69]. In [60], the ZF matrix is confined to the pseudo-inverse of the channel for the single receive antenna users with per-antenna power constraints. The sub-optimality of pseudo-inverse ZF beamforming subject to per-antenna power constraints was first shown in [65]. [68] presented the optimal precoder's structure using

the concept of generalized inverses, which lead to a non-convex optimization problem and its relaxed form required semi-definite programming (SDP) [70]. This was investigated only for single-antenna mobile users. [69] also used the generalized inverses for the single-antenna mobile users, but with multistage optimization algorithms.

Further improvement can be achieved by minimizing the mean square error (MMSE) between the estimate and the transmitted data. This is referred to as MMSE transceivers [46, 56, 71–74].

## 1.4 Implementation Challenges

Although theoretical perspective of multi-cell cooperative systems has been extensively researched in the recent years, the results of these efforts are all highly dependent to ideal assumptions such as high-capacity delay-free backhaul links and perfect channel knowledge (implying perfect channel estimation). In this section, we review some of the main challenges in practice. This dissertation is an effort to solve some of these challenges and build a foundation to study them.

### 1.4.1 Complexity

The complexity of finding the optimal precoding schemes increases with the number of users (or cells) participating in the cooperation (for example it has cubic order with the number of users [28, 69, 75]). Hence, investigating low complexity signal processing and coding techniques that approach ideal cooperative gains is of great interest. Most of the precoding and equalization designs contain sophisticated algorithms based on optimization toolboxes such as semidefinite programming (SDP) [70]. SDP-based algorithms are complex<sup>4</sup> and they do not give a closed-form structure for the solutions. Due to the non-convexity nature of the problem, a problem relaxation requires to apply convex optimization toolboxes or methods and consequently many of these algorithms reach a poor suboptimal solution. Furthermore, in practical systems

---

<sup>4</sup>The complexity of a SDP with  $n$  variables is  $\mathcal{O}(n^6)$  [70].

full data sharing and CSI may not be available and therefore efficient precoding techniques only relying on local CSI and local user data are also of research interest.

### **1.4.2 Synchronization**

Downlink multi-cell cooperation requires tight symbol and carrier synchronization between local BS oscillators. For outdoor BSs, global positioning signal (GPS) signal can be used for synchronization [76]. For the indoor BSs, the timing signal is sent from an outdoor GPS receiver. The BS carrier frequency offset estimation can be formed at the mobile users and then be fed back to the coordinated BSs [77]. This can also be done with remote radio heads for co-located BSs.

### **1.4.3 Channel estimation**

Coherent transmission and reception improves the performance significantly when the CSI is available. Therefore, system needs to allocate resources for pilot signals to estimate the channel. It is shown in [78] that the number of antennas participating in the joint coordination of network MIMO is not only limited by the complexity and limited backhaul link capacity but by the time and frequency variability of the fading channel. Therefore, there is a tradeoff between increasing the multi-cell network size, CSI estimation error, spectral resources allocated to training and the system performance. In frequency selective channels the channel needs to be estimated within its coherence time. The optimal channel training length is also studied in [79].

Note that in general the channel estimation is a multiuser MIMO challenge, but in multi-cell cooperative networks it is more complicated due to the size and the latency of estimation signals across the BSs.

## **1.5 Contributions**

The contributions of this dissertation can be listed as below:

- (i) We consider a more sophisticated approach to CoMP involving partial data sharing between the BSs. We also consider realistic per-antenna/per-BS power constraints and multiple antennas are deployed at both the BS and mobile user terminals. A novel model has been proposed to study CoMP, which is the MIMO interference channel with generalized power constraints. This model facilitates dynamic and distributed level of cooperation within the cellular network.
  
- (ii) Using this channel model, we focus on the linear processing schemes since they are easier to implement and more robust in the system. We begin with the ZF transmit precoding scheme. This scheme emerges as block diagonalization precoding technique when the users are employed with multiple antennas. We find the optimal block diagonalization precoders under per-antenna/per-BS power constraints. Our optimization is performed over the entire null space of other users' transmission and hence it is optimal. We obtain the optimal structure for the precoders and subsequently propose a simple iterative algorithm to find the precoders. Since ZF transmit precoding can serve limited number of users simultaneously, therefore a user selection algorithm is required prior to transmission. We also extend a semi-orthogonal user selection algorithm to the case where users are equipped with multiple antennas. This algorithm is less complex than greedy user selection algorithms due to reducing the size of search domain at each step to the users which have semi(almost)-orthogonal channel matrices to the users that have been already selected [80].
  
- (iii) Next, we include equalization into our design problem and optimize the precoders and equalizers jointly. We first review (and extend) the previous techniques to maximize the sum rate. Then, we address minimization of weighted sum of mean square errors of the estimated data symbols and propose two novel algorithms to design the precoders and equalizers. Compared to the previous techniques, these two are less complex and outperform earlier algorithms.

(iv) In the next stage, we consider imperfect CSI available at the BSs and address the robust design of transceivers. First, we consider that the channel estimation error is bounded and design worst-case robust transceiver, which guarantees a performance within the uncertainty region of the channel matrices. Next, we consider the case where the channel estimation error is a random matrix with specific statistical parameters and design statistically robust transceivers.

Throughout this dissertation, we have verified our algorithms within a realistic cellular model considering the channel parameters such as distance-dependent path loss, Rayleigh fading and log-normal shadowing. We drop the users randomly in the network and account for the incoming interference from the neighboring (non-coordinated) BSs.

# Chapter 2

## System Model and Preliminaries

In this chapter, we illustrate the system model which is used to study multicell coordinated systems in this dissertation. First, we discuss the arrangement of the cellular environment and the channel modelling. In CoMP, our main emphasis is on the multicell systems with partial cooperation. Therefore, we consider a partial cooperative channel model, which is called *MIMO interference channel with generalized constraints (MIMO-IFC-GC)*. Using this model, we formulate the problem that we will address throughout this dissertation, which is (weighted) sum-rate maximization in MIMO-IFC-GC over linear precoders and equalizer. This problem is in general a non-convex problem where the globally optimal solutions are not available through algorithms with reasonable complexity. An efficient concept in the design of precoders and equalizers in multiuser systems is uplink-downlink duality, which is extended to our channel model (MIMO-IFC-GC) in Section 2.4.

### 2.1 Channel Model and Configurations

We consider a cellular wireless network, where the users are distributed over the cells. We assume that each cell is served by one BS. A number of neighboring BSs are grouped together to build a so-called *cluster*. This grouping can be determined in the design or can be performed using one of scheduling algorithms in literature [81] that will not be discussed in this dissertation. Within each cluster, a form of multicell coordination can be used (e.g. interference/MIMO/partial coordination). Nevertheless, there is no inter-

cluster cooperation assumed in the network and the cluster-edge users suffer from inter-cluster interference (similar to inter-cell interference in a system without CoMP). We consider multiple-antennas at both BSs and the users. Our channel model consists of realistic cellular model. This means that the channel gains between each transmit antenna at the BS and each receive antenna at the user consists of three components: distance-dependent path loss, Rayleigh fading, and log-normal shadow fading.

A wireless channel is characterized due to the variation of the signal strength in time and frequency also known as *fading*. The signal attenuates with the distance from the source, which is referred to *path loss*. Thus, the attenuation is proportional with  $d^{-\beta}$  with  $d$  denotes the distance and  $\beta$  represents the path-loss exponent holding values between 2 and 4 (2 for free space and 4 for the reflection from ground plan, typically between 3 and 4 in urban areas). Another large-scale fading effect comes from shadowing by large objects such as buildings and hills. This phenomenon is called *shadowing* and it is observed that it follows the log-normal distribution. This can be modelled as  $\rho = 10^{\rho_{dBm}/10}$  where  $\rho_{dBm}$  follows a complex Gaussian distribution with zero mean and standard deviation of  $\sigma_\rho$  (i.e.  $\rho_{dBm} \sim \mathcal{CN}(0, \sigma_\rho^2)$ ). Typical value of the shadowing standard deviation is  $\sigma_\rho = 8$  dB [82].

Multiple paths between the transmitter and receiver cause constructive and destructive signals which occurs in scale of the carrier wavelength. This is dependent to the Doppler effect and delay spread. This effect is frequency dependent. A simple model for the variation of the channel gains (in specific frequency and delay time) is based on the existence a large number of statistically independent reflected and scattered path with random amplitude. This results in variation of the channel gain following a circular symmetric Gaussian distribution (i.e.  $\alpha \sim \mathcal{CN}(0, \sigma_h^2)$ ). The magnitude of the channel gain is exponentially distributed. This model is called *Rayleigh fading*<sup>1</sup>. Combining these effects, the channel gain can be modelled as

$$h = \alpha \sqrt{\rho d^{-\beta}} \quad (2.1)$$

---

<sup>1</sup>This will change when there is a line-of-sight path. In this case the magnitude of the channel gain follows Rician distribution [82].

Note that this is the channel model that we use in our numerical results and we often refer to it as *realistic* model since it accounts for all the variation of the channel gain in a cellular scenario.

In the case of a MIMO channel the channel gains between each transmit antenna and each receive antenna follow the same model. Thus, a MIMO channel with  $n_t$  transmit antenna and  $n_r$  receive antenna can be modelled as a channel matrix  $\mathbf{H} \in \mathbb{C}^{n_t \times n_r}$  such that each entry represents the channel gain between a transmit antenna and a receive antenna and it follows (2.1).

## 2.2 Downlink Transmission

In this dissertation, we focus on the downlink transmission and specifically on linear processing at the BSs and mobile users. In this section, we will detail the system model. Consider the MIMO downlink system illustrated in Fig.2.1 with  $M$  BSs (BSs) forming a set  $\mathcal{M}$ , and  $K$  users forming a set  $\mathcal{K}$ . The set  $\mathcal{M}$  forms a cluster which is assumed to have some form of coordination in between. Each BS is equipped with  $n_t$  transmit antennas and each mobile user employs  $n_r$  receive antennas. The  $m$ th BS is provided with the messages of its assigned users set  $\mathcal{K}_m \subseteq \mathcal{K}$ . In other words, the  $k$ th user receives its message from a subset of  $M_k$  BSs  $\mathcal{M}_k \subseteq \mathcal{M}$ . Notice that, if  $\mathcal{K}_m$  contains one user for each transmitter  $m$  and  $M_k = 1$ , then the model at hand reduces to a standard MIMO interference channel. Moreover, when all transmitters cooperate in transmitting to all the users, i.e.,  $\mathcal{K}_m = \mathcal{K}$  for all  $m \in \mathcal{M}$  or equivalently  $M_k = M$ , then we have a MIMO broadcast channel (BC). We now detail the signal model for the channel at hand, which is referred to as *MIMO interference channel with partial message sharing*. Define as  $\mathbf{u}_k = [u_{k,1} \dots u_{k,d_k}]^T \in \mathbb{C}^{d_k}$  the  $d_k \times 1$  complex vector representing the  $d_k \leq \min(M_k n_t, n_r)$  independent information streams intended for user  $k$ . We assume that  $\mathbf{u}_k \sim \mathcal{CN}(0, \mathbf{I})$ , where we assumed that the channel gains are normalized correspondingly. The data streams  $\mathbf{u}_k$  are known to all the BS in the set  $\mathcal{M}_k$ . In particular, if  $m \in \mathcal{M}_k$ , the  $m$ th BS precodes vector  $\mathbf{u}_k$  via a matrix  $\mathbf{F}_{k,m} \in \mathbb{C}^{n_t \times d_k}$ , so that the signal

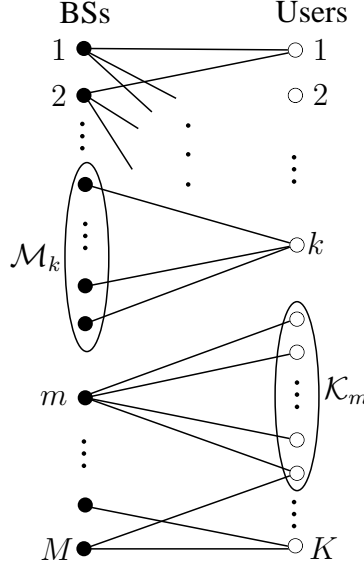


Figure 2.1: A downlink model with partial BS cooperation or equivalently partial message knowledge.

$\tilde{\mathbf{x}}_m \in \mathbb{C}^{n_t}$  sent by the  $m$ th BS can be expressed as

$$\tilde{\mathbf{x}}_m = \sum_{k \in \mathcal{K}_m} \mathbf{F}_{k,m} \mathbf{u}_k. \quad (2.2)$$

Imposing a per-BS power constraint, the following constraint must be then satisfied

$$\begin{aligned} \mathbb{E} [|\tilde{\mathbf{x}}_m|^2] &= \text{tr} \{ \mathbb{E} [\tilde{\mathbf{x}}_m \tilde{\mathbf{x}}_m^H] \} \\ &= \sum_{k \in \mathcal{K}_m} \text{tr} \{ \mathbf{F}_{k,m} \mathbf{F}_{k,m}^H \} \leq P_m, m = 1, \dots, M, \end{aligned} \quad (2.3)$$

where  $P_m$  is the power constraint of the  $m$ th BS. When per-antenna power constraints are enforced, the constraints can be seen as

$$\begin{aligned} [\mathbb{E} [|\tilde{\mathbf{x}}_m|^2]]_{i,i} &= \left[ \sum_{k \in \mathcal{K}_m} \text{tr} \{ \mathbf{F}_{k,m} \mathbf{F}_{k,m}^H \} \right]_{i,i} \leq P_{m,i}, \\ m &= 1, \dots, M, \quad i = 1, \dots, n_t \end{aligned} \quad (2.4)$$

where  $P_{m,i}$  is the power budget of the  $i$ th-antenna of the  $m$ th BS. The signal received at the  $k$ th user can be written as

$$\mathbf{y}_k = \sum_{m=1}^M \tilde{\mathbf{H}}_{k,m} \tilde{\mathbf{x}}_m + \tilde{\mathbf{n}}_k \quad (2.5)$$

$$= \sum_{m \in \mathcal{M}_k} \tilde{\mathbf{H}}_{k,m} \mathbf{B}_{k,m} \mathbf{u}_k + \sum_{l \neq k} \sum_{j \in \mathcal{M}_l} \tilde{\mathbf{H}}_{k,j} \mathbf{B}_{l,j} \mathbf{u}_l + \tilde{\mathbf{n}}_k, \quad (2.6)$$

where  $\tilde{\mathbf{H}}_{k,m} \in \mathbb{C}^{n_r \times n_t}$  is the channel matrix between the  $m$ th BS and  $k$ th user and  $\mathbf{n}_k$  is additive complex Gaussian noise  $\tilde{\mathbf{n}}_k \sim \mathcal{CN}(\mathbf{0}, \mathbf{I})$ . In case the noise is not uncorrelated across the antennas, each user can always whiten it as a linear pre-processing step. Therefore, a spatially uncorrelated noise can be assumed without loss of generality. The availability of channel state information at all nodes will be discussed in each of next chapters independently. In (2.6), we have distinguished between the first term, which represents useful signal, the second term, which accounts for interference, and the noise.

### 2.2.1 Equivalence with MIMO-IFC-GC

We now show that the MIMO interference channel with *partial message sharing and per-BS power constraints* described above is equivalent to a specific MIMO interference channel with *individual message knowledge and generalized linear constraints*, which we refer to as MIMO-IFC-GC.

**Definition 2.1.** (*MIMO-IFC-GC*) The MIMO-IFC-GC consists of  $K$  transmitters and  $K$  receiver, where the  $k$ th transmitter has  $m_{t,k}$  antennas and the  $k$ th receiver has  $m_{r,k}$  antennas. The received signal at the  $k$ th receiver is

$$\mathbf{y}_k = \mathbf{H}_{k,k} \mathbf{x}_k + \sum_{l \neq k} \mathbf{H}_{k,l} \mathbf{x}_l + \mathbf{n}_k, \quad (2.7)$$

where  $\mathbf{n}_k \sim \mathcal{CN}(\mathbf{0}, \mathbf{I})$ , the inputs are  $\mathbf{x}_k \in \mathbb{C}^{m_{t,k}}$  and the channel matrix between the  $l$ th transmitter and the  $k$ th receiver is  $\mathbf{H}_{k,l} \in \mathbb{C}^{m_{r,k} \times m_{t,k}}$ . The data vector intended for user  $k$  is  $\mathbf{u}_k \in \mathbb{C}^{d_k}$  with  $d_k \leq \min(m_{t,k}, m_{r,k})$  and  $\mathbf{u}_k \sim \mathcal{CN}(0, \mathbf{I})$ . The precoding matrix for user  $k$  is defined as  $\mathbf{F}_k \in \mathbb{C}^{m_{t,k} \times d_k}$  so that  $\mathbf{x}_k = \mathbf{F}_k \mathbf{u}_k$ . The inputs  $\mathbf{x}_k$  have to satisfy  $M$  generalized linear constraints

$$\sum_{k=1}^K \text{tr} \{ \Phi_{k,n} \mathbb{E} [\mathbf{x}_k \mathbf{x}_k^H] \} = \sum_{k=1}^K \text{tr} \{ \Phi_{k,m} \mathbf{B}_k \mathbf{B}_k^H \} \leq p_n, \quad (2.8)$$

for given weight matrices  $\Phi_{k,n} \in \mathbb{C}^{m_{t,k} \times m_{t,k}}$  and  $n = 1, \dots, N$ . The weight matrices are such that matrices  $\sum_{n=1}^N \Phi_{k,n}$  are positive definite for all  $k = 1, \dots, K$ .

We remark that the positive definiteness of matrices  $\sum_{n=1}^N \Phi_{k,n}$  guarantees that the system is not allowed to transmit infinite power in any direction [75].

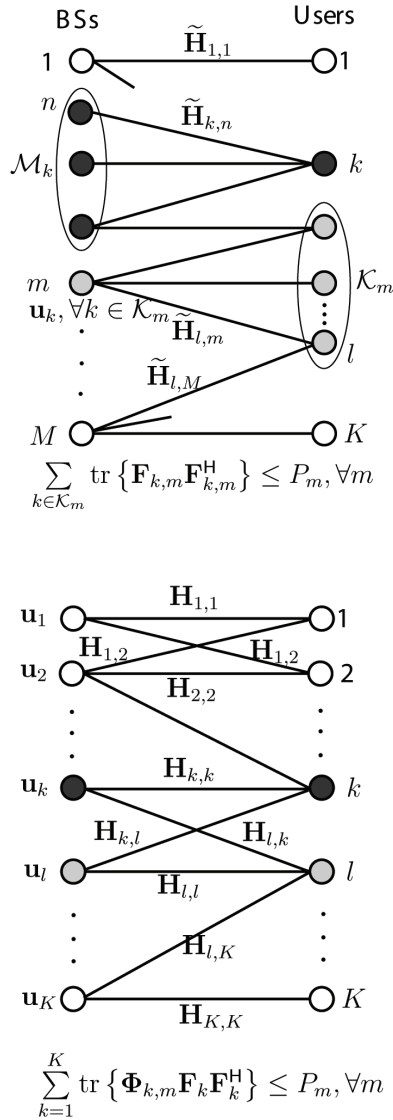


Figure 2.2: (a) A downlink model with partial BS cooperation or equivalently partial message knowledge, (b) The equivalent MIMO interference channel with generalized linear power constraints.

**Lemma 2.1.** *Let  $(l)_k$  be the  $l$ th BS in subset  $\mathcal{M}_k$  of BSs that know user  $k$ 's message. The MIMO interference channel with partial message sharing (and per-transmitter power constraints) is equivalent to a MIMO-IFC-GC. This equivalent MIMO-IFC-GC is defined with  $m_{t,k} = M_k n_t$ ,  $m_{r,k} = n_r$ , channel matrices*

$$\mathbf{H}_{k,l} = \left[ \tilde{\mathbf{H}}_{k,(1)_l} \cdots \tilde{\mathbf{H}}_{k,(M_l)_l} \right], \quad (2.9)$$

*beamforming matrices*

$$\mathbf{F}_k = \left[ \mathbf{F}_{k,(1)_k}^\top \cdots \mathbf{F}_{k,(M_k)_k}^\top \right]^\top \quad (2.10)$$

*and weight matrices  $\Phi_{k,n}$  and weight matrices  $\Phi_{k,n}$  corresponding to the*

- *$n$ th per-BS power constraints ( $N = Mn_t$ ), have to be all zero except that its  $l$ th  $n_t \times n_t$  submatrix on the main diagonal is  $\mathbf{I}_{n_t}$ , if  $m = (l)_k$ :*

$$\Phi_{k,m} = \begin{bmatrix} \mathbf{0}_{n_t} & \mathbf{0} & \cdots & \mathbf{0} \\ \mathbf{0} & \ddots & \ddots & \vdots \\ \vdots & \ddots & \mathbf{I}_{n_t} & \mathbf{0} \\ \mathbf{0} & \cdots & \mathbf{0} & \mathbf{0} \end{bmatrix}_{Mn_t \times Mn_t}, \quad (2.11)$$

*Notice that if  $k \notin \mathcal{K}_n$  then  $\Phi_{k,n} = \mathbf{0}$ .*

- *$n$ th per-antenna power constraint ( $N = Mn_t$ ), have to be all zero except a one in the main diagonal referring to the  $n$ th antenna:*

$$\Phi_{k,m} = \begin{bmatrix} 0 & 0 & \cdots & 0 \\ 0 & \ddots & \ddots & \vdots \\ \vdots & \ddots & 1 & 0 \\ 0 & \cdots & 0 & 0 \end{bmatrix}_{Mn_t \times Mn_t}, \quad (2.12)$$

- *sum power constraint ( $N = 1$ ), have to be equal to the identity matrix:*  
 $\Phi_{k,m} = \mathbf{I}_{Mn_t}$ .

*We emphasize that the definition of MIMO-IFC-GC and this equivalence rely on the assumption of linear processing at the transmitters.*

*Proof.* The proof follows by inspection. Notice that matrices  $\sum_{m=1}^M \Phi_{k,m}$  are positive definite by construction. In the common power condition scenarios (mentioned above) this summation is equal to an identity matrix which is positive definite.  $\square$

Given the generality of the MIMO-IFC-GC, which includes the scenario of interest of MIMO interference channel with partial message sharing as per the Lemma above, in the design of precoders and equalizers we focus on the MIMO-IFC-GC as defined above and return to the cellular application when we need to present numerical results.

In this dissertation, we also include the linear processing at the receivers. Therefore, the  $k$ th receiver estimates the intended vector  $\mathbf{u}_k$  using the receive processing (or equalization) matrix  $\mathbf{G}_k \in \mathbb{C}^{m_r, k \times d_k}$  as

$$\hat{\mathbf{u}}_k = \mathbf{G}_k \mathbf{y}_k. \quad (2.13)$$

The most common performance measures, such as weighted sum-rate or bit error rate, can be derived from the estimation error covariance matrix for each user  $k$ ,

$$\mathbf{E}_k = \mathbb{E} \left[ (\hat{\mathbf{u}}_k - \mathbf{u}_k) (\hat{\mathbf{u}}_k - \mathbf{u}_k)^H \right], \quad (2.14)$$

which is referred to as *Mean Square Error (MSE)-matrix* (see [83] for a review). The name comes from the fact that the  $j$ th term on the main diagonal of  $\mathbf{E}_k$  is the MSE

$$\text{MSE}_{k,j} = \mathbb{E}[|\hat{u}_{k,j} - u_{k,j}|^2] \quad (2.15)$$

on the estimation of the  $k$ th user's  $j$ th data stream  $u_{k,j}$ . Using the definition of MIMO-IFC-GC, it is easy to see that the MSE-matrix can be written as a function of the equalization matrix  $\mathbf{G}_k$  and *all* the transmit matrices  $\{\mathbf{F}_k\}_{k=1}^K$  as

$$\begin{aligned} \mathbf{E}_k &= \mathbf{G}_k \mathbf{H}_k \mathbf{F}_k \mathbf{F}_k^H \mathbf{H}_{k,k}^H \mathbf{G}_k^H - \mathbf{G}_k \mathbf{H}_{k,k} \mathbf{F}_k \\ &\quad - \mathbf{F}_k^H \mathbf{H}_{k,k}^H \mathbf{G}_k^H + \mathbf{G}_k \mathbf{\Omega}_k \mathbf{G}_k^H + \mathbf{I}_k. \end{aligned} \quad (2.16)$$

where  $\mathbf{\Omega}_k$  is the covariance matrix that accounts for noise and interference at user  $k$

$$\mathbf{\Omega}_k = \mathbf{I} + \sum_{l \neq k} \mathbf{H}_{k,l} \mathbf{F}_l \mathbf{F}_l^H \mathbf{H}_{k,l}^H. \quad (2.17)$$

## 2.2.2 Capacity Region

The capacity region of a MIMO BC with sum power constraint has been previously discussed in [39, 47, 48]. In this model, the transmitters know all

the users' messages and therefore in theory there is only one multiple-antenna transmitter. In this case,  $m_{t,k} = Mn_t$ . The sum capacity of a Gaussian vector broadcast channel under per-antenna power constraint is the saddle-point of a minimax problem [48]

$$\begin{aligned} \mathcal{C} = \max_{\mathbf{C}_x \succeq \mathbf{0}} \min_{\mathbf{C}_n \succeq \mathbf{0}} \quad & \log \frac{|\mathbf{H}\mathbf{C}_x\mathbf{H}^H + \mathbf{C}_n|}{|\mathbf{C}_n|} \\ \text{subject to} \quad & [\mathbf{C}_x]_{i,i} \leq p_i, \text{ for } i = 1, \dots, N \\ & \mathbf{C}_n^{(i)} = \sigma^2 \mathbf{I}_{n_r} \end{aligned} \quad (2.18)$$

where  $\mathbf{C}_n$  is the noise covariance matrix of  $\mathbf{n}$  in (2.7) such that  $\mathbf{n}^T = [\mathbf{n}_1^T \cdots \mathbf{n}_K^T]$ , and  $\mathbf{C}_n^{(i)}$  refers to the  $i$ th block-diagonal term of  $\mathbf{C}_n$ . The maximization is over all transmit covariance matrices  $\mathbf{C}_x$  and the minimization is over all off-block diagonal terms of the noise covariance matrix  $\mathbf{C}_n$ . This is due to the fact that the capacity of MIMO BC equals the Sato bound, which is the capacity of a cooperative system with the worst case noise  $\mathbf{C}_n$  [84]. The sum capacity of a MIMO BC with individual per-antenna transmit power constraints  $p_1, \dots, p_{N_t}$  is the same as the sum capacity of a dual MIMO MAC with a sum power constraint  $\sum_{i=1}^{N_t} p_i$  and with an uncertain noise  $\hat{\mathbf{C}}_n$  [30, 49, 85]. The Lagrangian dual of the minimax problem (2.18) can be stated as [30, 49]

$$\begin{aligned} \max_{\hat{\mathbf{C}}_x} \min_{\hat{\mathbf{C}}_n} \quad & \log \frac{|\mathbf{H}^H \hat{\mathbf{C}}_x \mathbf{H} + \hat{\mathbf{C}}_n|}{|\hat{\mathbf{C}}_n|} \\ \text{subject to} \quad & \text{tr}(\hat{\mathbf{C}}_x) \leq \text{tr}(\mathbf{P}) \\ & \text{tr}(\hat{\mathbf{C}}_n \mathbf{P}) \leq \text{tr}(\mathbf{C}) \\ & \hat{\mathbf{C}}_n \text{ is diagonal, } \hat{\mathbf{C}}_n \succeq 0, \hat{\mathbf{C}}_x \succeq 0 \end{aligned} \quad (2.19)$$

where  $\mathbf{P} = \text{diag}(p_1, \dots, p_{N_t})$  is a diagonal matrix of individual maximum transmit powers,  $\text{tr}(\cdot)$  denotes the trace of a matrix, and that  $\succeq$  in the matrix inequalities means  $\hat{\mathbf{C}}_n$  and  $\hat{\mathbf{C}}_x$  are positive semi-definite matrices. Thus, the Lagrangian dual corresponds to a MAC with linearly constrained noise. This duality result has been generalized to the entire capacity region [30]. The dual minimax problem is convex-concave and thus the original downlink optimization problem can be much more efficiently solved in the dual domain. An efficient algorithm using Newton's method [50] is used in [85] and [30] to

solve the dual minimax problem; it finds an efficient search direction for the simultaneous maximization and minimization. This capacity result is used to characterize the sum capacity of the multi-base coordinated network and thus constitutes the performance limit for the proposed transmission schemes.

## 2.3 Problem Formulation

Generally, we are interested in the (weighted) sum-rate maximization of the system under the specified (individual) power constraints. The optimization variables of this problem are linear precoders and equalizers of the users. The achievable rate of user  $k$  is given by [2]

$$R_k = \log |\mathbf{I} + \mathbf{H}_{k,k} \mathbf{F}_k \mathbf{F}_k^H \mathbf{H}_{k,k}^H \mathbf{\Omega}_k^{-1}| \quad (2.20)$$

where the interference between users data streams are simply considered as noise. Consequently, the weighted sum-rate maximization problem can be translated as an optimization problem

$$\begin{aligned} & \underset{\mathbf{F}_k, \forall k}{\text{maximize}} && \sum_{k=1}^K \mu_k R_k, \\ & \text{subject to} && \mathbf{F}_k \in \mathcal{F}, \forall k \end{aligned} \quad (2.21)$$

where  $\mathcal{F}$  is the set of precoding matrices which satisfy specified power constraints. The weights  $\mu_k \geq 0$  are user rate priorities defined based on the scheduling algorithm (a higher level protocol) and will be explained later. As discussed in the previous section, the constraints of problem (2.21) are generally defined in a linear format (affine conditions). It can be simply verified that the objective function of problem (2.21) is non-convex. Even for a single-user case where the interference plus noise covariance matrix is an identity matrix, it is non-convex. When the users are equipped with a single antenna only, there is a particular formulation of the problem above that enjoys efficient and global optimal solution. This formulation is the minimization of the transmit power across the BSs subject to SINR constraints. This formulation fits applications where the system has fixed quality of service constraints (for

feasible values of  $\gamma_k$ s). The formulation is given by

$$\begin{aligned} & \underset{\mathbf{f}_k, \forall k}{\text{minimize}} && \sum_{k=1}^K \|\mathbf{f}_k\|^2 \\ & \text{subject to} && \frac{|\mathbf{h}_{k,k}\mathbf{f}_k|^2}{1+\sum_{l \neq k} |\mathbf{h}_{k,l}\mathbf{f}_l|^2} \geq \gamma_k, \forall k \end{aligned}, \quad (2.22)$$

Nevertheless, we require the schemes where the BSs can find an optimal solution jointly without excessive exchange of channel state information. Therefore, downlink-uplink duality is a useful concept in this direction. The problem of multi-cell transmit downlink beamforming was first considered in a classic work by Rashid-Farrokhi et al [29], where the BSs employ multiple antennas and the users are single-antenna. The transmit beamforming optimization is formulated as the minimization of total transmit power while the SINR at each link satisfies a minimum target. Rashidi-Farrokhi et al proposed an iterative algorithm to achieve the optimal solution for this problem. This algorithm is based on establishing a virtual uplink network with transmitters and receivers reversed and the uplink channels equal to the Hermitian transpose of the downlink channels, but with the same achievable SINR sets. The algorithm finds the optimal uplink receivers, which are indeed minimum mean squared error (MMSE) receivers. These virtual uplink MMSE receivers give the transmitters for the downlink system. Next, the virtual uplink powers and correspondingly the downlink powers are updated. The algorithm iterates until convergence. Later, it is shown that the downlink-uplink duality may be unified under a Lagrangian duality in optimization [30]. Note that the formulation of the transmit beamforming problem as a minimization of the total power constraint enables global optimization of this problem. With this formulation, the SINR constraints can be transformed into a second-order-cone constraint [31] and therefore solving the problem via convex optimization. Although the downlink-uplink duality can be extended to the systems with multiple-antenna users [32], the iterative transmit/receive beamformer and the power will not converge to the global optimal solution and only local optimal solution is guaranteed so far. This is due to the non-convexity nature of joint transmit/receive beamforming optimization problem. In the following section, we have extended the uplink-downlink duality to the

MIMO interference channel with single linear power constraint.

## 2.4 Uplink-Downlink Duality

The concept of SINR duality has been discussed in the literature between the MIMO BC and multiple access channel under the sum power constraints [86–88] and under linear power constraints [49, 89]. The SINR duality has been discussed for the interference networks under single sum power constraint in [71] but its extension to a linear constraint requires invertibility on the weight matrices. In this section, we generalize the SINR duality results in [89] to MIMO-IFC-GC with a user-weighted linear power constraints given by

$$\sum_{k=1}^K \text{tr} \{ \mathbf{\Phi}_k \mathbf{F}_k \mathbf{F}_k^H \} \leq P \quad (2.23)$$

and then we use this result for the case of multiple linear constraints. Since this extension does not require the inversion of weight matrices, it can be used for any linear power constraints including per-BS power constraints where the weight matrices can be non-singular .

**Definition 2.2.** The dual of a MIMO-IFC-GC with the power constraint (2.23) is an interference channel with channel matrices equal to the conjugate transposed channel matrices of the MIMO-IFC-GC, i.e. the channel matrix of the dual MIMO-IFC-GC from the  $k$ th user to the  $l$ th transmitter is  $\mathbf{H}_{k,l}^H$ , and the  $k$ th user noise covariance matrix is  $\mathbf{\Phi}_k$ . The dual MIMO-IFC-GC contains  $\tilde{\mathbf{g}}_{k,j}$  as a normalized transmit beamforming vector for the  $j$ th data substream for the user  $k$  and  $\tilde{\mathbf{f}}_{k,j}$  as a normalized receive processing vector at the  $k$ th transmitter for the  $j$ th data substream.

The corresponding dual power constraint is also given as

$$\sum_{k=1}^K \text{tr} \{ \mathbf{G}_k \mathbf{G}_k^H \} \leq P \quad (2.24)$$

where  $\hat{\Sigma}_k = \mathbf{G}_k \mathbf{G}_k^H$  is the transmit covariance matrix for the  $k$ th user at the dual MIMO-IFC-GC. Figure 2.2 summarizes the duality results. The power

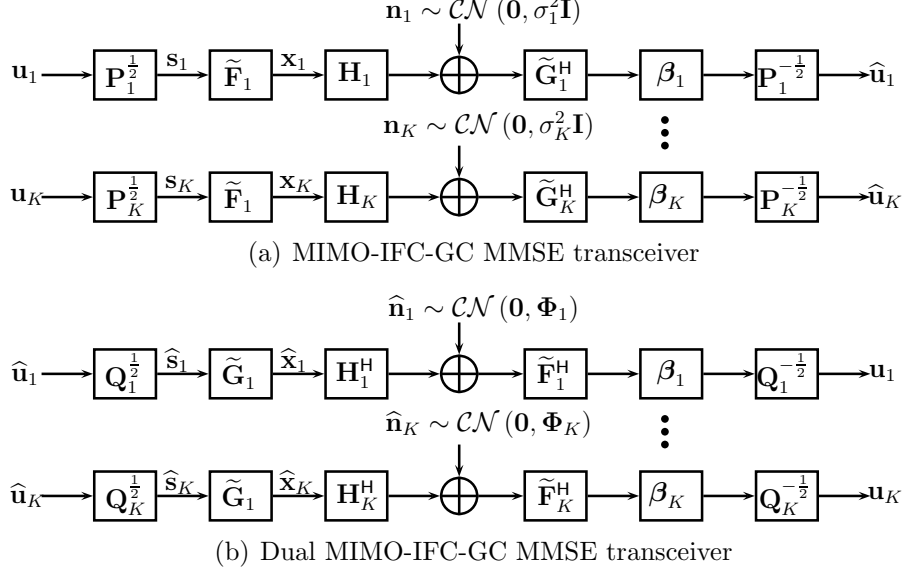


Figure 2.3: Duality for the MIMO-IFC-GC model.

allocated to the  $j$ th data substream of the  $k$ th user is  $p_{k,j}$  and consequently the power vector is defined as

$$\mathbf{p} = [p_{1,1}, \dots, p_{1,d_1}, \dots, p_{K,1}, \dots, p_{K,d_K}]^\top. \quad (2.25)$$

The power allocated to the  $j$ th data substream of the  $k$ th user of the dual MIMO-IFC-GC model is  $q_{k,j}$  and thus the dual power vector is denoted as

$$\mathbf{q} = [q_{1,1}, \dots, q_{1,d_1}, \dots, q_{K,1}, \dots, q_{K,d_K}]^\top. \quad (2.26)$$

The immediate extension of the results in [89] to the interference network with the user-weighted linear power constraint (2.23) is as follows:

**Lemma 2.2.** (*SINR Duality*) *If a set of SINRs  $\gamma$  is achieved by the linear processing strategy  $(\{\tilde{\mathbf{f}}\}, \{\tilde{\mathbf{g}}\}, \mathbf{p})$  in MIMO-IFC-GC under the power constraint (2.23), then  $\gamma$  is also achievable in the corresponding dual MIMO-IFC-GC with the linear beamforming strategy  $(\{\tilde{\mathbf{g}}\}, \{\tilde{\mathbf{f}}\}, \mathbf{q})$  under the sum power constraint (2.24). The reverse is also true.*

*Proof.* Assuming linear processing at the transmitters and the receivers, the SINR of the  $j$ th data substream at the  $k$ th user can be written as

$$\text{SINR}_{k,j} = \frac{p_{k,j} |\tilde{\mathbf{g}}_{k,j}^H \mathbf{H}_{k,k} \tilde{\mathbf{f}}_{k,j}|^2}{1 + \sum_{(l,i) \neq (k,j)} p_{l,i} |\tilde{\mathbf{g}}_{k,j}^H \mathbf{H}_{k,l} \tilde{\mathbf{f}}_{l,i}|^2}. \quad (2.27)$$

The achievable rate of user  $k$  can be defined immediately as

$$R_k = \sum_{j=1}^{d_k} \log(1 + \text{SINR}_{k,j}). \quad (2.28)$$

Following definition of the dual MIMO-IFC-GC, its corresponding SINR for the  $j$ th data substream of the  $k$ th user can be expressed as

$$\widehat{\text{SINR}}_{k,j} = \frac{q_{k,j} |\tilde{\mathbf{f}}_{k,j}^H \mathbf{H}_{k,k}^H \tilde{\mathbf{g}}_{k,j}|^2}{\tilde{\mathbf{f}}_{k,j}^H \left( \sum_{(l,i) \neq (k,j)} q_{l,i} \mathbf{H}_{l,k}^H \tilde{\mathbf{g}}_{l,i} \tilde{\mathbf{g}}_{l,i}^H \mathbf{H}_{l,k} + \Phi_k \right) \tilde{\mathbf{f}}_{k,j}} \quad (2.29)$$

We introduce the cross-talk matrix  $\Psi \in \mathbb{R}_{+}^{\sum_k d_k \times \sum_k d_k}$  between different data substreams of the users in the system [87]. We denote the  $(\sum_{n=1}^{k-1} + j, \sum_{m=1}^{l-1} + i)$ th element of  $\Psi$  as  $\Psi_{k,j}^{l,i}$  which represents the interference power from the  $l$ th user's  $i$ th data substream to the  $k$ th user's  $j$ th data substream and is given by

$$\Psi_{k,j}^{l,i} = \begin{cases} \left| \tilde{\mathbf{g}}_{k,j}^H \mathbf{H}_{k,l} \tilde{\mathbf{f}}_{l,i} \right|^2 & (l,i) \neq (k,j) \\ 0 & \text{otherwise.} \end{cases} \quad (2.30)$$

Further we introduce a diagonal matrix  $\mathbf{D} \in \mathbb{R}_{+}^{\sum_k d_k \times \sum_k d_k}$  with the  $(\sum_{n=1}^{k-1} + j)$ th diagonal element denoted by  $\mathbf{D}^{k,j}$  and is defined as

$$\mathbf{D}^{k,j} = \frac{\gamma_{k,j}}{|\tilde{\mathbf{g}}_{k,j}^H \mathbf{H}_{k,k} \tilde{\mathbf{f}}_{k,j}|^2}. \quad (2.31)$$

Let the noise power vector defined as

$$\boldsymbol{\eta} = [\eta_{1,1}, \dots, \eta_{1,d_1}, \dots, \eta_{K,1}, \dots, \eta_{K,d_K}]^T \quad (2.32)$$

where  $\eta_{k,j} = \tilde{\mathbf{f}}_{k,j}^H \Phi_k \tilde{\mathbf{f}}_{k,j}$ . Note that the  $\widehat{\text{SINR}}_{k,j}$  can be rewritten as [71]

$$\widehat{\text{SINR}}_{k,j} = \frac{q_{k,j} |\tilde{\mathbf{f}}_{k,j}^H \mathbf{H}_{k,k}^H \tilde{\mathbf{g}}_{k,j}|^2}{\sum_{(l,i)} q_{(l,i)} \Psi_{l,i}^{k,j} + \eta_{k,j}}. \quad (2.33)$$

Setting  $\widehat{\text{SINR}}_{k,j} = \gamma_{k,j}$  and using (2.33) and (2.31), we can obtain

$$\frac{q_{k,j}}{\Psi_{k,j}^T \mathbf{q} + \eta_{k,j}} = \mathbf{D}^{k,j} \quad (2.34)$$

where  $\Phi_{k,j}^T$  is the corresponding  $(k,j)$ th row of  $\Psi^T$ . By simplifying this equation, we can obtain a vector equation

$$\mathbf{q} = \mathbf{D} (\Psi^T \mathbf{q} + \boldsymbol{\eta}). \quad (2.35)$$

Hence, the power allocation  $\mathbf{q}$  at the dual MIMO-IFC-GC is given by

$$\mathbf{q} = (\mathbf{D}^{-1} - \mathbf{\Psi}^\top)^{-1} \boldsymbol{\eta}. \quad (2.36)$$

Since  $\mathbf{D}^{-1} - \mathbf{\Psi}^\top$  is a Stieltjes matrix which is a real symmetric positive definite matrix with non-positive off-diagonal entries, it is invertible to a nonsingular symmetric matrix with nonnegative entries [90]. Hence, the dual power vector has non-negative elements (i.e.  $\mathbf{q} \succeq 0$ ). The power constraint (2.23) can be simplified as

$$\begin{aligned} \sum_{k=1}^K \text{tr} \{ \mathbf{\Phi}_k \boldsymbol{\Sigma}_k \} &= \sum_{k=1}^K \sum_{j=1}^{d_k} p_{k,j} \text{tr} \left\{ \tilde{\mathbf{f}}_{k,j}^\text{H} \mathbf{\Phi}_k \tilde{\mathbf{f}}_{k,j} \right\} \\ &= \sum_{k=1}^K \sum_{j=1}^{d_k} p_{k,j} \eta_{k,j} \leq P \end{aligned} \quad (2.37)$$

Correspondingly, to obtain same set of SINRs as dual MIMO-IFC-GC, the power allocation at the MIMO-IFC-GC is given by [87]

$$\mathbf{p} = (\mathbf{D}^{-1} - \mathbf{\Psi})^{-1} \mathbf{1} \quad (2.38)$$

where  $\mathbf{1}$  is a vector with entries equal to 1. The power constraint at the MIMO-IFC-GC can be written as

$$\mathbf{p}^\top \boldsymbol{\eta} = \mathbf{1}^\top (\mathbf{D}^{-1} - \mathbf{\Psi}^\top)^{-1} \boldsymbol{\eta} = \mathbf{1}^\top \mathbf{q} = \sum_{k=1}^K \sum_{j=1}^{d_k} q_{k,j} \leq P \quad (2.39)$$

where the equalities holds due to (2.38) and (2.36). Thus, the power constraints at the MIMO-IFC-GC and its dual are equivalent.  $\square$

The MSE duality between MIMO BC and MIMO multiple access channel (MAC) with sum power constraint is shown in [91]. The MSE duality relies on the SINR duality established in the previous section. In this section, this has been extended to the interference network with partial user message knowledge and under a single user-weighted linear power constraint.

Consider the MIMO-IFC-GC discussed in Section 2.2 with the power constrain given by (2.23). The estimated  $j$ th data symbol of the  $k$ th user

can be obtained from (2.13) as

$$\begin{aligned}\widehat{u}_{k,j} &= \beta_{k,j} \widetilde{\mathbf{g}}_{k,j}^H \mathbf{H}_{k,k} \widetilde{\mathbf{f}}_{k,j} u_{k,j} \\ &+ \sum_{(l,i) \neq (k,j)} \beta_{k,j} p_{k,j}^{-\frac{1}{2}} \widetilde{\mathbf{g}}_{k,j}^H \mathbf{H}_{k,l} p_{l,i}^{\frac{1}{2}} \widetilde{\mathbf{f}}_{l,i} u_{l,i} + \beta_{k,j} p_{k,j}^{\frac{1}{2}} \widetilde{\mathbf{g}}_{k,j}^H z_{k,j}\end{aligned}\quad (2.40)$$

where  $\beta_{k,j}$  is the normalizing parameter for the estimation of  $j$ th data substream of the  $k$ th user. The MSE for the  $j$ th data substream of the  $k$ th user at the MIMO-IFC-GC can be expressed as

$$\begin{aligned}\text{MSE}_{k,j} &= \mathbb{E} [|\widehat{u}_{k,j} - u_{k,j}|^2] \\ &= \beta_{k,j}^2 p_{k,j}^{-1} \widetilde{\mathbf{g}}_{k,j}^H \left( \sum_{(l,i)} \mathbf{H}_{k,l} p_{l,i} \widetilde{\mathbf{f}}_{l,i} \widetilde{\mathbf{f}}_{l,i}^H \mathbf{H}_{k,l}^H \right) \widetilde{\mathbf{g}}_{k,j} \\ &\quad - 2\beta_{k,j} \mathbb{R} \{ \widetilde{\mathbf{g}}_{k,j}^H \mathbf{H}_{k,k} \widetilde{\mathbf{f}}_{k,j} \} + \beta_{k,j}^2 p_{k,j}^{-1} \sigma_{k,j}^2 + 1\end{aligned}\quad (2.41)$$

Correspondingly, the MSE for the  $j$ th data substream of the  $k$ th user in the dual MIMO-IFC-GC MSE can be written as

$$\begin{aligned}\widehat{\text{MSE}}_{k,j} &= \beta_{k,j}^2 q_{k,j}^{-1} \widetilde{\mathbf{f}}_{k,j}^H \left( \sum_{(l,i)} \mathbf{H}_{k,l}^H q_{l,i} \widetilde{\mathbf{g}}_{l,i} \mathbf{g}_{l,i}^H \mathbf{H}_{k,l} \right) \widetilde{\mathbf{f}}_{k,j} \\ &\quad - 2\beta_{k,j} \mathbb{R} \{ \widetilde{\mathbf{f}}_{k,j}^H \mathbf{H}_{k,k}^H \widetilde{\mathbf{g}}_{k,j} \} + \beta_{k,j}^2 q_{k,j}^{-1} \eta_{k,j} + 1\end{aligned}\quad (2.42)$$

**Lemma 2.3.** (*MSE Duality*) For any MSE values achieved at the MIMO-IFC-GC with linear beamforming strategy  $(\{\widetilde{\mathbf{f}}\}, \{\widetilde{\mathbf{g}}\}, \mathbf{p})$  and under power constraint (2.23), the same MSE values can be achieved by linear beamforming strategy  $(\{\widetilde{\mathbf{g}}\}, \{\widetilde{\mathbf{f}}\}, \mathbf{q})$  at its dual MIMO-IFC-GC under the power constraint (2.24).

*Proof.* From Theorem 1, the same set of SINRs can be achieved by both the MIMO-IFC-GC system and its dual system. The achieved SINR for the  $j$ th data substream of the  $k$ th user is denoted by  $\gamma_{k,j}$ . Hence, using  $\text{SINR}_{k,j} = \gamma_{k,j}$  and  $\widehat{\text{SINR}}_{k,j} = \gamma_{k,j}$ , it can be easily verified that

$$\begin{aligned}\text{MSE}_{k,j} &= \widehat{\text{MSE}}_{k,j} = \frac{\beta_{k,j}^2}{\mathbf{D}_{k,j}^{k,j}} + \beta_{k,j}^2 \left| \widetilde{\mathbf{g}}_{k,j}^H \mathbf{H}_{k,k} \widetilde{\mathbf{f}}_{k,j} \right|^2 \\ &\quad - 2\beta_{k,j} \mathbb{R} \{ \widetilde{\mathbf{f}}_{k,j}^H \mathbf{H}_{k,k}^H \widetilde{\mathbf{g}}_{k,j} \}\end{aligned}\quad (2.43)$$

Hence, the same feasible MSE values are achieved at both links.  $\square$

**Corollary 2.1.** The power allocation required at the dual MIMO-IFC-GC to achieve the same MSE values obtained at the MIMO-IFC-GC is given by (2.36).

Although, we can obtain the duality for the interference channel with single linear power constraint, it is not valid for the case of multiple linear power constraints (To the best of our knowledge such duality concept does not exist). Therefore, to solve the joint linear precoding and equalization problem we must use another approach. In the following chapters we will discuss and propose efficient algorithm to find the solution to this problem. Note that due to the non-convex nature of the problem, only suboptimal solutions are available with reasonable complexity and strong performance.

## 2.5 Conclusions

In this chapter, we presented the channel model and cellular configuration first. Then, we proposed a model to study a CoMP system with partial cooperation, which is MIMO interference channel with generalized constraints. Then, we discussed the problem considered in this paper, which is (weighted) sum-rate maximization. This problem is in general non-convex. A common tool to study multiuser MIMO systems is the concept of uplink-downlink duality, where we extended it to the MIMO interference channel with single linear power constraint. However, based on our knowledge, this duality is not available for the MIMO-IFC with multiple linear power constraints. Therefore, this motivates finding suboptimal solutions for our problem with reasonable complexity and strong performance.

# Chapter 3

## Multi-cell Block Diagonalization

### 3.1 Motivation

As discussed in the previous chapters, the CoMP transmission/reception approach increases the number of transmit antennas used in transmission to each user and hence the capacity increases dramatically compared to conventional MIMO networks without coordination [51, 59, 92]. Moreover, inter-cell scheduled transmission benefits from the increased *multiuser diversity* gain [93]. Multiuser diversity comes from the fact that in a large wireless network where users are faded independently, it is highly probable that there exist a user with good channel condition at any time. The capacity region of network MIMO coordination as a MIMO BC has been previously established under sum power constraint [39,47,48,53,84] using uplink-downlink duality and under more realistic per-antenna/per-BS power constraints in [30, 49] using Lagrangian duality framework in convex optimization [50] to explore the capacity region. It is known that the capacity region is achievable with dirty paper coding (DPC). However, DPC is too complex for practical implementations. Consequently, due to their simplicity, linear precoding schemes such as multiuser zero-forcing (ZF) or *block diagonalization* (BD) are considered [64, 94].

In this chapter, we focus on the multi-cell multiuser ZF or multicell BD. Multicell BD is an extension of transmit zero-forcing technique in multi-antenna scenario (at both terminals). Moreover, we are particularly interested in per-antenna/per-BS power constraints (multiple linear power constraints)

and multiple antennas at the mobile terminals.

## 3.2 Introduction

The key idea of BD (multiuser ZF) is linear precoding of data in such a way that transmission for each user lies within the null space of other users' transmissions. Therefore, the interference to other users is eliminated. Multi-cell BD has been employed explicitly for network MIMO coordinated systems in [8, 65–67] with the diagonal structure of the precoders and the sum power constraint [64]. Although there were attempts in these works to optimize the precoders to satisfy per-base-station and per-antenna power constraints, this structure of the precoders is no longer optimal for such power constraints and must be revised [65, 68, 69]<sup>1</sup>. In [60], the ZF matrix is confined to the pseudo-inverse of the channel for the single receive antenna users with per-antenna power constraints. The sub-optimality of pseudo-inverse ZF beamforming subject to per-antenna power constraints was first shown in [65]. [68] presented the optimal precoders' structure using the concept of generalized inverses which lead to a non-convex optimization problem and the relaxed form requires semi-definite programming (SDP) [70]. This is investigated only for single-antenna mobile users. [69] also uses the generalized inverses for the single-antenna mobile users, but using a multistage optimization algorithms.

In this chapter, we aim to maximize the throughput of CoMP with partial cooperation (MIMO-IFC-GC) employing multiple antennas both at the BSs and the mobile users through optimization of precoders. Optimal form of BD is introduced by extending the search domain of precoding matrices to the entire null space of other users' transmissions [62]. Following this idea [95] has optimized the precoders by defining the problem with respect to the transmit covariance matrices. The throughput maximization problem in general is a non-convex problem. Therefore, [95] consider the transmit covariance matrix optimization problem and relax the rank constraint. Consequently, the problem

---

<sup>1</sup>We have discussed the optimality of BD using so-called water-filling algorithm under sum power constraint in Appendix B.

is simplified to a convex form and can be solved using SDP for example [68, 69, 95].

We have given a solution to this problem in [63], where the dual of throughput maximization problem is utilized to obtain a simple iterative gradient descent method [50] to find the optimal linear precoding matrices efficiently and globally. A more general approach is given in this chapter as we consider any number of data streams transmitted by each user and the optimization is performed over the precoding matrices rather than the transmit covariance matrices. Our approach is specifically adopted for our partial cooperative system (MIMO-IFC-GC).

The remainder of this chapter is organized as follows. In Section 3.3 the multi-cell BD scheme is studied and its comparison with the conventional BD is presented, which motivates research on optimal multi-cell BD under per-antenna power constraints. The optimal multi-cell BD scheme is proposed in Section 3.3.2. Comprehensive numerical results are presented in Section 3.5 following the discussion of the simulation setup in Section 3.4. Conclusions are given in Section 3.6.

### 3.3 Multi-cell Multiuser ZF

In this chapter, we follow the system model introduced in Chapter 2. Therefore, the received signal at the  $k$ th mobile user can be expressed as

$$\mathbf{y}_k = \mathbf{H}_{k,k}\mathbf{F}_k\mathbf{u}_k + \sum_{l \neq k} \mathbf{H}_{k,l}\mathbf{F}_l\mathbf{u}_l + \mathbf{n}_k, \quad (3.1)$$

where  $\mathbf{n}_k \sim \mathcal{CN}(\mathbf{0}, \mathbf{I})$  is the normalized AWGN, the data vectors are  $\mathbf{u}_k \in \mathbb{C}^{d_k}$  and the channel matrices are denoted by  $\mathbf{H}_{k,l} \in \mathbb{C}^{m_r,k \times m_t,l}$ .  $\mathbf{F}_k \in \mathbb{C}^{m_t,k \times d_k}$  denotes the precoding matrix.

To remove the intra-cluster interference, a linear zero-forcing technique will be employed in this chapter. When multiple antennas are employed at both terminals (BSs and mobile users) the multiuser zero-forcing is in the form of a technique called block diagonalization [64] rather than channel inversion. Assuming the downlink transmission setup described in Chapter 2, each user's

data  $\mathbf{u}_k$  is precoded with the matrix  $\mathbf{F}_k$ , such that

$$\mathbf{H}_{k,l}\mathbf{F}_l = 0 \quad \text{for all } l \neq k \quad \text{and} \quad 1 \leq k, l \leq K. \quad (3.2)$$

Hence the received signal for user  $k$  can be simplified to

$$\mathbf{y}_k = \mathbf{H}_{k,k}\mathbf{F}_k\mathbf{u}_k + \mathbf{n}_k. \quad (3.3)$$

Let  $\tilde{\mathbf{H}}_k = [\mathbf{H}_{1,k}^\top \cdots \mathbf{H}_{k-1,k}^\top \mathbf{H}_{k+1,k}^\top \cdots \mathbf{H}_{K,k}^\top]^\top$ . Zero-interference constraint in (3.2) forces  $\mathbf{F}_k$  to lie in the null space of  $\tilde{\mathbf{H}}_k$  which requires a dimension condition  $m_{t,k} \geq d_k + \sum_{l \neq k} m_{r,l}$  to be satisfied. This directly comes from the definition of null space in linear algebra [96]. We refer to this condition as *ZF feasibility condition*. Now, consider a multicell MIMO BC model where each BS in the cluster transmits to all the users within the cluster. Each of  $M$  BSs in the cluster is equipped with  $n_t$  transmit antennas and each user employs  $n_r$  antennas. The BSs transmit  $d_k = n_r$  data streams to each user. Consequently, the ZF feasibility condition will be simplified as  $Mn_t \geq Kn_r$ . Hence, the maximum number of users that can be served in a time slot is  $K = \lfloor \frac{Mn_t}{n_r} \rfloor$ . In our analysis, we focus on the number of  $K$  users where the ZF transmit precoding is feasible (following the ZF feasibility condition). These users are selected through a scheduling algorithm and assigned to one orthogonal dimension. The remaining unserved users are referred to other orthogonal dimensions or will be scheduled in other time slots. Assume that  $\tilde{\mathbf{H}}_k$  is a full rank matrix  $\text{rank}(\tilde{\mathbf{H}}_k) = \sum_{l \neq k} m_{r,l}$ , which holds with probability one due to the randomness of entries of channel matrices. We perform singular value decomposition (SVD)

$$\tilde{\mathbf{H}}_k = \mathbf{U}_k \mathbf{\Lambda}_k [\mathbf{\Upsilon}_k \mathbf{V}_k]^\mathbf{H} \quad (3.4)$$

where  $\mathbf{\Upsilon}_k$  holds the first  $\sum_{l \neq k} m_{r,l}$  right singular vectors corresponding to non-zero singular values, and  $\mathbf{V}_k \in \mathbb{C}^{m_{t,k} \times (m_{t,k} - \sum_{l \neq k} m_{r,l})}$  contains the last  $\tilde{m}_{r,k} = m_{t,k} - \sum_{l \neq k} m_{r,l}$  right singular vectors corresponding to zero singular values of  $\tilde{\mathbf{H}}_k$ . The orthonormality of  $\mathbf{V}_k$  means that  $\mathbf{V}_k^\mathbf{H} \mathbf{V}_k = \mathbf{I}_{\tilde{m}_{r,k}}$ . The columns of  $\mathbf{V}_k$  form a basis set in the null space of  $\tilde{\mathbf{H}}_k$ , and hence  $\mathbf{F}_k$  can be any linear combination of the columns of  $\mathbf{V}_k$ , i.e.

$$\mathbf{F}_k = \mathbf{V}_k \check{\mathbf{F}}_k, \quad k = 1, \dots, K \quad (3.5)$$

where  $\check{\mathbf{F}}_k \in \mathbb{C}^{\tilde{m}_{r,k} \times m_{r,k}}$  can be any arbitrary matrix subject to the specified power constraints [62]. Conventional BD scheme proposed in [64] assumes only linear combinations of a diagonal form to simplify it to a power allocation algorithm through water-filling. The conventional BD is optimal only when sum power constraint is applied [97], and it is not optimal under per-antenna (or any linear) power constraints [65, 68, 69].

### 3.3.1 Conventional BD

In *conventional BD* [64], the sum power constraint is applied to the throughput maximization problem and further simplified to a water-filling power allocation algorithm. In this scheme, the linear combination introduced in (3.5) is confined to have a form given by

$$\check{\mathbf{F}}_k^{\text{CBD}} = \tilde{\mathbf{V}}_k \mathbf{\Theta}_k^{\frac{1}{2}}, \quad k = 1, \dots, K \quad (3.6)$$

where  $\tilde{\mathbf{V}}_k \in \mathbb{C}^{\tilde{m}_{r,k} \times m_{r,k}}$  are the right singular vectors of  $\mathbf{H}_k \mathbf{V}_k$  corresponding to its non-zero singular values. Hence, the aggregate precoding matrix of the conventional scheme,  $\mathbf{F}_{\text{CBD}}$ , is defined as

$$\mathbf{F}_{\text{CBD}} = \begin{bmatrix} \mathbf{V}_1 \tilde{\mathbf{V}}_1 & \mathbf{V}_2 \tilde{\mathbf{V}}_2 & \cdots & \mathbf{V}_K \tilde{\mathbf{V}}_K \end{bmatrix} \mathbf{\Theta}^{\frac{1}{2}} \quad (3.7)$$

where  $\mathbf{\Theta} = \text{bdiag}[\mathbf{\Theta}_1, \dots, \mathbf{\Theta}_K]$  is a diagonal matrix whose elements scale the power transmitted into each of the columns of  $\mathbf{F}_{\text{CBD}}$ . The sum power constraint implies that

$$\sum_{k=1}^K \text{tr} \left\{ \mathbf{V}_k \tilde{\mathbf{V}}_k \mathbf{\Theta}_k \tilde{\mathbf{V}}_k^H \mathbf{V}_k^H \right\} = \sum_{k=1}^K \text{tr} \{ \mathbf{\Theta}_k \} \quad (3.8)$$

This simplifies the problem to an optimization over the diagonal terms of  $\mathbf{\Theta}_k$ . Consequently, this problem can be interpreted as a power allocation problem and solved by the well-known *water-filling* algorithm over the diagonal terms of  $\mathbf{\Theta}$  [64]. However, this form of BD cannot be extended as an optimal precoder to the case of per-antenna (or generalized linear) power constraints. Indeed, the generalized linear power constraints (which have per-antenna and per-BS power constraints embedded in them) can be written as

$$\sum_{k=1}^K \text{tr} \left\{ \Phi_{k,n} \mathbf{V}_k \tilde{\mathbf{V}}_k \mathbf{\Theta}_k \tilde{\mathbf{V}}_k^H \mathbf{V}_k^H \right\} \leq p_n, \quad n = 1, \dots, N \quad (3.9)$$

which is a function of all the elements of the matrices  $\Theta_k$  rather than the diagonal terms. Therefore, for the cases other than the case with a single sum power constraint, the selection of  $\Theta_k$ s as diagonal matrices reduces the search domain size of the optimization and hence does not lead to the optimal solution. In addition, computing  $\tilde{\mathbf{V}}_k$  adds  $K$  SVD operations to the precoding computation procedure (one for each served users). Therefore, the generalized linear power constraints (including per-antenna power constraints) do not allow the optimization to be reduced in form of water-filling algorithm. Previous work on BD with per-antenna (similarly with per-base-station) power constraints for a case of multiple-receive antennas employs this conventional BD and optimizes diagonal terms of  $\Theta$  [8, 65, 66]. Hence, they are not optimal indeed. The optimal form of BD proposed in this chapter includes the optimization over the entire null space of other users' channel matrices resulting in optimal precoders under generalized linear power constraints which can accommodate per-antenna or per-BS power constraints. Moreover, we address the general case where any number of data streams can be sent out for each user  $\forall d_k \leq n_r$ .

The numerical results in Fig. 3.1 compare maximized sum rate of a MIMO BC system with conventional BD [64] and the optimal scheme proposed later in this chapter. There are 12 transmit antennas at the base station and 2 receive antennas at each mobile user.  $M = 1$  is considered to specifically show the difference between the two BD schemes. Note that the conventional BD has a domain of  $\mathbb{R}_+^{Mn_t}$  while the optimal BD searches over all possible  $K$  symmetric (covariance) matrices and therefore has a larger domain of  $\mathbb{C}_{++}^{Km_{r,k}(m_{r,k}-1)/2}$  and grows when number of users per cell increases. As a consequence, the difference between these two schemes increases with the number of users per cell. Details of the simulation setup are given in Section 3.4. In the following section the optimal BD scheme is introduced and discussed in detail, and the algorithm to find the precoders is presented.

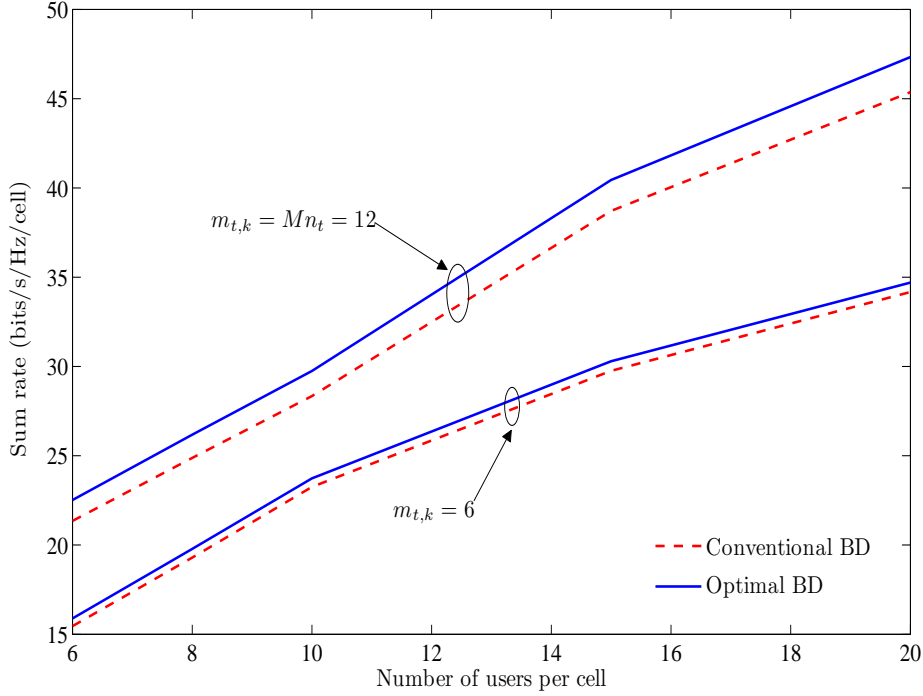


Figure 3.1: Comparison of sum rates for conventional BD vs. the proposed optimal BD for  $M = 1$ ,  $m_{t,k} = Mn_t = 6, 12$ ,  $d_k = n_r = 2$  using maximum sum rate scheduling.

### 3.3.2 Optimal Multi-Cell BD

The focus of this section is on the design of optimal multi-cell BD precoder matrices  $\mathbf{F}_k$  to maximize the throughput while the generalized linear power constraints are enforced (e.g. per-antenna/per-BS power constraints). In this scheme, we search over the entire null space of other users channel matrices ( $\tilde{\mathbf{H}}_k$ ), i.e.  $\check{\mathbf{F}}_k$  can be any arbitrary matrix of  $\mathbb{C}^{\tilde{m}_{r,k} \times m_{r,k}}$  subject to the power constraints.

Following the design of precoders according to (3.5), the received signal for user  $k$  can be expressed as

$$\mathbf{y}_k = \mathbf{H}_k \mathbf{V}_k \check{\mathbf{F}}_k \mathbf{u}_k + \mathbf{n}_k. \quad (3.10)$$

The rate of  $k$ th user is given by

$$R_k = \log \left| \mathbf{I} + \mathbf{H}_k \mathbf{V}_k \check{\mathbf{F}}_k \check{\mathbf{F}}_k^H \mathbf{V}_k^H \mathbf{H}_k^H \right| \quad (3.11)$$

$$= \log \left| \mathbf{I} + \check{\mathbf{F}}_k^H \mathbf{V}_k^H \mathbf{H}_k^H \mathbf{H}_k \mathbf{V}_k \check{\mathbf{F}}_k \right| \quad (3.12)$$

$$= \log \left| \mathbf{I} + \check{\mathbf{F}}_k^H \check{\mathbf{H}}_k \check{\mathbf{H}}_k^H \check{\mathbf{F}}_k \right|. \quad (3.13)$$

where we have used  $\log |\mathbf{I} + \mathbf{AB}| = \log |\mathbf{I} + \mathbf{BA}|$  and defined  $\check{\mathbf{H}}_k = \mathbf{H}_k \mathbf{V}_k$  to express the rate for user  $k$ . Therefore, sum rate maximization problem can be expressed as

$$\begin{aligned} & \underset{\check{\mathbf{F}}_k, \forall k}{\text{maximize}} && \sum_{k=1}^K \log \left| \mathbf{I} + \check{\mathbf{F}}_k^H \check{\mathbf{H}}_k \check{\mathbf{H}}_k^H \check{\mathbf{F}}_k \right| \\ & \text{subject to} && \sum_{k=1}^K \text{tr} \left\{ \check{\Phi}_{k,n} \mathbf{V}_k \check{\mathbf{F}}_k \check{\mathbf{F}}_k^H \mathbf{V}_k^H \right\} \leq p_n, \quad n = 1, \dots, N \end{aligned} \quad (3.14)$$

where the maximization is over all matrices  $\check{\mathbf{F}}_k \in \mathbb{C}^{\tilde{m}_{r,k} \times d_k}$ . The power constraints follow the MIMO-IFC-GC model described in Chapter 2. As discussed previously, proper selection of the weight matrices  $\check{\Phi}_{k,n}$  can accommodate the sum power, per-antenna, per-BS, or any linear power constraints.

*Remark 3.1.* Note that replacing  $\mathbf{S}_{\check{\mathbf{F}}_k} = \check{\mathbf{F}}_k \check{\mathbf{F}}_k^H$  in the rate definition (3.11), the throughput maximization problem can be reformulated with respect to the covariance matrices  $\mathbf{S}_{\check{\mathbf{F}}_k}$  as

$$\begin{aligned} & \underset{\mathbf{S}_{\check{\mathbf{F}}_k}, \forall k}{\text{maximize}} && \sum_{k=1}^K \log \left| \mathbf{I} + \check{\mathbf{H}}_k \mathbf{S}_{\check{\mathbf{F}}_k} \check{\mathbf{H}}_k^H \right| \\ & \text{subject to} && \sum_{k=1}^K \text{tr} \left\{ \check{\Phi}_{k,n} \mathbf{V}_k \mathbf{S}_{\check{\mathbf{F}}_k} \mathbf{V}_k^H \right\} \leq p_n, \quad n = 1, \dots, N \\ & && \mathbf{S}_{\check{\mathbf{F}}_k} \succeq \mathbf{0}, \\ & && \text{rank}(\mathbf{S}_{\check{\mathbf{F}}_k}) \leq d_k, \quad k = 1, \dots, K \end{aligned} \quad (3.15)$$

The rank constraint makes this problem non-convex. However, by relaxing this constraint then the problem is convex and can be categorized as a semi-definite program [70]. [95] solves this problem by using this relaxation and finding the solutions based on the convexity of this optimization problem. We instead address this optimization problem with respect to the precoders. Hence, we avoid the rank constraints but the non-convex form still holds due to the non-convex objective function.

**Theorem 3.1.** *If there exist the optimal solution  $\tilde{\mathbf{F}}_k, k = 1, \dots, K$  which together with a Lagrangian multiplier  $\tilde{\boldsymbol{\lambda}}$  that has at least  $m_{t,k} - \sum_{l \neq k} m_{r,k}$  non-zero components, satisfy the conditions*

$$\nabla_{\tilde{\mathbf{F}}_k} \mathcal{L} = \mathbf{0}, \quad k = 1, \dots, K \quad (3.16)$$

$$\sum_{k=1}^K \text{tr} \left\{ \mathbf{V}_k^H \Phi_{k,n} \mathbf{V}_k \tilde{\mathbf{F}}_k \tilde{\mathbf{F}}_k^H \right\} \leq p_n, \quad n = 1, \dots, N \quad (3.17)$$

of the problem (3.14), then the optimal BD precoder must have the following structure

$$\mathbf{F}_k^{\text{BD}\star} = \mathbf{V}_k \left[ \mathbf{V}_k^H \left( \sum_{n=1}^N \tilde{\lambda}_n \Phi_{k,n} \right) \mathbf{V}_k \right]^{-\frac{1}{2}} \tilde{\mathbf{U}}_k \tilde{\boldsymbol{\Sigma}}_k, \quad k = 1, \dots, K. \quad (3.18)$$

where  $\tilde{\mathbf{U}}_k$  is an orthonormal matrix containing the eigenvectors of the matrix  $\Phi_k(\tilde{\boldsymbol{\lambda}})^{-\frac{1}{2}} \check{\mathbf{H}}_k^H \check{\mathbf{H}}_k \Phi_k(\tilde{\boldsymbol{\lambda}})^{-\frac{1}{2}}$  with its  $d_k$  largest eigenvalues given by  $\gamma_{k,1} \geq \dots \geq \gamma_{k,d_k}$ .  $\tilde{\boldsymbol{\Sigma}}_k$  is a diagonal matrix with diagonal elements given by  $\tilde{\sigma}_{k,i} = \sqrt{\left[ 1 - \frac{1}{\gamma_{k,i}(\tilde{\boldsymbol{\lambda}})} \right]^+}$ ,  $i = 1, \dots, d_k, \forall k$ . We have used simplification  $\Phi_k(\tilde{\boldsymbol{\lambda}}) = \mathbf{V}_k^H \left( \sum_{n=1}^N \tilde{\lambda}_n \Phi_{k,n} \right) \mathbf{V}_k$  and the operator  $[\cdot]^+ = \max(\cdot, 0)$ .

*Proof.* The proof is given in Section 3.A. □

Inspired by this theorem, we propose an algorithm to find the optimal BD precoders. In order to find the optimal Lagrangian multipliers, we minimize the dual function with respect to  $\boldsymbol{\lambda} \succeq 0$ . This can be performed by sub-gradient update given by

$$\lambda_n^{(j)} = \lambda_n^{(j-1)} + \delta \left( p_n - \sum_{k=1}^K \text{tr} \left\{ \Phi_{k,n} \mathbf{F}_k \mathbf{F}_k^H \right\} \right) \quad (3.19)$$

so as to satisfy the power constraints. Therefore, the resulting algorithm has two loops; an outer loop which updates the auxiliary variable  $\boldsymbol{\lambda}$  using the sub-gradient update and the inner loop which finds the optimal BD precoder when  $\boldsymbol{\lambda}$  is fixed using the structure discussed in the above theorem. The details of this algorithm are given in Table 3.1

Table 3.1: BD precoder optimization algorithm

---

Find the right singular vectors of  $\tilde{\mathbf{H}}_k$ ,  $k = 1, \dots, K$  (i.e.  $\mathbf{V}_k$ ).  
Initialize  $\boldsymbol{\lambda} \succeq 0$   
**Repeat**  
Update  $\boldsymbol{\Phi}_k(\boldsymbol{\lambda}) = \mathbf{V}_k^H \left( \sum_{n=1}^N \lambda_n \boldsymbol{\Phi}_{k,n} \right) \mathbf{V}_k, \forall k$   
Find  $\check{\mathbf{H}}_k = \mathbf{H}_k \mathbf{V}_k, \forall k$   
Find the  $d_k$  largest eigenvalues and corresponding eigenvectors  
of the matrix  $\boldsymbol{\Phi}_k(\boldsymbol{\lambda})^{-\frac{1}{2}} \check{\mathbf{H}}_k^H \check{\mathbf{H}}_k \boldsymbol{\Phi}_k(\boldsymbol{\lambda})^{-\frac{1}{2}}$  (i.e.  $\gamma_{k,i} \geq \dots \geq \gamma_{k,d_k}$  and  $\mathbf{U}_k, \forall k$ ).  
Update  $\sigma_{k,i} = \sqrt{\left[ 1 - \frac{1}{\gamma_{k,i}(\boldsymbol{\lambda})} \right]^+}$ ,  $i = 1, \dots, d_k, \forall k$ .  
Establish the optimal BD precoder as  
 $\mathbf{F}_k(\boldsymbol{\lambda}) = \mathbf{V}_k \boldsymbol{\Phi}_k(\boldsymbol{\lambda})^{-\frac{1}{2}} \mathbf{U}_k \boldsymbol{\Sigma}_k, k = 1, \dots, K$ .  
Update  $\lambda_n \leftarrow \lambda_n + \delta \left( p_n - \sum_{k=1}^K \text{tr} \{ \boldsymbol{\Phi}_{k,n} \mathbf{F}_k(\boldsymbol{\lambda}) \mathbf{F}_k(\boldsymbol{\lambda})^H \} \right)$   
**Until**  $\sum_n \left| \lambda_n \left( p_n - \sum_{k=1}^K \text{tr} \{ \boldsymbol{\Phi}_{k,n} \mathbf{F}_k(\boldsymbol{\lambda}) \mathbf{F}_k(\boldsymbol{\lambda})^H \} \right) \right| \leq \epsilon_0$

---

### 3.4 Simulation Setup

The propagation model between each base station's transmit antenna and mobile user's receive antenna includes three factors: a path loss component proportional to  $d_{kb}^{-\beta}$  (where  $d_{k,m}$  denotes distance from BS  $m$  to the mobile user  $k$  and  $\beta = 3.8$  is the path loss exponent), and two random components representing lognormal shadow fading and Rayleigh fading. The channel gain between transmit antenna  $t$  of the base station  $m$  and receive antenna  $r$  of the  $k$ th user is given by

$$[\mathbf{H}_{k,m}]_{(r,t)} = \alpha_{k,m}^{(r,t)} \sqrt{\rho_{k,m} \left( \frac{d_{k,m}}{d_0} \right)^{-\beta}} \Gamma \quad (3.20)$$

where  $[\mathbf{H}_{k,m}]_{(r,t)}$  is the  $(r, t)$  element of the channel matrix  $\mathbf{H}_{k,m} \in \mathbb{C}^{n_r \times n_t}$  from the base station  $m$  to the mobile user  $k$ ,  $\alpha_{k,m}^{(r,t)} \sim \mathcal{CN}(0, 1)$  represents independent Rayleigh fading,  $d_0 = 1$  km is the cell radius, and  $\rho_{k,m} = 10^{\rho_{k,m}^{(\text{dBm})}/10}$  is the lognormal shadow fading variable between  $m$ th base station and  $k$ th user, where  $\rho_{k,m}^{(\text{dBm})} \sim \mathcal{CN}(0, \sigma_\rho)$  and  $\sigma_\rho = 8$  dB is its standard deviation. A reference SNR,  $\Gamma = 20$  dB is a typical value of the interference-

free SNR at the cell boundary (as in [59] and [9]).

Our cellular network setup involves clustering. Since global coordination is not feasible, clustering with cluster sizes of up to  $M = 7$  is considered. The cellular network layout is shown in Fig. 3.2. A base station is located at the center of each hexagonal cell. Each base station is equipped with  $n_t$  transmit antennas. There are  $n_r$  receive antennas on each mobile user and there are  $K$  users per cell per subband. All  $m_{t,k} = Mn_t$  base stations' transmit antennas in each cluster are coordinated to transmit to each user. Hence, a MIMO BC model is evolved. In Fig. 3.2 the clusters of sizes 3 and 7 are shown. For cluster size 7, one wrap-around layer of clusters is considered to contribute inter-cluster interference, while for  $M = 3$  two tiers of interfering cells are accounted for. User locations are generated randomly, uniformly and independently in each cell. For each drop of users (random realization of the user distribution), the distance of users from base stations in the network is computed and path loss, lognormal and Rayleigh fading are included in the channel gain calculations. To compare the results all the sum rates achieved through network MIMO coordination are normalized by the size of clusters  $M$ . Base stations causing inter-cluster interference are assumed to transmit at full power, which is the worst case scenario.

### 3.4.1 User Selection

As discussed in the previous sections, transmit ZF precoding has limitations on the number of users that can be served simultaneously. To obtain multiuser diversity a user selection procedure is applied prior to precoding. Generally, total number of receive antennas must be less than or equal to the total number of transmit antennas<sup>2</sup>. In this chapter, we employ two types of user selection criteria; maximum sum rate scheduling and proportionally-fair criteria with the updated weights for the rate of each user as in [98–100]. In the following discussion, first we briefly review these two scheduling methods. Then, we review greedy user selection algorithm and propose the extension of a semi-

---

<sup>2</sup>Selection of maximum number of users does not achieve maximum throughput necessarily.

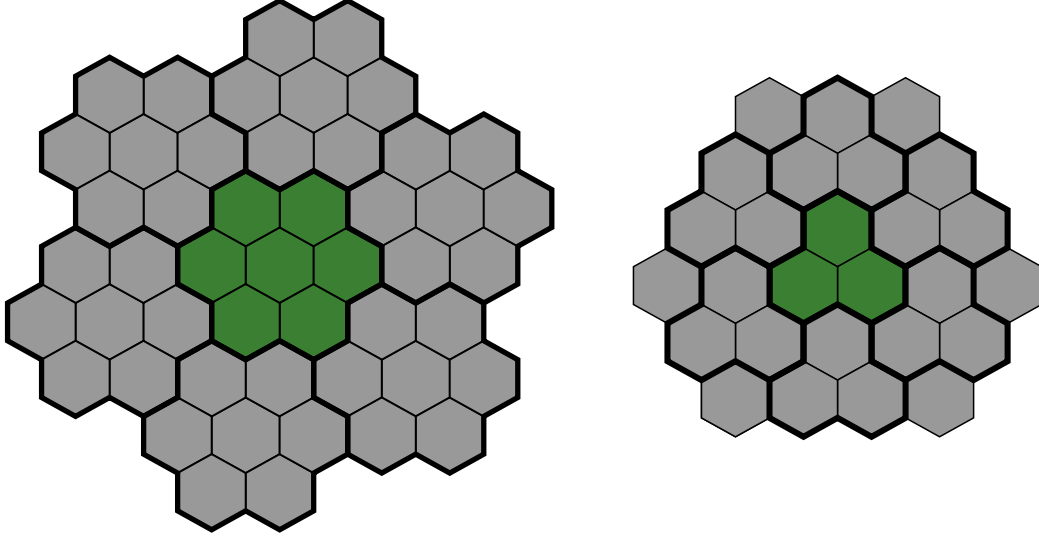


Figure 3.2: The cellular layout of  $M = 3$  and  $M = 7$  clustered network MIMO joint processing. The borders of clusters are bold. Green colored cells represent the analyzed center cluster and the grey cells are causing inter-cell interference. For  $M = 7$ , one tier of interfering clusters is considered, while for  $M = 3$  two tiers of interfering cells are accounted for.

orthogonal user selection algorithm [101] to the multiple-antenna user case.

Assume that set of all users are denoted as  $\mathcal{U}$ . In general, the user selection criteria is to maximize a weighted sum rate of the system as

$$\hat{\mathcal{U}} = \underset{\tilde{\mathcal{U}} \subseteq \mathcal{U}}{\operatorname{argmax}} \sum_{k \in \tilde{\mathcal{U}}} \mu_k R_k \quad (3.21)$$

where  $\mu_k$  are selected based on the scheduling procedure and  $K_{\max}$  is the maximum number of users that can be served simultaneously. The optimal solution for this maximization problem can be obtained through exhaustive search. However, the exhaustive search requires searching over all subsets of  $\mathcal{U}$  with the size less than or equal  $K_{\max}$ . The complexity of the exhaustive search is even higher in the multicell network MIMO scenario with large number of users and transmit antennas. Alternatively, there are other approaches such as greedy, genetic, and semi-orthogonal user selection algorithms [80,99,101–104]. The greedy user selection algorithm has been investigated in [103] and further extended in [99,104]. In this algorithm, in each step a user is selected which maximizes the increase in the (weighted) sum rate. When adding any user does not increase the (weighted) sum rate of the system the user selection

algorithm will be terminated. Most common criterion to select the users is the weighted sum rate with the weights selected based on proportional fair schedule or maximized sum rate schedule. In the former, in each scheduling interval  $t$ , greedy algorithm picks the user  $\hat{k}$  which maximizes the increase in the weighted sum rate

$$\sum_{k \in \hat{\mathcal{U}} \cap \hat{k}} \mu_k(t) R_k(t) \quad (3.22)$$

where  $\mu_k(t)$  and  $R_k(t)$  are respectively the rate weight and the supported rate during  $t$ th scheduling interval for the  $k$ th user. The weights are defined as  $\mu_k(t) = 1/\bar{R}_k(t)$  where  $\bar{R}_k(t)$  is the average throughput that is achieved by user  $k$  up to time  $t$ , which is updated as in [105]

$$\bar{R}_k(t+1) = \left(1 - \frac{1}{\tau}\right) \bar{R}_k(t) + \frac{1}{\tau} R_k(t) \quad (3.23)$$

where  $R_k(t)$  is equal to zero when the user  $k$  is not scheduled in the  $t$ th time interval.  $\tau$  is the sliding window width where the throughput of user  $k$  is monitored and the priority weights  $\mu_k(t)$  is updated according the users achieved rate in that interval. In our simulations for proportional fair scheduling algorithm  $\tau = 10$  is considered. The user selection algorithm based on maximum sum rate criterion is when  $\mu_k = 1, k = 1, \dots, K$  are selected.

## 3.5 Numerical Results

In this section, the performance results (obtained via Monte Carlo simulations) of the proposed optimal BD scheme in a network MIMO coordinated system are discussed. The network MIMO coordination exhibits several system advantages, which are exposed in the following.

### 3.5.1 Network MIMO Gains

While the universal network MIMO coordination is practically impossible, clustering is a practical scheme, which also benefits the network MIMO coordination gains and reduces the amount of feedback required at the base stations [8, 9]. The size of clusters,  $M$ , is a parameter in network MIMO coordination.  $M = 1$  means no coordination with optimal BD scheme applied.

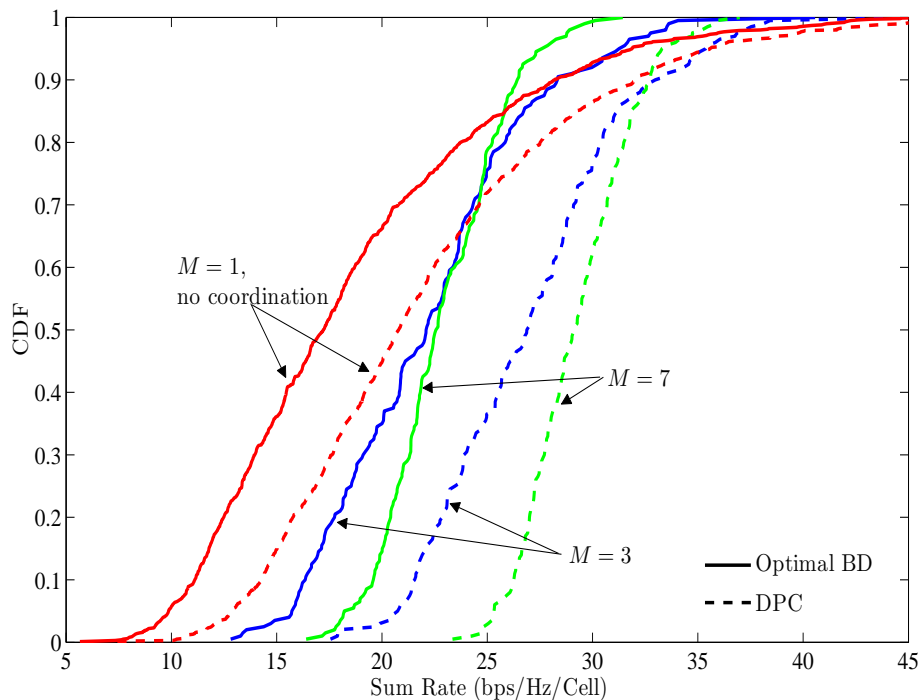


Figure 3.3: CDF of sum rate with different cluster sizes  $M = 1, 3, 7$ ,  $n_t = 4$ ,  $n_r = 2$  and 10 users per cell (network MIMO joint processing).

Fig. 3.3 shows that with increasing cluster size throughput of the system increases. System throughput is computed using MSR scheduling and averaged over several channel realizations for a large number of user locations generated randomly. The normalized throughput for different cluster sizes is compared, which means that the total throughput in each cluster is divided by the number of cells in each cluster  $M$ . The normalized sum rate has lower variance in larger clusters, which shows that the performance of the system is less dependent on the position of users and that network MIMO coordination brings more stability to the system.

### 3.5.2 Multiple-Antenna Gains

The inter-cell interference mitigation through coordination of base stations enables the cellular network to enjoy the great spectral efficiency improvement associated with employing multiple antennas. Fig. 3.4 shows the linear growth

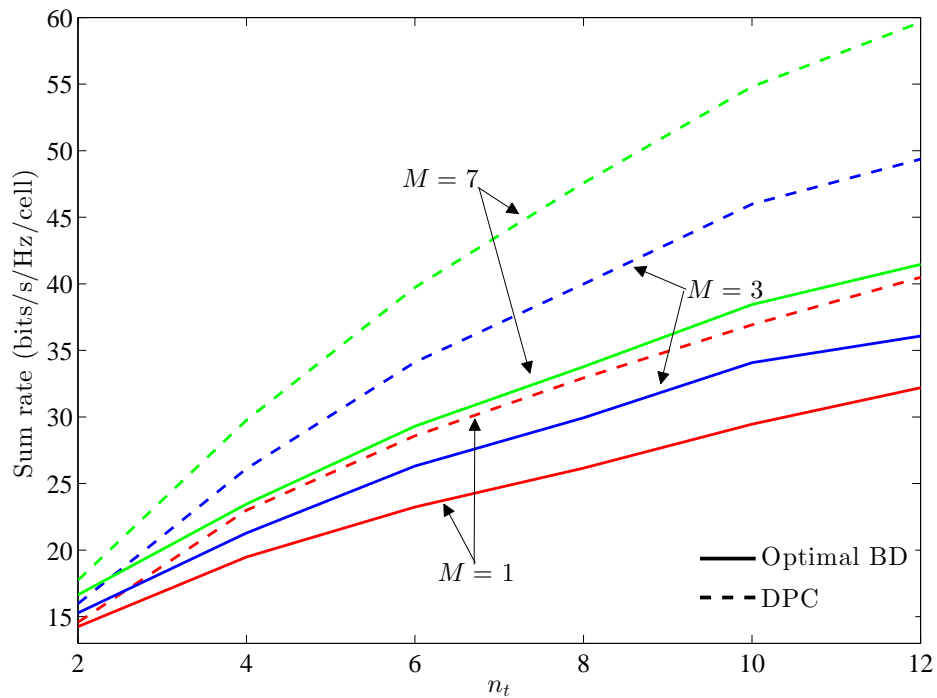


Figure 3.4: Sum-rate increase with the number of antennas per base station.  $n_r = 2$ .

of the maximum throughput achievable through the proposed optimal multi-cell BD and the capacity limits of DPC [30]. The number of receive antennas at each mobile user is fixed to  $n_r = 2$  and the number of transmit antennas  $n_t$  at each base station is increasing. When the cluster size grows, the slope of spectral efficiency also increases. The maximum power on each transmit antenna is normalized such that total power at each base station for different  $n_t$  is constant.

### 3.5.3 Multiuser Diversity

Multi-cell coordination benefits from increased multiuser diversity, since the number of users scheduled at each time interval is  $B$  times of that without coordination. In Fig. 3.5, the multiuser diversity gain of network MIMO is shown with up to 10 users per cell. The MSR scheduling is applied for each drop of users and averaged over several channel realizations.

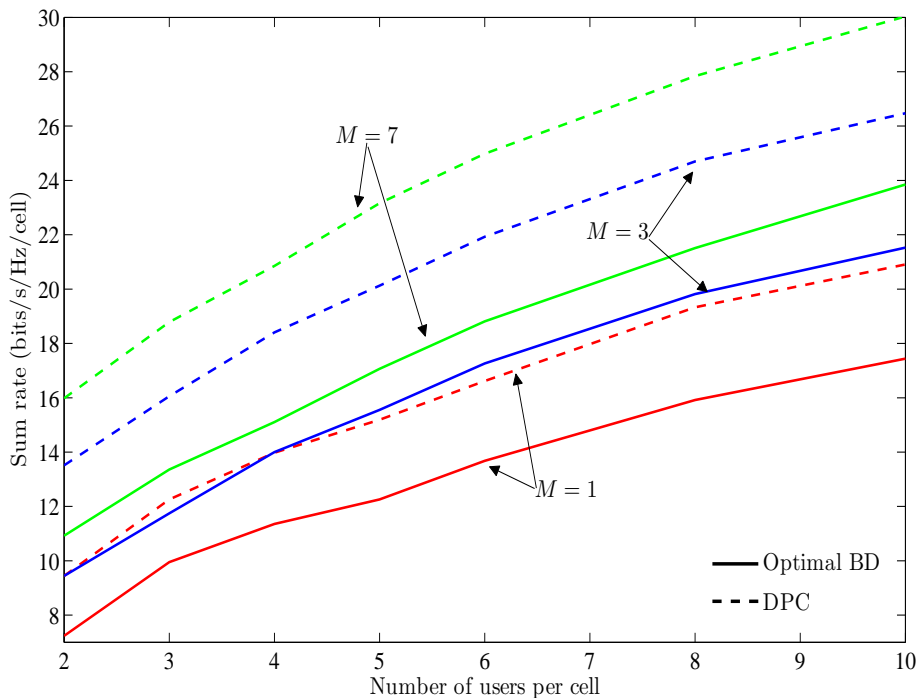


Figure 3.5: Sum rate per cell achieved with the proposed optimal BD and the capacity limits of DPC for cluster sizes  $M = 1, 3, 7$ ;  $n_t = 4$ ,  $n_r = 2$ .

### 3.5.4 Fairness Advantages

One of the main purposes of network MIMO coordination is that the cell-edge users gain from neighboring base stations signals. In Fig. 3.6, the cumulative distribution functions (CDFs) of mean rates for users are shown and compared for  $M = 1$  (i.e. beamforming without coordination) and  $M = 3, 7$  for the proposed optimal BD scheme. There are 10 users per cell randomly and uniformly dropped in the network for each simulation. For each drop of users, the proportionally fair scheduling algorithm is applied over hundreds of scheduling time intervals using sliding window width  $\tau = 10$  time slots (see [47]). Each user's rates achieved in all time intervals are averaged to find the mean rates per user and their CDF for several user locations is plotted. As shown by the plots, for  $M = 3$  and  $M = 7$  network MIMO coordination nearly 70% and 80% users have mean rate larger than 1 bps/Hz, respectively, while for the scheme without coordination it is 45% of users. However, fairness among

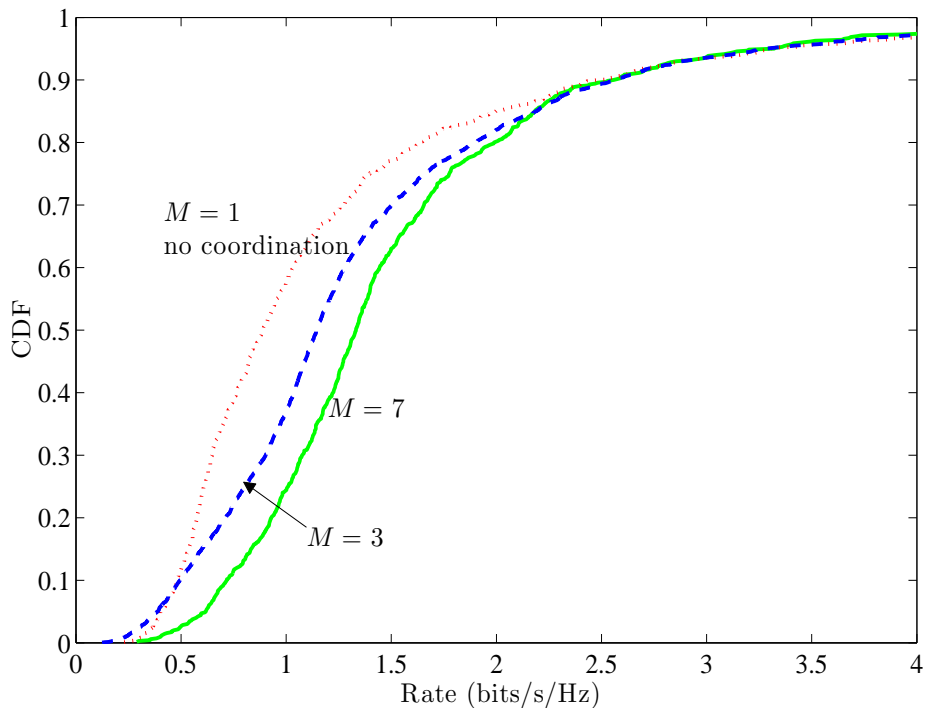


Figure 3.6: CDF of the mean rates in the clusters of sizes  $M = 3, 7$  and comparison with  $M = 1$  (no coordination) using the proposed optimal BD.

users does not seem to be improved when cluster size increases. This is due to the existence of larger number of cell-edge users when cluster size increases (the area that cell-edge users are located in the network grows quadratically with the radius of the cluster).

### 3.5.5 Convergence

Convergence of the gradient descent method proposed in Section 3.3.2 is illustrated in Fig. 3.7. The normalized sum rates obtained after each iteration with respect to the optimal target values versus the number of iterations are depicted. The convergence behavior of the algorithm for 20 independent and randomly generated user location sets is shown, and their channel realizations are tested with the proposed iterative algorithm and the values of sum rate after each iteration divided by the target value are monitored. Nearly all of the optimizations converge to the target value within only 10 first iterations

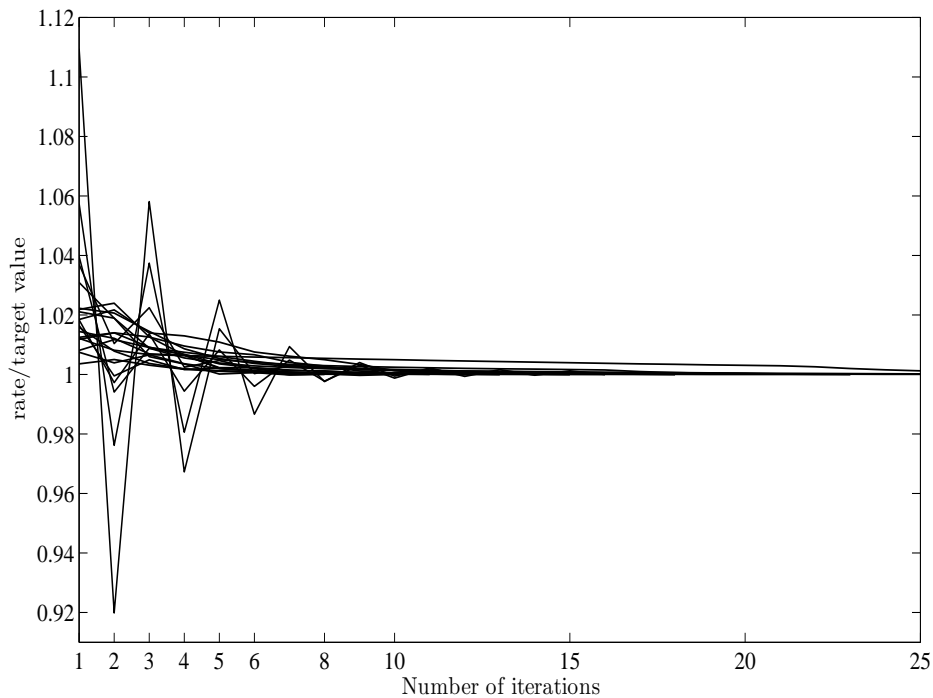


Figure 3.7: Convergence of the gradient descent method for the proposed optimal BD for  $M = 3$ ,  $n_t = 4$ ,  $n_r = 2$ , and 8 users per cell.

with 1% error.

### 3.6 Conclusions

In this chapter, a multi-cell coordinated downlink MIMO transmission has been considered under individual (per-antenna/per-BS) power constraints. Sub-optimality of the conventional block diagonalization (BD) has been discussed and it has motivated the search for the optimal BD scheme. The optimal BD scheme for network MIMO coordinated system under individual power constraints has been proposed in this chapter. As a result, a simple iterative algorithm has been proposed to obtain the optimal precoders for multi-cell BD. The comprehensive simulation results have demonstrated advantages achieved by using multi-cell coordinated transmission under more practical individual power constraints.

### 3.A Proof of Theorem 3.1

First note that the maximum of the objective function of the problem (3.14) is attained when  $\mathbf{I} + \check{\mathbf{F}}_k^H \check{\mathbf{H}}_k^H \check{\mathbf{H}}_k \check{\mathbf{F}}_k$  is diagonal. To prove this, we assume that the maximum is reached at  $\check{\mathbf{F}}_k^*$ . Then, one can always find a unitary matrix  $\mathbf{\Pi}_k \in \mathbb{C}^{d_k \times d_k}$  such that the matrix  $\bar{\mathbf{F}}_k = \check{\mathbf{F}}_k^* \mathbf{\Pi}_k$  diagonalizes

$$\mathbf{I} + \bar{\mathbf{F}}_k^H \check{\mathbf{H}}_k^H \check{\mathbf{H}}_k \bar{\mathbf{F}}_k = \mathbf{\Pi}_k^H \left( \mathbf{I} + \check{\mathbf{F}}_k^H \check{\mathbf{H}}_k^H \check{\mathbf{H}}_k \check{\mathbf{F}}_k \right) \mathbf{\Pi}_k. \quad (3.24)$$

Nevertheless, the value of the objective function is still fixed due to the unitary structure of  $\mathbf{\Pi}_k$ s. Moreover, the power constraints are also unchanged due to the fact that  $\bar{\mathbf{F}}_k \bar{\mathbf{F}}_k^H = \check{\mathbf{F}}_k^* \check{\mathbf{F}}_k^{*H}$ . This proves our claim.

Although, the optimization problem (3.14) is non-convex we can use the Karush-Kuhn-Tucker (KKT) conditions as the necessary conditions of this problem. The Lagrangian function of this problem can be formed as

$$\begin{aligned} \mathcal{L}(\check{\mathbf{F}}_k, \boldsymbol{\lambda}) = & - \sum_{k=1}^K \log \left| \mathbf{I} + \check{\mathbf{F}}_k^H \check{\mathbf{H}}_k^H \check{\mathbf{H}}_k \check{\mathbf{F}}_k \right| \\ & + \sum_{k=1}^K \text{tr} \left\{ \mathbf{V}_k^H \left( \sum_{n=1}^N \lambda_n \boldsymbol{\Phi}_{k,n} \right) \mathbf{V}_k \check{\mathbf{F}}_k \check{\mathbf{F}}_k^H \right\} - \sum_{n=1}^N \lambda_n p_n \end{aligned} \quad (3.25)$$

Thus, there exist a Lagrange multiplier vector  $\tilde{\boldsymbol{\lambda}} = (\tilde{\lambda}_1, \dots, \tilde{\lambda}_N)$  such that together with  $\tilde{\mathbf{F}}_k, k = 1, \dots, K$  satisfies the KKT conditions of the problem (3.14). The zero gradient condition can be expressed as

$$\begin{aligned} \nabla_{\tilde{\mathbf{F}}_k} \mathcal{L} = & - \check{\mathbf{H}}_k^H \check{\mathbf{H}}_k \tilde{\mathbf{F}}_k \left( \mathbf{I} + \tilde{\mathbf{F}}_k^H \check{\mathbf{H}}_k^H \check{\mathbf{H}}_k \tilde{\mathbf{F}}_k \right)^{-1} \\ & + \mathbf{V}_k^H \left( \sum_{n=1}^N \tilde{\lambda}_n \boldsymbol{\Phi}_{k,n} \right) \mathbf{V}_k \tilde{\mathbf{F}}_k = \mathbf{0}, \quad k = 1, \dots, K \end{aligned} \quad (3.26)$$

Now, we know that  $\mathbf{I} + \tilde{\mathbf{F}}_k^H \check{\mathbf{H}}_k^H \check{\mathbf{H}}_k \tilde{\mathbf{F}}_k$  and consequently  $\tilde{\mathbf{F}}_k^H \check{\mathbf{H}}_k^H \check{\mathbf{H}}_k \tilde{\mathbf{F}}_k$  are diagonal matrices. Pre-multiplying (3.26) by  $\tilde{\mathbf{F}}_k^H$ , we obtain

$$\tilde{\mathbf{F}}_k^H \check{\mathbf{H}}_k^H \check{\mathbf{H}}_k \tilde{\mathbf{F}}_k \left( \mathbf{I} + \tilde{\mathbf{F}}_k^H \check{\mathbf{H}}_k^H \check{\mathbf{H}}_k \tilde{\mathbf{F}}_k \right)^{-1} = \tilde{\mathbf{F}}_k^H \mathbf{V}_k^H \left( \sum_{n=1}^N \tilde{\lambda}_n \boldsymbol{\Phi}_{k,n} \right) \mathbf{V}_k \tilde{\mathbf{F}}_k \quad (3.27)$$

where has the left-side in a diagonal form. Therefore, the right side of this equation must be also in a diagonal form. For simplicity, we introduce  $\boldsymbol{\Phi}_k(\tilde{\boldsymbol{\lambda}}) =$

$\mathbf{V}_k^H \left( \sum_{n=1}^N \tilde{\lambda}_n \Phi_{k,n} \right) \mathbf{V}_k$ . If at least there are  $\tilde{m}_{r,k}$  non-zero  $\tilde{\lambda}_n, \forall n$ , then  $\Phi_k(\tilde{\lambda})$  is a non-singular matrix. This can be easily verified due to the structure of  $\Phi_{k,n}$ . Consequently, we can write  $\tilde{\mathbf{F}}_k^H \Phi_k(\tilde{\lambda}) \tilde{\mathbf{F}}_k = \mathbf{D}_k$  where  $\mathbf{D}_k \in \mathbb{C}^{d_k \times d_k}$  diagonal matrix. Hence, we can write

$$\Phi_k(\tilde{\lambda})^{\frac{1}{2}} \tilde{\mathbf{F}}_k = \tilde{\mathbf{U}}_k \tilde{\Sigma}_k, \quad k = 1, \dots, K \quad (3.28)$$

where  $\tilde{\mathbf{U}}_k \in \mathbb{C}^{m_{i,k} \times d_k}$  is an orthonormal matrix (i.e.  $\tilde{\mathbf{U}}_k^H \tilde{\mathbf{U}}_k = \mathbf{I}$ ) and  $\tilde{\Sigma}_k$  is a  $d_k \times d_k$  diagonal matrix with the real diagonal terms  $\tilde{\sigma}_{k,i} \geq 0$ . Therefore, we can write

$$\tilde{\mathbf{F}}_k = \Phi_k(\tilde{\lambda})^{-\frac{1}{2}} \tilde{\mathbf{U}}_k \tilde{\Sigma}_k, \quad k = 1, \dots, K \quad (3.29)$$

Replacing this structure, we have

$$\tilde{\mathbf{F}}_k^H \check{\mathbf{H}}_k^H \check{\mathbf{H}}_k \tilde{\mathbf{F}}_k = \tilde{\Sigma}_k^H \tilde{\mathbf{U}}_k^H \Phi_k(\tilde{\lambda})^{-\frac{1}{2}} \check{\mathbf{H}}_k^H \check{\mathbf{H}}_k \Phi_k(\tilde{\lambda})^{-\frac{1}{2}} \tilde{\mathbf{U}}_k \tilde{\Sigma}_k = \mathbf{D}_k \quad (3.30)$$

and consequently the orthonormal matrix  $\tilde{\mathbf{U}}_k$  must contain the eigenvectors of  $\Phi_k(\tilde{\lambda})^{-\frac{1}{2}} \check{\mathbf{H}}_k^H \check{\mathbf{H}}_k \Phi_k(\tilde{\lambda})^{-\frac{1}{2}}$ . Consequently,  $\mathbf{D}_k = \tilde{\Sigma}_k^H \tilde{\Gamma}_k(\tilde{\lambda}) \tilde{\Sigma}_k$ . Now, plugging (3.30) into (3.27), we obtain

$$\tilde{\Sigma}_k^H \tilde{\Gamma}_k(\tilde{\lambda}) \tilde{\Sigma}_k \left( \mathbf{I} + \tilde{\Sigma}_k^H \tilde{\Gamma}_k(\tilde{\lambda}) \tilde{\Sigma}_k \right)^{-1} = \tilde{\Sigma}_k^H \tilde{\Sigma}_k, \quad k = 1, \dots, K \quad (3.31)$$

This can be simplified in a scalar form as

$$\gamma_{k,i}(\tilde{\lambda}) = \left( 1 + \tilde{\sigma}_{k,i}^2 \gamma_{k,i}(\tilde{\lambda}) \right). \quad (3.32)$$

Therefore, the diagonal terms of  $\tilde{\Sigma}_k$  are given by

$$\tilde{\sigma}_{k,i} = \sqrt{\left[ 1 - \frac{1}{\gamma_{k,i}(\tilde{\lambda})} \right]^+}, \quad k = 1, \dots, K, \quad i = 1, \dots, d_k \quad (3.33)$$

Consequently, structure given by (3.18) evolves for the optimal precoders.

# Chapter 4

## MMSE Precoding and Equalization

In this chapter, we focus on the optimization of linear precoding strategies at the BSs and equalization at the users for network MIMO with partial cooperation. We consider the model introduced in Chapter 2, MIMO Interference channel with generalized constraints, when individual power constraints at the BSs are enforced. We also account constraints on the number of streams per user. Our optimization approach is based on minimization of weighted sum of mean square error values of the estimated data vector. Therefore, the proposed algorithms in this chapter can be categorized as MMSE precoding and equalization.

We focus on the sum-rate maximization (SRM) and on the minimization of weighted sum-MSE (WSMSE) under per-BS power constraints and constraints on the number of streams per user. Moreover, although non-linear processing techniques such as vector precoding [106,107] may generally be useful, we focus on more practical linear processing techniques. Both the SRM and WSMSE minimization (WSMMSE) problems are non-convex [50], and thus suboptimal design strategies of reasonable complexity are called for.

The contributions of this chapter are as follows:

- (i) We review the available suboptimal techniques that have been proposed for the SRM problem [46,56,71] and extend them to the MIMO-IFC-GC scenario where necessary in Sec. 4.2. Since these techniques are generally unable to enforce constraints on the number of streams, we also review

and generalize techniques that are based on the idea of interference alignment [44] and are able to impose such constraints;

- (ii) Then, we propose two novel suboptimal solutions for the WSMMSE problem in Sec. 4.3 under arbitrary constraints on the number of streams. It is noted that the WSMMSE problem without such constraints would be trivial, as it would result in zero MMSE and no stream transmitted. The proposed solutions are based on a novel insight into the single-user MMSE problem with multiple linear constraints, which is discussed in Sec. 4.3.2;
- (iii) Finally, extensive numerical simulations are provided in Sec. 4.4 to compare performance of the proposed schemes in realistic cellular systems.

In this chapter, we include linear processing at the BSs and at the users. The system model and preliminaries has been reviewed in 2.2.1.

## 4.1 Problem Definition and Preliminaries

In this chapter, we consider the optimization of the sum of some specific functions  $f_k(\mathbf{E}_k)$  of the MSE-matrices  $\mathbf{E}_k$  of all users  $k = 1, \dots, K$  for the MIMO-IFC-GC. Specifically, we address the following constrained optimization problem

$$\begin{aligned} & \underset{\mathbf{F}_k, \mathbf{G}_k, \forall k}{\text{minimize}} && \sum_{k=1}^K f_k(\mathbf{E}_k) \\ & \text{subject to} && \sum_{k=1}^K \text{tr} \{ \Phi_{k,m} \mathbf{F}_k \mathbf{F}_k^H \} \leq P_m, m = 1, \dots, M, \end{aligned} \quad (4.1)$$

where the optimization is over all transmit beamforming matrices  $\mathbf{F}_k$  and equalization matrices  $\mathbf{G}_k$ . Specifically, we focus on the *weighted sum-MSE functions* (WSMSE)

$$f_k(\mathbf{E}_k) = \text{tr} \{ \mathbf{W}_k \mathbf{E}_k \} = \sum_{j=1}^{d_k} w_{kj} \text{MSE}_{kj} \quad (4.2)$$

with given diagonal weight matrices  $\mathbf{W}_k \in \mathbb{C}^{d_k \times d_k}$  where the main diagonal of  $\mathbf{W}_k$  is given by  $[w_{k,1}, \dots, w_{k,d_k}]$  with non-negative weights  $w_{kj} \geq 0$ . With cost function (4.2), we refer to the problem (4.1) as the *weighted sum-MSE* minimization (*WSMMSE*) problem.

Of more direct interest for communications systems is the maximization of the sum-rate. This is obtained from (4.1) by selecting the *sum-rate (SR) functions*

$$f_k(\mathbf{E}_k) = \log |\mathbf{E}_k|. \quad (4.3)$$

With cost function (4.3), problem (4.1) is referred to as the *sum-rate maximization* (SRM) problem. In fact, from information-theoretic considerations, it can be seen that (4.3) is the maximum achievable rate (in bits per channel use) for the  $k$ th user where the signals of the other users are treated as noise (see, e.g., [83]).

*Remark 4.1.* Consider an iterative algorithm where at each iteration a WSMMSE problem is solved with the weight matrices  $\mathbf{W}_k$  assumed to be non-diagonal and selected based on the previous MSE-matrix  $\mathbf{E}_k$ . This algorithm can approximate the solution of (4.1) for any general cost function  $f_k(\mathbf{E}_k)$ . This was first pointed out in [108] for the weighted SRM problem in a MIMO BC, then in [72] for the single-antenna interference channel and a general utility function, and has been generalized to a MIMO (broadcast) interference channel in [109] with conventional power constraints. It is not difficult to see that this result extends also to the MIMO-IFC-GC, which is not subsumed in the model of [109] due to the generalized linear constraints. We explicitly state this conclusion below.

**Lemma 4.1.** [109] *For strictly concave utility functions  $f_k(\cdot)$  for all  $k$ , the global optimal solution of problem (4.1) and the solution of*

$$\begin{aligned} & \underset{\mathbf{F}_k, \mathbf{G}_k, \mathbf{W}_k, \forall k}{\text{minimize}} && \sum_{k=1}^K \{ \text{tr} \{ \mathbf{W}_k \mathbf{E}_k \} - \text{tr} \{ \mathbf{W}_k g_k(\mathbf{W}_k) \} \\ & && + f_k(g_k(\mathbf{W}_k)) \} \\ & \text{subject to} && \sum_{k=1}^K \text{tr} \{ \Phi_{k,m} \mathbf{F}_k \mathbf{F}_k^H \} \leq P_m, m = 1, \dots, M, \end{aligned} \quad (4.4)$$

where  $g_k(\cdot)$  is the inverse function of the  $\nabla f_k(\cdot)$ , are the same.

Consequently, in order to find an approximate solution of (4.1), at each step matrices  $\mathbf{W}_k$  for  $k = 1, \dots, K$  are updated by solving (4.4) with respect to  $\mathbf{W}_k$  only (i.e., we keep  $(\mathbf{G}_k, \mathbf{F}_k), \forall k$  unchanged in this step). Then, using the obtained matrices  $\mathbf{W}_k$ , for  $k = 1, \dots, K$ , the problem (4.4) reduces to a WSM MSE problem with respect to matrices  $\mathbf{G}_k$  and  $\mathbf{F}_k$  for  $k = 1, \dots, K$  (i.e., matrices  $\mathbf{W}_k$  are kept fixed). This results in the iterative algorithm, that is discussed in Remark 1 and that leads to a suboptimal solution of (4.1). In the special case of the SRM problem, we have  $f_k(\mathbf{E}_k) = \log |\mathbf{E}_k|$  and  $g_k(\mathbf{W}_k) = \mathbf{W}_k^{-1}$ , in which problem (4.4) is then equivalent to the problem

$$\begin{aligned} & \underset{\mathbf{F}_k, \mathbf{G}_k, \mathbf{W}_k, \forall k}{\text{minimize}} && \sum_{k=1}^K \text{tr} \{ \mathbf{W}_k \mathbf{E}_k \} - \sum_{k=1}^K \log |\mathbf{W}_k| \\ & \text{subject to} && \sum_{k=1}^K \text{tr} \{ \Phi_{k,m} \mathbf{F}_k \mathbf{F}_k^H \} \leq P_m, m = 1, \dots, M. \end{aligned} \quad (4.5)$$

The optimization problem (4.5) can be solved in an iterative fashion, where at each iteration the weights are selected as  $\mathbf{W}_k^* = \mathbf{E}_k^{-1}$  and then the WSM MSE problem is solved with respect to matrices  $(\mathbf{G}_k, \mathbf{F}_k)$  for  $k = 1, \dots, K$ .

## 4.2 Known Techniques

The SRM problem for a number of users  $K > 1$  is non-convex even when removing the constraints on the number of streams per user. The general problem in fact remains non-convex and is NP-hard [110]. Therefore, since finding the global optimal has prohibitive complexity, one needs to resort to suboptimal solutions with reasonable complexity. In this section, we review several suboptimal solutions to the SRM problem that have been proposed in the literature. Since some of these techniques were originally proposed for a scenario that does not subsume the considered MIMO-IFC-GC, we also propose the necessary modifications required for application to the MIMO-IFC-GC. Note that these techniques perform an optimization over the transmit covariance matrices by relaxing the rank constraint due to the number of users per streams (see discussion below). Therefore, we also review and modify when necessary a different class of algorithms that solve problems related to SRM but are able to enforce constraints on the number of transmitting streams per

user. The WSMMSE problem does not seem to have been addressed previously for the MIMO-IFC-GC and will be studied in the next section.

### 4.2.1 Soft Interference Nulling

A solution to the SRM problem for the MIMO-IFC-GC was proposed in [56]. In this technique the optimization is over all transmit covariance matrices  $\mathbf{\Sigma}_k = \mathbf{F}_k \mathbf{F}_k^H \in \mathbb{C}^{m_{t,k} \times m_{t,k}}$ . The constraints on the number of streams would impose a rank constraint on  $\mathbf{\Sigma}_k$  as  $\text{rank}(\mathbf{\Sigma}_k) = d_k$ . Here, and in all the following reviewed techniques below, unless stated otherwise, such rank constraints are relaxed by assuming that the number of transmitting data streams is equal to the transmitting antennas to that user, i.e.  $d_k = m_{t,k}$ . From (4.3) and (4.23), we can rewrite the (negative) sum-rate as

$$\sum_{k=1}^K \log |\mathbf{E}_k| = - \sum_{k=1}^K \log |\mathbf{\Omega}_k + \mathbf{H}_{k,k} \mathbf{\Sigma}_k \mathbf{H}_{k,k}^H| + \log |\mathbf{\Omega}_k|, \quad (4.6)$$

where  $\mathbf{\Omega}_k$  is defined in (2.17). Notice that it is often convenient to work with the covariance matrices instead of the beamforming matrices  $\mathbf{F}_k$ , since this change of variables may render the optimization problem convex as, for instance, when minimizing the first term only in (4.6). It can then be seen that the SRM problem is, however, non-convex due to the presence of the  $-\log |\mathbf{\Omega}_k|$  term, which is indeed a concave function of the matrices  $\mathbf{\Sigma}_k$ .

An approximate solution is then be found in [56] via an iterative scheme, whereby at each  $(j+1)$ th iteration, given the previous solution  $\mathbf{\Sigma}_k^{(j)}$  the non-convex term  $-\log |\mathbf{\Omega}_k|$  is approximated using a first-order Taylor expansion as

$$-\log |\mathbf{\Omega}_k| \simeq -\log |\mathbf{\Omega}_k^{(j)}| - \sum_{l \neq k} \text{tr} \left\{ \left( \mathbf{\Omega}_k^{(j)} \right)^{-1} \mathbf{H}_{k,l} \left( \mathbf{\Sigma}_l - \mathbf{\Sigma}_l^{(j)} \right) \mathbf{H}_{k,l}^H \right\}, \quad (4.7)$$

where  $\mathbf{\Omega}_k^{(j)} = \mathbf{I} + \sum_{l \neq k} \mathbf{H}_{k,l} \mathbf{\Sigma}_k^{(j)} \mathbf{H}_{k,l}^H$ . Since the resulting problem

$$\begin{aligned}
& \underset{\boldsymbol{\Sigma}_k, k=1, \dots, K}{\text{minimize}} && - \sum_{k=1}^K \log |\boldsymbol{\Omega}_k + \mathbf{H}_{k,k} \boldsymbol{\Sigma}_k \mathbf{H}_{k,k}^{\text{H}}| \\
& && + \sum_{l \neq k} \text{tr} \left\{ \left( \boldsymbol{\Omega}_k^{(j)} \right)^{-1} \mathbf{H}_{k,l} \boldsymbol{\Sigma}_l \mathbf{H}_{k,l}^{\text{H}} \right\} \\
& \text{subject to} && \text{tr} \{ \boldsymbol{\Phi}_{k,m} \boldsymbol{\Sigma}_k \} \leq P_m, \quad m = 1, \dots, M,
\end{aligned} \tag{4.8}$$

is convex, a solution can be found efficiently. Following the original reference [56], we refer to this scheme as ‘‘soft interference nulling’’. We refer to [56] for further details about the algorithm.

## 4.2.2 SDP Relaxation

A related approach is taken in [46] for the SRM problem<sup>1</sup> for a MIMO-IFC with regular per-transmitter, rather than generalized, power constraints. Similarly to the previous technique, the optimization is over the transmit covariance matrices and under the relaxed rank constraints. In particular, the authors first approximate the problem by using the approach in [108]. Then, an iterative solution is proposed by linearizing a non-convex term similar to soft interference nulling as reviewed above. It turns out that such linearized problem can be solved using semi-definite programming (SDP). Specifically, denoting with  $\boldsymbol{\Omega}_k^{(j)}$  the matrix (2.17) corresponding to the solution  $\mathbf{F}_k^{(j)}$  at the previous iteration  $j$ , i.e.,  $\boldsymbol{\Omega}_k^{(j)} = \mathbf{I} + \sum_{l \neq k} \mathbf{H}_{k,l} \mathbf{F}_l^{(j)} \mathbf{F}_l^{(j)\text{H}} \mathbf{H}_{k,l}^{\text{H}}$ , the SDP problem to be solved to find the solutions  $\mathbf{F}_k^{(j+1)}$  for the  $(j+1)$ th iteration is given by

$$\begin{aligned}
& \underset{\mathbf{Y}_k, \boldsymbol{\Sigma}_k, \forall k}{\text{minimize}} && \sum_{k=1}^K \text{tr} \{ \mathbf{Y}_k \} + \sum_{k=1}^K \text{tr} \left\{ \mathbf{C}_k^{(j)} \boldsymbol{\Sigma}_k \right\} \\
& \text{subject to} && \sum_{k=1}^K \text{tr} \{ \boldsymbol{\Phi}_{k,m} \boldsymbol{\Sigma}_k \} \leq P_m, \quad m = 1, \dots, M \\
& && \begin{bmatrix} \mathbf{H}_{k,k} \boldsymbol{\Sigma}_k \mathbf{H}_{k,k}^{\text{H}} + \boldsymbol{\Omega}_k^{(j)} & \left( \mathbf{W}_k^{(j)} \boldsymbol{\Omega}_k^{(j)} \right)^{\frac{1}{2}} \\ \left( \mathbf{W}_k^{(j)} \boldsymbol{\Omega}_k^{(j)} \right)^{\frac{1}{2}} & \mathbf{Y}_k \end{bmatrix} \succeq 0, \\
& && \text{and } \boldsymbol{\Sigma}_k \succeq 0, \quad k = 1, \dots, K
\end{aligned}$$

where

$$\mathbf{W}_k^{(j)} = \mathbf{I} + \mathbf{H}_{k,k} \boldsymbol{\Sigma}_k^{(j)} \mathbf{H}_{k,k}^{\text{H}} \boldsymbol{\Omega}_k^{(j)-1}, \tag{4.9}$$

---

<sup>1</sup>More generally, the reference studies the weighted SRM problem.

$$\begin{aligned} \mathbf{C}_k^{(j)} &= \sum_{i \neq k} \mathbf{H}_{i,k}^H \left( \mathbf{I} + \sum_l \mathbf{H}_{i,l} \Sigma_l^{(j)} \mathbf{H}_{i,l}^H \right)^{-1} \mathbf{W}_i^{(j)} \times \\ &\quad \mathbf{H}_i \Sigma_i^{(j)} \mathbf{H}_i^H \left( \mathbf{I} + \sum_l \mathbf{H}_{i,l} \Sigma_l^{(j)} \mathbf{H}_{i,l}^H \right)^{-1} \mathbf{H}_{i,k}, \end{aligned} \quad (4.10)$$

and  $\mathbf{Y}_k$  is an auxiliary optimization variable, defined using the Schur complement as  $\mathbf{Y}_k = \mathbf{W}_k \Omega_k^{(j)} \left( \mathbf{H}_{k,k} \Sigma_k \mathbf{H}_{k,k}^H + \Omega_k^{(j)} \right)^{-1}$  to convert the original optimization problem to an SDP problem [46]. The derivation requires minor modifications with respect to [46] and is therefore not detailed. The scheme is referred to as ‘‘SDP relaxation’’ in the following. We refer to [46] for further details about the algorithm.

### 4.2.3 Polite Waterfilling

Reference [75] studied the (weighted) SRM problem for a general model that includes the MIMO-IFC-GC. We review the approach here for completeness. Two algorithms are proposed, whose basic idea is to search iteratively for a solution of the KKT conditions [50] for the (weighted) SRM problem. Notice that, since the problem is non-convex, being a solution of the KKT conditions is only necessary (as proved in [75]) but not sufficient to guarantee global optimality. It is shown in [75] that any solution  $\Sigma_k$ ,  $k = 1, \dots, K$ , of the KKT conditions must have a specific structure that is referred to as ‘‘polite waterfilling’’, which is reviewed below for the SRM problem.

**Lemma 4.2.** [75] *For a given set of Lagrange multipliers  $\boldsymbol{\lambda} = (\mu\lambda_1, \dots, \mu\lambda_M)$ , where  $\mu > 0$  and  $\lambda_i \geq 0$  for  $i = 1, \dots, M$ , associated with the  $M$  power constraints in (4.1), define the covariance matrices*

$$\hat{\Omega}_k = \sum_{m=1}^M \lambda_m \Phi_{k,m} + \sum_{j \neq k} \mathbf{H}_{j,k}^H \hat{\Sigma}_j \mathbf{H}_{j,k}, \quad (4.11)$$

with

$$\hat{\Sigma}_k = \frac{1}{\mu} \left( \Omega_k^{-1} - \left( \Omega_k + \mathbf{H}_{k,k} \Sigma_k \mathbf{H}_{k,k}^H \right)^{-1} \right). \quad (4.12)$$

An optimal solution  $\Sigma_k$ ,  $k = 1, \dots, K$ , of the SRM problem must have the ‘‘polite waterfilling’’ form

$$\Sigma_k = \hat{\Omega}_k^{-\frac{1}{2}} \mathbf{V}_k \mathbf{P}_k \mathbf{V}_k^H \hat{\Omega}_k^{-\frac{1}{2}}, \quad (4.13)$$

where the columns of  $\mathbf{V}_k$  are the right singular vectors of the “pre- and post-whitened channel matrix”  $\mathbf{\Omega}_k^{-\frac{1}{2}} \mathbf{H}_{k,k} \hat{\mathbf{\Omega}}_k^{-\frac{1}{2}}$  with (2.17) for  $k = 1, \dots, K$ , and  $\mathbf{P}_k$  is a diagonal matrix with diagonal elements  $p_{k,i}$ . The powers  $p_{k,i}$  must satisfy

$$p_{k,i} = \left[ \frac{1}{\mu} - \frac{1}{\gamma_{k,i}} \right]^+, \quad (4.14)$$

where  $\sqrt{\gamma_{k,i}}$  is the  $i$ th singular value of the whitened matrix  $\mathbf{\Omega}_k^{-\frac{1}{2}} \mathbf{H}_{k,k} \hat{\mathbf{\Omega}}_k^{-\frac{1}{2}}$ . Parameter  $\mu \geq 0$  is selected so as to satisfy the constraint

$$\sum_{m=1}^M \lambda_m \sum_{k=1}^K \text{tr} \{ \mathbf{\Phi}_{k,m} \mathbf{\Sigma}_k \} \leq \sum_{m=1}^M \lambda_m P_m, \quad (4.15)$$

which implied by the constraints of the original problem (4.1). Moreover, parameters  $\lambda_i \geq 0$  are to be chosen so as to satisfy each individual constraint in (4.1).

In order to obtain a solution  $\mathbf{\Sigma}_k$ ,  $k = 1, \dots, K$ , according to polite waterfilling form as described in Lemma 6, [75] proposes to use the interpretation of  $\hat{\mathbf{\Omega}}_k$  in (4.11) as the interference plus noise covariance matrix and  $\hat{\mathbf{\Sigma}}_k$  in (4.12) as the transmit covariance matrix both at the “dual” system<sup>2</sup>.

Based on this observation, the algorithm proposed in [75] works as follows. At each  $j$ th iteration, first one calculates the covariance matrices  $\mathbf{\Sigma}_k^{(j)}$  in the original system using the polite waterfilling solution of Lemma 6; then one calculates the matrices  $\hat{\mathbf{\Sigma}}_k^{(j)}$  using again polite waterfilling in the dual system as explained above. Finally, at the end of each  $j$ th iteration, one updates the Lagrange multipliers as

$$\lambda_m^{(j+1)} = \lambda_m^{(j)} \frac{\sum_{k=1}^K \text{tr} \{ \mathbf{\Phi}_{k,m} \mathbf{\Sigma}_k^{(j)} \}}{P_m}, \quad (4.16)$$

thus forcing the solution to satisfy the constraints of the SRM problem (4.1).

For details on the algorithm, we refer to [75].

---

<sup>2</sup>In the “dual” system the role of transmitters and receivers is switched, i.e., the  $k$ th transmitter in the original system becomes the  $k$ th receiver in the “dual” system. The channel matrix between the  $k$ th transmitter and the  $l$ th receiver in the dual system is given by  $\mathbf{H}_{l,k}^H$ .

*Remark 4.2.* Other notable algorithms designed to solve the SRM problem for the special case of a MIMO-BC with generalized constraints are [28, 69]. As explained in [75], these schemes are not easily generalized to the scenario at hand where the cost function is not convex. As such, they will not be further studied here.

#### 4.2.4 Leakage Minimization

While the techniques discussed above do not enforce constraints on the number of stream per users, here we extend a technique previously proposed in [111] that aims at aligning interference through minimizing the interference leakage and is able to enforce the desired rank constraints. It is known that this approach solves the SRM problem for high signal-to-noise-ratio (SNR). In this algorithm, it is assumed that the power budget is divided equally between the data streams and the precoding matrix of user  $k$  from BS  $m$  is given as  $\mathbf{F}_{k,m} = \sqrt{\frac{P_m}{K_m d_k}} \bar{\mathbf{F}}_{k,m}$  where  $\bar{\mathbf{F}}_{k,m}$  is a  $n_t \times d_k$  matrix of orthonormal columns (i.e.  $\bar{\mathbf{F}}_{k,m}^H \bar{\mathbf{F}}_{k,m} = \mathbf{I}$ ). The equalization matrices are also assumed to have orthonormal columns (i.e.  $\mathbf{G}_k^H \mathbf{G}_k = \mathbf{I}$ ). Hence, there is no inter-stream interference for each user. Total interference leakage at user  $k$  is given by

$$I = \sum_k \text{tr} \{ \mathbf{G}_k^H \mathbf{Q}_k \mathbf{G}_k \}. \quad (4.17)$$

where  $\mathbf{Q}_k = \sum_{j \neq k} \sum_{m \in \mathcal{M}_j} \frac{P_m}{K_m d_j} \tilde{\mathbf{H}}_{k,m} \bar{\mathbf{F}}_{k,m} \bar{\mathbf{F}}_{k,m}^H \tilde{\mathbf{H}}_{j,m}^H$ . To minimize the interference leakage, the equalization matrix  $\mathbf{G}_k$  for user  $k$  can be obtained as  $\mathbf{G}_k = v_{d_k}(\mathbf{Q}_k)$  where  $v_{d_k}(\mathbf{A})$  represents a matrix with columns given by the eigenvectors corresponding to the  $d_k$  smallest eigenvalues of  $\mathbf{A}$ . Now, for fixed matrices  $\mathbf{G}_k$ , the cost function (4.17) can be rewritten as

$$I = \sum_k \sum_{m \in \mathcal{M}_k} \text{tr} \{ \bar{\mathbf{F}}_{k,m}^H \hat{\mathbf{Q}}_{k,m} \bar{\mathbf{F}}_{k,m} \} \quad (4.18)$$

where  $\hat{\mathbf{Q}}_{k,m} = \sum_{j \neq k, j \in \mathcal{K}_m} \frac{P_m}{K_m d_k} \tilde{\mathbf{H}}_{j,m}^H \mathbf{G}_j \mathbf{G}_j^H \tilde{\mathbf{H}}_{j,m}$ .<sup>3</sup> Minimizing over the matrices  $\bar{\mathbf{F}}_k$  leads to choosing  $\bar{\mathbf{F}}_{k,m} = v_{d_k}(\hat{\mathbf{Q}}_{k,m})$ . The algorithm iterates until convergence. We refer to this scheme as “min leakage” in the following.

<sup>3</sup>In the original work [111] which is proposed for the interference channels, the algorithm iteratively exchanges the role of transmitters and receivers to update the precoding and equalization matrices similarly.

### 4.2.5 Max-SINR

Another algorithm called “max-SINR” has been proposed in [111] which is based on the maximization of SINR, rather than directly the sum-rate. This algorithm is also able to enforce rank constraints. The max-SINR algorithm assumes equal power allocated to the data streams and attempts at maximizing the SINR for each stream by selecting the receive filters. Then, it exchanges the role of transmitter and receiver to obtain the transmit precoding matrices which maximizes the max-SINR. This iterates until convergence. A modification of this algorithm is given in [112] by maximizing the ratio of the average signal power to the interference plus noise power (SINR-like) term. However, these techniques are only given for standard MIMO interference channels and not for MIMO-IFC-GC.

## 4.3 MSE Minimization

In this section, we propose two suboptimal techniques to solve the WSM MSE problem. We recall that with the WSM MSE problem enforcing the constraint on  $d_k$  is necessary in order to avoid trivial solutions. Performance comparison among all the considered schemes will be provided in Sec. 4.4 for a multi-cell system with network MIMO.

### 4.3.1 MMSE Interference Alignment

A technique referred to as MMSE interference alignment (MMSE-IA) was presented in [72] for an interference channel with per-transmitter power constraints and where each receiver is endowed with a single antenna. Here we extend the approach to to the MIMO-IFC-GC.

The idea is to approximate the solution of the WSM MSE problem by optimizing the precoding matrices  $\mathbf{F}_k$  followed by the equalization matrices  $\mathbf{G}_k$  and iterating the procedure. Specifically, initialize  $\mathbf{F}_k$  arbitrarily. Then, at each iteration  $j$ : (i) For each user  $k$ , evaluate the equalization matrices using the MMSE solution (4.23), obtaining  $\mathbf{G}_k^{(j)} = \left( \mathbf{H}_{k,k} \mathbf{F}_k^{(j-1)} \mathbf{F}_k^{(j-1)\text{H}} \mathbf{H}_{k,k}^{\text{H}} + \boldsymbol{\Omega}_k^{(j-1)} \right)^{-1} \mathbf{H}_{k,k} \mathbf{F}_k^{(j-1)}$ , where from (2.17) we have  $\boldsymbol{\Omega}_k^{(j-1)} = \mathbf{I} + \sum_{l \neq k} \mathbf{H}_{k,l} \mathbf{F}_l^{(j-1)} \mathbf{F}_l^{(j-1)\text{H}} \mathbf{H}_{k,l}^{\text{H}}$ ; (ii) Given

the matrices  $\mathbf{G}_k^{(j)}$ , the WSM MSE problem becomes

$$\begin{aligned} & \underset{\mathbf{F}_k, k=1, \dots, K}{\text{minimize}} && \sum_{k=1}^K \text{tr} \left\{ \mathbf{W}_k \mathbf{E}_k^{(j)} \right\} \\ & \text{subject to} && \sum_{k=1}^K \text{tr} \left\{ \Phi_{k,m} \mathbf{F}_k \mathbf{F}_k^H \right\} \leq P_m, \forall m \in \mathcal{M} \end{aligned}, \quad (4.19)$$

where  $\mathbf{E}_k^{(j)}$  is (2.16) with  $\mathbf{G}_k^{(j)}$  in place of  $\mathbf{G}_k$ . Fixing the equalization matrices  $\mathbf{G}_k^{(j)}, \forall k$ , this problem is convex in  $\mathbf{F}_k$  and can be solved by enforcing the KKT conditions. Therefore, matrices  $\mathbf{F}_k^{(j)}$  for the  $j$ th iteration can be obtained as follows.

**Lemma 4.3.** *For given equalization matrices  $\mathbf{G}_k^{(j)}$ , a solution  $\mathbf{F}_k^{(j)}$ ,  $k = 1, \dots, K$ , of the WSM MSE problem is given by*

$$\mathbf{F}_k^{(j)} = \left( \sum_{l=1}^K \mathbf{H}_{l,k}^H \mathbf{G}_l^{(j)} \mathbf{W}_l \mathbf{G}_l^{(j)H} \mathbf{H}_{l,k} + \sum_m \mu_m \Phi_{k,m} \right)^{-1} \times \mathbf{H}_{k,k}^H \mathbf{G}_k^{(j)} \mathbf{W}_k \quad (4.20)$$

where  $\mu_m$  are Lagrangian multipliers satisfying

$$\mu_m \geq 0 \quad (4.21)$$

$$\mu_m \left( \sum_{k=1}^K \text{tr} \left\{ \Phi_{k,m} \mathbf{F}_k^{(j)} \mathbf{F}_k^{(j)H} \right\} - P_m \right) = 0 \quad (4.22)$$

and the power constraints  $\sum_{k=1}^K \text{tr} \left\{ \Phi_{k,m} \mathbf{F}_k^{(j)} \mathbf{F}_k^{(j)H} \right\} \leq P_m$  for all  $m$ .

Once obtained the matrices  $\mathbf{F}_k^{(j)}$  using the results in Lemma 4.3, the iterative procedure continues with the  $(j+1)$ th iteration. We refer to this scheme as extended MMSE-IA, or eMMSE-IA.

*Remark 4.3.* The algorithm proposed above reduces to the one introduced in [72] in the special case of per-transmitter power constraints and single-antenna receivers. It is noted that in such case, problem (4.19) can be solved in a distributed fashion, so that each transmitter  $k$  can calculate its matrix (more precisely vector, given the single antenna at the receivers) independently from the other transmitters. In the MIMO-IFC-GC, the power constraints couple the solutions of the different users and thus make a distributed approach infeasible.

### 4.3.2 Diagonalized MMSE

#### The Single-User Case ( $K = 1$ )

The WSM MSE and SRM problems are non-convex and thus global optimization is generally prohibitive. In this section, we address the case of a single user ( $K = 1$ ). In particular, the SRM problem with  $K = 1$  is non-convex if one includes constraints on the number of streams  $d_1$ , but is otherwise convex and in this special case can be solved efficiently [83]. The global optimal solution for the single-user problem with multiple linear power constraint (and a rank constraint) is still unknown [113]. The WSM MSE problem is trivial without rank constraint, as explained above, and is non-convex. Here we first review a key result in [83] [114] that shows with  $K = 1$  and a single constraint ( $M = 1$ ) the solution of the WSM MSE problem can be, however, found efficiently. We then discuss that with multiple constraints ( $M > 1$ ), this is not the case, and a solution of the WSM MSE problem even with  $K = 1$  must be found through some complex global optimization strategies. One such technique was recently proposed in [113] based on a sophisticated gradient approach. At the end of this section we then propose a computationally and conceptually simpler solution based on a novel result (Lemma 4.6), that our numerical result have shown to have excellent performance. This will be then leveraged in Sec. 4.3.2 to propose a novel solution for the general multiuser case.

To elaborate, consider a scenario where the noise-plus-interference matrix  $\mathbf{\Omega}_k$  (2.17) is fixed and given (i.e., not subject to optimization). Now, we solve the WSM MSE problem with  $K = 1$  for specified weight matrices  $\mathbf{W}$  and  $\mathbf{\Phi}_m$ . For the rest of this section, we drop the index  $k = 1$  from all quantities for simplicity of notation. We proceed by solving the problem at hand, first with respect to  $\mathbf{G}$  for fixed  $\mathbf{F}$ , and then with respect to  $\mathbf{F}$  without loss of optimality. The first optimization, over  $\mathbf{G}$ , is easily seen to be a convex problem (without constraints) whose solution is given by the minimum MSE equalization matrix

$$\mathbf{G} = (\mathbf{H}\mathbf{F}\mathbf{F}^H\mathbf{H}^H + \mathbf{\Omega})^{-1} \mathbf{H}\mathbf{F}. \quad (4.23)$$

Plugging (4.23) in the MSE matrix (2.16), we obtain

$$\mathbf{E} = (\mathbf{I} + \mathbf{B}^H \mathbf{H}^H \Omega^{-1} \mathbf{H} \mathbf{F})^{-1}. \quad (4.24)$$

We now need to optimize over  $\mathbf{F}$  the following problem

$$\begin{aligned} & \underset{\mathbf{F}}{\text{minimize}} && \text{tr} \left\{ \mathbf{W} (\mathbf{I} + \mathbf{F}^H \mathbf{H}^H \Omega^{-1} \mathbf{H} \mathbf{F})^{-1} \right\} \\ & \text{subject to} && \text{tr} \left\{ \Phi_m \mathbf{F} \mathbf{F}^H \right\} \leq P_m, m = 1, \dots, M \end{aligned}, \quad (4.25)$$

Consider first the single-constraint problem, i.e.,  $M = 1$ . The global optimal solution for single-user WSMSE problem with  $M = 1$  is given in [114] [113] and reported below. Recall that, according to Definition 2.1, matrix  $\Phi_1$  is positive definite.

**Lemma 4.4.** [114] *The optimal solution of the WSMSE problem with  $K = 1$  and a single trace constraint ( $M = 1$ ) is given by*

$$\mathbf{F} = \Phi_1^{-\frac{1}{2}} \mathbf{U} \Sigma, \quad (4.26)$$

where  $\mathbf{U} \in \mathbb{C}^{m_t \times d}$  is the matrix of eigenvectors of matrix  $\Phi_1^{-\frac{1}{2}} \mathbf{H} \Omega^{-1} \mathbf{H}^H \Phi_1^{-\frac{1}{2}}$  corresponding to its largest eigenvalues  $\gamma_1 \geq \dots \geq \gamma_d$  and  $\Sigma$  is a diagonal matrix with the diagonal terms  $\sqrt{p_i}$  defined as

$$p_i = \left[ \sqrt{\frac{w_i}{\mu \gamma_i}} - \frac{1}{\gamma_i} \right]^+, \quad (4.27)$$

with  $\mu \geq 0$  being the “waterfilling” level chosen so as to satisfy the single power constraint  $\text{tr} \left\{ \Phi_1 \mathbf{F} \mathbf{F}^H \right\} = P_1$ .

*Proof.* Introducing the “effective” precoding matrix  $\bar{\mathbf{F}} = \Phi_1^{1/2} \mathbf{F}$  and “effective” channel matrix  $\bar{\mathbf{H}} = \mathbf{H} \Phi_1^{-\frac{1}{2}}$ , the problem is equivalent to the one discussed in [114, Theorem 1].  $\square$

In the case of multiple constraints the approach used in Lemma 4.4 cannot be leveraged. Here we propose a simple, but effective, approach, which is based on the following considerations summarized in the following two lemmas.

**Lemma 4.5.** *The precoding matrix (4.26)-(4.27) for a given fixed  $\mu > 0$  minimizes the Lagrangian function*

$$\begin{aligned} \mathcal{L}(\bar{\mathbf{F}}; \mu) = & \text{tr} \left\{ \mathbf{W} \left( \mathbf{I} + \bar{\mathbf{F}}^H \Phi_1^{-\frac{1}{2}} \mathbf{H}^H \Omega^{-1} \mathbf{H} \Phi_1^{-\frac{1}{2}} \bar{\mathbf{F}} \right)^{-1} \right\} \\ & + \mu \text{tr} \left\{ \bar{\mathbf{F}} \bar{\mathbf{F}}^H \right\} \end{aligned} \quad (4.28)$$

where  $\bar{\mathbf{F}}$  is the effective precoding matrix defined above.

*Proof.* We first note that (4.28) is the Lagrangian function of the single-user single-constraint problem solved in Lemma 4.4. Then, we prove (4.28) by contradiction. Assume that the minimum of the Lagrangian function is attained where the corresponding  $\mathbf{E}$  is not diagonal. Then, one can always find a unitary matrix  $\mathbf{Q} \in \mathbb{C}^{d \times d}$  such that the matrix  $\bar{\mathbf{F}}^* = \bar{\mathbf{F}}\mathbf{Q}$  diagonalizes  $\mathbf{E}$  since with  $\bar{\mathbf{F}}^*$  we have  $\mathbf{E} = \mathbf{Q}^H \left( \mathbf{I} + \bar{\mathbf{B}}^H \Phi_1^{-\frac{1}{2}} \mathbf{H}^H \Omega^{-1} \mathbf{H} \Phi_1^{-\frac{1}{2}} \bar{\mathbf{F}} \right)^{-1} \mathbf{Q}$  [114]. The function  $\text{tr}\{\mathbf{W}\mathbf{E}\}$  is Schur concave, and therefore the matrix  $\bar{\mathbf{F}}^*$  does not decrease the function  $\text{tr}\{\mathbf{W}\mathbf{E}\}$  with respect to  $\bar{\mathbf{F}}$ , while  $\bar{\mathbf{F}}\bar{\mathbf{F}}^H = \bar{\mathbf{F}}^*\bar{\mathbf{F}}^{*H}$ . This implies that the minimum of  $\text{tr}\{\mathbf{W}\mathbf{E}\}$  is reached when the MSE matrix is diagonalized. Therefore, we can set without loss of generality  $\bar{\mathbf{F}} = \mathbf{U}\boldsymbol{\Sigma}$  where  $\mathbf{U}$  is defined as in Lemma 4.4 and  $\boldsymbol{\Sigma}$  is diagonal with non-negative elements on the main diagonal. Substituting this form of  $\bar{\mathbf{F}}$  into the Lagrangian function, we obtain a convex problem in the diagonal elements of  $\boldsymbol{\Sigma}$ , whose solution can be easily shown to be given by (4.27) for the given  $\mu$ . This concludes the proof.  $\square$

**Lemma 4.6.** *Let  $p^*$  be the optimal value of the single-user WSM MSE problem with multiple constraints ( $K = 1, M \geq 1$ ). We have*

$$p^* \geq \max_{\boldsymbol{\lambda} \geq 0} \inf_{\mathbf{F}} \mathcal{L}(\mathbf{F}; \boldsymbol{\lambda}), \quad (4.29)$$

where

$$\begin{aligned} \mathcal{L}(\mathbf{F}; \boldsymbol{\lambda}) = & \text{tr} \left\{ \mathbf{W} \left( \mathbf{I} + \mathbf{F}^H \mathbf{H}^H \Omega \mathbf{H} \mathbf{F} \right)^{-1} \right\} \\ & + \sum_{m=1}^M \lambda_m \left( \text{tr} \{ \Phi_m \mathbf{F} \mathbf{F}^H \} - P_m \right) \end{aligned} \quad (4.30)$$

is the Lagrangian function of the single-user WSM MSE problem at hand and  $\boldsymbol{\lambda} = (\lambda_1, \dots, \lambda_M)$ . Moreover, if there exists an optimal solution  $\tilde{\mathbf{F}}$  achieving  $p^*$  that, together with a strictly positive Lagrange multiplier  $\tilde{\boldsymbol{\lambda}} > 0$ , satisfies the conditions

$$\nabla_{\mathbf{F}} \mathcal{L} = 0, \quad (4.31)$$

$$\text{tr} \left\{ \Phi_m \tilde{\mathbf{F}} \tilde{\mathbf{F}}^H \right\} = P_m, \quad \forall m \quad (4.32)$$

then (4.29) holds with equality.

*Proof.* The inequality (4.29) follows from weak Lagrangian duality. We now prove the second part of the statement. Recognizing now that  $\text{tr}\{\mathbf{W}\mathbf{E}\}$  with (4.24) is a Schur-concave function of the diagonal elements of (4.24)<sup>4</sup>, it can be argued that the minimum is attained when  $\mathbf{E}$  is diagonalized as we did for Lemma 4. Defining  $\mathbf{R} = \mathbf{H}^H \mathbf{\Omega}^{-1} \mathbf{H}$ , we can conclude that  $\mathbf{F}^H \mathbf{R} \mathbf{F}$  must be also diagonal in this search domain. Now assume that an optimal solution of the single-user WSMSE problem is denoted as  $\tilde{\mathbf{F}}$ . Without loss of generality we can assume that this solution diagonalizes the MSE matrices. The necessity of the KKT conditions can be proved as in [75] and in special cases such as the MIMO interference channel with partial message sharing of Sec. 2.2.1, it also follows from linear independence constraint qualification conditions [115].

Hence, there exists a Lagrange multiplier vector  $\tilde{\boldsymbol{\lambda}}$  which together with  $\tilde{\mathbf{F}}$  satisfies the KKT conditions of the WSMSE problem (4.25) [108] [115]. As it is stated in the Lemma, we consider the case that  $\tilde{\lambda}_m$  are also strictly positive (i.e.  $\tilde{\lambda}_m > 0$  for all  $m$ ). Simplifying the KKT condition (4.31), we have<sup>5</sup>

$$\nabla_{\mathbf{F}} \mathcal{L} = -\mathbf{R} \tilde{\mathbf{F}} \tilde{\mathbf{E}} \mathbf{W} \tilde{\mathbf{E}} + \sum_{m=1}^M \tilde{\lambda}_m \boldsymbol{\Phi}_m \tilde{\mathbf{F}} = \mathbf{0} \quad (4.33)$$

Left-multiplying (4.33) by  $\tilde{\mathbf{F}}^H$  gives us

$$\tilde{\mathbf{F}}^H \mathbf{R} \tilde{\mathbf{F}} \tilde{\mathbf{E}} \mathbf{W} \tilde{\mathbf{E}} = \tilde{\mathbf{F}}^H \left( \sum_m \tilde{\lambda}_m \boldsymbol{\Phi}_m \right) \tilde{\mathbf{F}}. \quad (4.34)$$

Since  $\tilde{\mathbf{F}}^H \mathbf{R} \tilde{\mathbf{F}}$  and correspondingly  $\tilde{\mathbf{E}}$  are diagonal matrices,  $\tilde{\mathbf{F}}^H \left( \sum_m \tilde{\lambda}_m \boldsymbol{\Phi}_m \right) \tilde{\mathbf{F}}$  must also be diagonal. For simplicity, we introduce  $\boldsymbol{\Phi}(\tilde{\boldsymbol{\lambda}}) = \sum_{m=1}^M \tilde{\lambda}_m \boldsymbol{\Phi}_m$ . Since  $\tilde{\lambda}_m > 0$  for every  $m$ , therefore  $\boldsymbol{\Phi}(\tilde{\boldsymbol{\lambda}})$  is a non-singular matrix. This can be easily verified due to the structure of  $\boldsymbol{\Phi}_m$ . Hence, we can write  $\tilde{\mathbf{F}}^H \boldsymbol{\Phi}(\tilde{\boldsymbol{\lambda}}) \tilde{\mathbf{F}} = \tilde{\boldsymbol{\Delta}}$  where  $\tilde{\boldsymbol{\Delta}} \in \mathbb{C}^{d \times d}$  is a diagonal matrix. Therefore, we can write

$$\boldsymbol{\Phi}(\tilde{\boldsymbol{\lambda}})^{1/2} \tilde{\mathbf{F}} = \tilde{\mathbf{U}} \tilde{\boldsymbol{\Sigma}} \quad (4.35)$$

<sup>4</sup>A Schur-concave function  $f(\mathbf{x})$  of vector  $\mathbf{x} = (x_1, \dots, x_d)$  is such that  $f(\mathbf{x}) \leq f(\mathbf{x}')$  if  $\mathbf{x}$  majorizes  $\mathbf{x}'$ , that is, if  $\sum_{i=1}^j x_{[i]} \geq \sum_{i=1}^j x'_{[i]}$  for all  $j = 1, \dots, d$ , where  $x_{[i]}$  (and  $x'_{[i]}$ ) represents the vector sorted in decreasing order, i.e.,  $x_{[1]} \geq \dots \geq x_{[d]}$  (and  $x'_{[1]} \geq \dots \geq x'_{[d]}$ ).

<sup>5</sup>We use differentiation rule  $\nabla_{\mathbf{X}} \text{tr}\{\mathbf{G}\mathbf{X}^H \mathbf{F}\} = \mathbf{F}\mathbf{G}$  and  $\nabla_{\mathbf{X}} \text{tr}\{\mathbf{Y}^{-1}\} = -\mathbf{Y}^{-1} (\nabla_{\mathbf{X}} \mathbf{Y}) \mathbf{Y}^{-1}$ . For the complex gradient operator each matrix and its conjugate transpose are treated as independent variables [116].

where  $\tilde{\mathbf{U}} \in \mathbb{C}^{m_t \times d}$  consists of orthonormal columns (i.e.  $\tilde{\mathbf{U}}^H \tilde{\mathbf{U}} = \mathbf{I}$ ) and  $\tilde{\mathbf{\Sigma}} \in \mathbb{C}^{d \times d}$  is a diagonal matrix with the diagonal terms of  $\sqrt{\tilde{p}_i}$ . Hence, we can write

$$\tilde{\mathbf{F}} = \mathbf{\Phi}(\tilde{\boldsymbol{\lambda}})^{-1/2} \tilde{\mathbf{U}} \tilde{\mathbf{\Sigma}}. \quad (4.36)$$

Replacing the structure of  $\tilde{\mathbf{F}}$  given in (4.36), we can write

$$\tilde{\mathbf{F}}^H \mathbf{R} \tilde{\mathbf{F}} = \tilde{\mathbf{\Sigma}}^H \tilde{\mathbf{U}}^H \mathbf{\Phi}(\tilde{\boldsymbol{\lambda}})^{-\frac{1}{2}} \mathbf{R} \mathbf{\Phi}(\tilde{\boldsymbol{\lambda}})^{-\frac{1}{2}} \tilde{\mathbf{U}} \tilde{\mathbf{\Sigma}} = \mathbf{D} \quad (4.37)$$

Thus, we can conclude from the equation above that  $\tilde{\mathbf{U}}$  must contain the eigenvectors of  $\mathbf{\Phi}(\tilde{\boldsymbol{\lambda}})^{-\frac{1}{2}} \mathbf{R} \mathbf{\Phi}(\tilde{\boldsymbol{\lambda}})^{-\frac{1}{2}}$ .

Now, plugging (4.36) into (4.31) and left-multiply it with  $\mathbf{\Phi}^{-\frac{1}{2}}$ , we get

$$\tilde{\mathbf{\Gamma}} \tilde{\mathbf{\Sigma}} \left( \mathbf{I} + \tilde{\mathbf{\Gamma}} \tilde{\mathbf{\Sigma}}^2 \right)^{-1} \mathbf{W} \left( \mathbf{I} + \tilde{\mathbf{\Gamma}} \tilde{\mathbf{\Sigma}}^2 \right)^{-1} = \tilde{\mathbf{\Sigma}} \quad (4.38)$$

where  $\tilde{\mathbf{\Gamma}}(\tilde{\boldsymbol{\lambda}}) = \text{diag}[\gamma_1(\tilde{\boldsymbol{\lambda}}) \cdots \gamma_d(\tilde{\boldsymbol{\lambda}})]$  is a diagonal matrix with the diagonal terms of the  $d$  largest eigenvalues of  $\mathbf{\Phi}(\tilde{\boldsymbol{\lambda}})^{-\frac{1}{2}} \mathbf{R} \mathbf{\Phi}(\tilde{\boldsymbol{\lambda}})^{-\frac{1}{2}}$ . Since all the matrices are diagonal, (4.38) reduces to the scalar equations:

$$\frac{w_i \gamma_i(\tilde{\boldsymbol{\lambda}})}{(1 + \tilde{p}_i \gamma_i(\tilde{\boldsymbol{\lambda}}))^2} = 1 \quad (4.39)$$

Solving these equations gives us the optimal  $\tilde{p}_i$  given by

$$\tilde{p}_i = \left[ \sqrt{\frac{w_i}{\gamma_i(\tilde{\boldsymbol{\lambda}})}} - \frac{1}{\gamma_i(\tilde{\boldsymbol{\lambda}})} \right]^+, \quad (4.40)$$

Thus, for the given Lagrange multiplier  $\tilde{\boldsymbol{\lambda}}$  which together with  $\tilde{\mathbf{F}}$ , satisfying the KKT conditions of (4.25),  $\tilde{\mathbf{F}}$  must satisfy (4.36) and (4.40). If all power constraints are satisfied with equality by this solution, then (4.36) and (4.40) also solves the single constraint problem

$$\begin{aligned} & \underset{\mathbf{F}}{\text{minimize}} \quad \text{tr} \left\{ \mathbf{W} \left( \mathbf{I} + \mathbf{F}^H \mathbf{H}^H \mathbf{\Omega}^{-1} \mathbf{H} \mathbf{F} \right)^{-1} \right\} \\ & \text{subject to} \quad \text{tr} \left\{ \mathbf{\Phi}(\tilde{\boldsymbol{\lambda}}) \mathbf{F} \mathbf{F}^H \right\} \leq \sum_{m=1}^M \tilde{\lambda}_m P_m, \end{aligned} \quad (4.41)$$

The solution of this problem is given in Lemma 3 as

$$\mathbf{F}(\tilde{\boldsymbol{\lambda}}) = \mathbf{\Phi}(\tilde{\boldsymbol{\lambda}})^{-\frac{1}{2}} \mathbf{U} \mathbf{\Sigma} \quad (4.42)$$

where  $\mathbf{U}$  consists of  $d$  eigenvectors of  $\Phi(\tilde{\boldsymbol{\lambda}})^{-\frac{1}{2}}\mathbf{R}\Phi(\tilde{\boldsymbol{\lambda}})^{-\frac{1}{2}}$  corresponding to its largest eigenvalues and  $\boldsymbol{\Sigma}$  is a diagonal matrix with the diagonal elements of  $\sqrt{p_i}$ , which is given by

$$p_{k,i} = \left[ \sqrt{\frac{w_i}{\mu\gamma_i(\tilde{\boldsymbol{\lambda}})}} - \frac{1}{\gamma_i(\tilde{\boldsymbol{\lambda}})} \right]^+, \quad (4.43)$$

for a waterfilling value of  $\mu \geq 0$  which satisfies the power constraint

$$\text{tr} \left\{ \Phi(\tilde{\boldsymbol{\lambda}})\mathbf{F}(\tilde{\boldsymbol{\lambda}})\mathbf{F}(\tilde{\boldsymbol{\lambda}})^H \right\} \leq \sum_m \tilde{\lambda}_m P_m. \quad (4.44)$$

On the other hand, summing up the KKT conditions  $\tilde{\lambda}_m (P_m - \text{tr} \{ \Phi_m \mathbf{F} \mathbf{F}^H \}) = 0$  for all  $m$ , we obtain that

$$\text{tr} \left\{ \left( \sum_m \tilde{\lambda}_m \Phi_m \right) \tilde{\mathbf{F}} \tilde{\mathbf{F}}^H \right\} = \sum_m \tilde{\lambda}_m P_m \quad (4.45)$$

If we set  $\mu = 1$  and comparing (4.40) and (4.43), we can conclude that  $\tilde{p}_i = p_i, \forall i$  which together with comparison of (4.42) and (4.36) we can conclude that  $\mathbf{F}(\tilde{\boldsymbol{\lambda}}) = \tilde{\mathbf{F}}$  and the  $\mu = 1$  is the optimal Lagrange multiplier of the single-constraint WSM MSE problem (4.41). Following Lemma 4, this precoding matrix is also a result of minimization of the Lagrangian function (4.28) when  $\mu = 1$  and  $\Phi_1 = \Phi(\tilde{\boldsymbol{\lambda}})$ , which means

$$p^* = \inf_{\mathbf{F}} \mathcal{L}(\mathbf{F}; \tilde{\boldsymbol{\lambda}}). \quad (4.46)$$

On the other hand, we have

$$\max_{\boldsymbol{\lambda} \geq 0} \inf_{\mathbf{F}} \mathcal{L}(\mathbf{F}; \boldsymbol{\lambda}) \geq \inf_{\mathbf{F}} \mathcal{L}(\mathbf{F}; \tilde{\boldsymbol{\lambda}}) \quad (4.47)$$

which in concert with (4.29) and (4.46) results in

$$p^* = \inf_{\mathbf{F}} \mathcal{L}(\mathbf{F}; \tilde{\boldsymbol{\lambda}}) = \max_{\boldsymbol{\lambda} \geq 0} \inf_{\mathbf{F}} \mathcal{L}(\mathbf{F}; \boldsymbol{\lambda}), \quad (4.48)$$

thus concluding the proof.  $\square$

Lemma 4.6 suggests that to solve the single-user multiple-constraint problem, under some technical conditions, one can minimize instead the dual problem on the right-hand side of (4.29). Lemma 4.4 showed that this is always

possible with a single constraint. The conditions in Lemma 4.6 hold in most cases where the power constraints for the optimal solution are satisfied with equality. While this may not be always the case, in practice, e.g., if the power constraints represent per-BS power constraints, this condition can be shown to hold [117].

Inspired by Lemma 4.6, here we propose an iterative approach to the solution of the WSM MSE problem with  $K = 1$  that is based on solving the dual problem  $\max_{\boldsymbol{\lambda} \succeq 0} \min_{\mathbf{F}} \mathcal{L}(\mathbf{F}; \boldsymbol{\lambda})$ . Specifically, in order to maximize  $\inf_{\mathbf{F}} \mathcal{L}(\mathbf{F}; \boldsymbol{\lambda})$  over  $\boldsymbol{\lambda} \succeq 0$ , in the proposed algorithm, the auxiliary variables  $\boldsymbol{\lambda}$  are updated at the  $j$ th iteration via a subgradient update given by [75]

$$\lambda_m^{(j)} = \lambda_m^{(j-1)} + \delta (P_m - \text{tr} \{ \Phi_m \mathbf{F} \mathbf{F}^H \}), \quad \forall m, \quad (4.49)$$

so as to attempt to satisfy the power constraints. Having fixed the vector  $\boldsymbol{\lambda}^{(j)}$ , problem  $\min_{\mathbf{F}} \mathcal{L}(\mathbf{F}, \boldsymbol{\lambda})$  reduces to minimizing (4.28) with  $\Phi_1 = \Phi(\boldsymbol{\lambda}^{(j)}) = \sum_m \lambda_m^{(j)} \Phi_m$  and  $\mu = 1$ . This can be done using Lemma 4.4, so that from (4.26)-(4.27), at the  $j$ th iteration,  $\mathbf{F}^{(j)}$  is obtained as  $\Phi(\boldsymbol{\lambda}^{(j)})^{-\frac{1}{2}} \mathbf{U}^{(j)} \boldsymbol{\Sigma}^{(j)}$  where  $\mathbf{U}^{(j)}$  is the matrix of eigenvectors of matrix  $\Phi(\boldsymbol{\lambda}^{(j)})^{-\frac{1}{2}} \mathbf{H} \mathbf{H}^H \Phi(\boldsymbol{\lambda}^{(j)})^{-\frac{1}{2}}$  corresponding to its largest eigenvalues  $\gamma_1 \geq \dots \geq \gamma_d$  and  $\boldsymbol{\Sigma}^{(j)}$  is a diagonal matrix with the diagonal terms  $\sqrt{p_i} = \sqrt{\left[ \sqrt{\frac{w_i}{\gamma_i}} - \frac{1}{\gamma_i} \right]^+}$ . We now propose an iterative optimization strategy inspired by the single-user algorithm that we put forth in Sec. 4.3.2. At the  $(j+1)$ th iteration, given the matrices obtained at the previous iteration, we proceed as follows. The weighted sum-MSE (4.2) with the definition of MSE-matrices (2.16) is a convex function in each  $\mathbf{G}_k$  and  $\mathbf{F}_k$  when  $(\mathbf{F}_j, \mathbf{G}_j), \forall j \neq k$  are fixed. Nevertheless, it is not jointly convex in terms of both  $(\mathbf{G}_k, \mathbf{F}_k)$ . Inspired by Lemma 4.6 for the corresponding single-user problem, we propose a (suboptimal) solution based on the solution of the dual problem for calculation of  $(\mathbf{G}_k, \mathbf{F}_k)$ . To this end, we first obtain  $\mathbf{G}_k$  as (4.23). Then, we simplify the Lagrangian function with respect to  $\mathbf{F}_k$  by removing the terms independent of  $\mathbf{F}_k$ . Specifically, by defining  $\Upsilon_k = \sum_{l \neq k} \mathbf{H}_{l,k}^H \mathbf{G}_l \mathbf{W}_l \mathbf{G}_l^H \mathbf{H}_{l,k}$ , we

have that the Lagrangian function at hand is given by

$$\begin{aligned}\mathcal{L}(\mathbf{F}_k; \boldsymbol{\lambda}) &= \text{tr} \left\{ \mathbf{W}_k \left( \mathbf{I} + \mathbf{F}_k^H \mathbf{H}_{k,k}^H \boldsymbol{\Omega}_k^{-1} \mathbf{H}_{k,k} \mathbf{F}_k \right)^{-1} \right\} \\ &\quad + \text{tr} \left\{ \boldsymbol{\Upsilon}_k \mathbf{F}_k \mathbf{F}_k^H \right\} \\ &\quad + \text{tr} \left\{ \left( \sum_m \lambda_m \boldsymbol{\Phi}_{k,m} \right) \mathbf{F}_k \mathbf{F}_k^H \right\}\end{aligned}\quad (4.50)$$

This Lagrangian function for user  $k$  is the same as the Lagrangian function (4.30) of single-user WSMMSE problem when  $\boldsymbol{\Phi}(\boldsymbol{\lambda})$  is replaced with  $\mathbf{F}_k(\boldsymbol{\lambda}) = \boldsymbol{\Upsilon}_k + \sum \lambda_m \boldsymbol{\Phi}_{k,m}$ . Matrix  $\mathbf{F}_k(\boldsymbol{\lambda})$  is non-singular and therefore, using the same argument as in the proof of Lemma 4.6, for a given Lagrange multipliers  $\boldsymbol{\lambda}$  and given other users' transmission strategies  $(\mathbf{G}_l, \mathbf{F}_l), \forall l \neq k$ , the optimal transmit precoding matrix can be obtained as

$$\mathbf{F}_k = \mathbf{F}_k(\boldsymbol{\lambda})^{-\frac{1}{2}} \mathbf{U}_k \boldsymbol{\Sigma}_k, \quad (4.51)$$

where  $\mathbf{U}_k \in \mathbb{C}^{m_{t,k} \times d_k}$  is the eigenvectors of  $\mathbf{F}_k(\boldsymbol{\lambda})^{-\frac{1}{2}} \mathbf{H}_{k,k}^H \boldsymbol{\Omega}_k^{-1} \mathbf{H}_{k,k} \mathbf{F}_k(\boldsymbol{\lambda})^{-\frac{1}{2}}$  corresponding to its largest eigenvalues  $\gamma_{k,1} \geq \dots \geq \gamma_{k,d_k}$  and  $\boldsymbol{\Sigma}_k$  is diagonal matrices with the elements  $\sqrt{p_{k,i}}$  given by

$$p_{k,i} = \left[ \sqrt{\frac{w_{k,i}}{\gamma_{k,i}}} - \frac{1}{\gamma_{k,i}} \right]^+, \quad (4.52)$$

with  $\boldsymbol{\lambda} \succeq 0$  being the Lagrangian multipliers satisfy the power constraints. Since this scheme diagonalizes the MSE matrices defined in (2.14), it is referred to as diagonalized MMSE (DMMSE).

To summarize, the proposed algorithm at each iteration  $j$  ( $i$ ) evaluates the transmit precoding matrices  $\mathbf{F}_k^{(j)}$  given other users' transmission strategies  $(\mathbf{G}_l^{(j-1)}, \mathbf{F}_l^{(j-1)})$  using (4.51)-(4.52) ( $ii$ ) updates the equalization matrices using the MMSE solution (4.23); ( $iii$ ) updates the  $\boldsymbol{\lambda}$  via a subgradient update

$$\lambda_m^{(j+1)} = \lambda_m^{(j)} + \delta \left( P_m - \sum_{k=1}^K \text{tr} \left\{ \boldsymbol{\Phi}_{k,m} \mathbf{F}_k \mathbf{F}_k^H \right\} \right) \quad (4.53)$$

to satisfy the power constraints.

*Remark 4.4.* In this chapter, we assume perfect knowledge of channel state information (CSI). Therefore, each transmitter and receiver has sufficient

information to calculate the resulting precoders and equalizers by running the proposed algorithms. Under this assumption, which is common to other reviewed works such as [56] [46], no exchange of precoder and equalizer vectors is required between the transmitters and receivers. Nevertheless, in practice, the CSI may only be available locally, in the sense that transmitter  $k$  knows channel matrices  $\mathbf{H}_{l,k}$ , for all  $l = 1, \dots, K$ , whereas receiver  $k$  is aware of channel matrices  $\mathbf{H}_{k,l}$ , for all  $l = 1, \dots, K$ . The proposed DMMSE and the reviewed PWF [71] [75] algorithms require, beside the local CSI, that the transmitter  $k$  has available also the interference plus noise covariance matrix,  $\mathbf{\Omega}_k$ , and the current equalization matrices  $\mathbf{G}_l$  for all  $l = 1, \dots, K$  in order to update the precoder for user  $k$ . Hence, to enable DMMSE and PWF with local CSI, exchange of the equalizer matrices is needed between the nodes. Similarly, the proposed eMMSEIA, and min leakage and Max-SINR algorithms [111], require the transmitters to know the equalizing matrices  $\mathbf{G}_l$  for  $l = 1, \dots, K$  at each iteration, in addition to the local CSI. Moreover, each receiver must know the current precoders  $\mathbf{F}_l$  for all  $l = 1, \dots, K$ . Therefore, the overhead for the proposed eMMSEIA and the min leakage and Max-SINR algorithms involves the exchange of equalizer and precoder matrices between the transmitters and receivers. However, these latter algorithms can also be adapted using the bi-directional optimization process proposed in [118]. This process involves bi-directional training followed by data transmission. In the forward direction, the training sequences are sent using the current precoders. Then, at the user receivers the equalizers are updated to minimize the least square error cost function. In the backward training phase, the current equalizers are used to send the training sequences and the precoders are updated accordingly. Finally, the SIN [56] and SDP relaxation [46] techniques are applied in a centralized fashion (rather than by updating the transmitter and receiver for each user at each iteration), and they require centralized full knowledge of all channel matrices.

*Remark 4.5.* Reference [46] addresses the SRM problem for a MIMO-IFC with regular per-transmitter, rather than generalized, power constraints. The

problem is addressed by solving an SDP problem at each iteration. Moreover, the optimization is over the transmit covariance matrices and under the relaxed rank constraint. This enforces a constraint on the number of transmitted streams per user. References [71]- [75] study the (weighted) SRM problem by decomposing the multiuser problem into single-user problems for each user. Each single-user problem is a standard single-user SRM problem with an additional interference power constraint. The approach used in [71]- [75] assumes that the number of transmitted streams is equal to  $n_r$ . Here, we address WSMSE problem and allow for an arbitrary number of streams ( $d_k \leq n_r$ ).

*Remark 4.6.* Our algorithms consists of an inner loop, which solves the WSMSE problem, and an outer loop, which is the subgradient algorithm to update  $\boldsymbol{\lambda}$ . The subgradient algorithm in the outer loop is convergent (with a proper selection of the step sizes [115]) due to the fact that the dual function  $\inf_{\mathbf{F}} \mathcal{L}(\mathbf{F}; \boldsymbol{\lambda})$  is a concave function with respect to  $\boldsymbol{\lambda}$  [50]. The inner loops of the proposed algorithms in this chapter (i.e. eMMSEIA and DMMSE) are convergent since the objective function decreases at each iteration. A discussion of the convergence for a special case of the eMMSEIA algorithm can be found in [72]. However, the original problem is non-convex and our solutions are only local minima. Nevertheless, the DMMSE algorithm is shown to converge to a local minimum with better performance compared to the previously known schemes in Sec. 4.4.

## 4.4 Numerical Results

We consider a hexagonal cellular system where each BS is equipped with  $n_t$  transmit antennas and each user has  $n_r$  receive antennas. The users are located uniformly at random. Two tiers of surrounding cells are considered as interference for each cluster. We consider the worst-case scenario for the inter-cluster interference, which will be the condition that interfering BSs transmit at the full allowed power [8, 9, 63, 119]. We define the cooperation factor  $\kappa$  as a number of BSs cooperating on transmission to each user. The  $\kappa$

BSs are assigned to each user so that the corresponding channel norms (or, alternatively, the corresponding received SNRs) are the largest.

The propagation channel between each BS's transmit antennas and mobile user's receive antenna is characterized by path loss, shadowing and Rayleigh fading. The path loss component is proportional to  $d_{km}^{-\beta}$ , where  $d_{km}$  denotes distance from base station  $m$  to mobile user  $k$  and  $\beta = 3.8$  is the path loss exponent. The channel from the transmit antenna  $t$  of the base station  $b$  at the receive antenna  $r$  of the  $k$ th user is given by [9]

$$\mathbf{H}_{k,b}^{(r,t)} = \alpha_{k,b}^{(r,t)} \sqrt{\gamma_0 \rho_{k,b} A \left( \Theta_{k,b}^{(t)} \right) \left( \frac{d_{k,b}}{d_0} \right)^{-\beta}} \quad (4.54)$$

where  $\alpha_{k,b}^{(r,t)} \sim \mathcal{CN}(0, 1)$  represents Rayleigh fading,  $\rho_{k,b}^{(\text{dBm})}$  is the lognormal shadow fading between  $b$ th BS and  $k$ th user with standard deviation of 8 dB, and  $d_0 = 1$  km is the cell radius.  $\gamma_0$  is the interference-free SNR at the cell boundary. We consider one user randomly located per cell for the numerical results.

When sectorization is employed, the transmit antennas are equally divided among the sectors of a cell. Each transmit antenna has a parabolic beam pattern as a function of the direction of the user from the broadside direction of the antenna (For more details refer to [9,120]). The antenna gain is a function of the direction of the user  $k$  from the broadside direction of the  $t$ th transmit antenna of the  $b$ th base station denoted by  $\Theta_{k,b}^{(t)} \in [-\pi, \pi]$ ;  $\Theta_{3\text{dB}}$  is the half-power angle and  $A_s$  is the sidelobe gain. The antenna gain is given as [120]

$$A \left( \Theta_{k,b}^{(t)} \right)_{\text{dB}} = - \min \left( 12 \left( \frac{\Theta_{k,b}^{(t)}}{\Theta_{3\text{dB}}} \right)^2, A_s \right) \quad (4.55)$$

For the 3,6-sector cells  $A_s = 20, 23$  dB and  $\Theta_{3\text{dB}} = \frac{70\pi}{180}, \frac{35\pi}{180}$ , respectively [9, 120, 121]. When there is no sectorization we set  $A = 1$ .

We first compare different algorithms (for the solution of the SRM problem) without enforcing rank constraints on SIN, PWF, SDP relaxation and setting  $d_k = \min(m_{t,k}, m_{r,k}) = n_r$  for the eMMSEIA and DMMSE algorithms. To solve the SRM problem, the weight matrices in the eMMSEIA and DMMSE

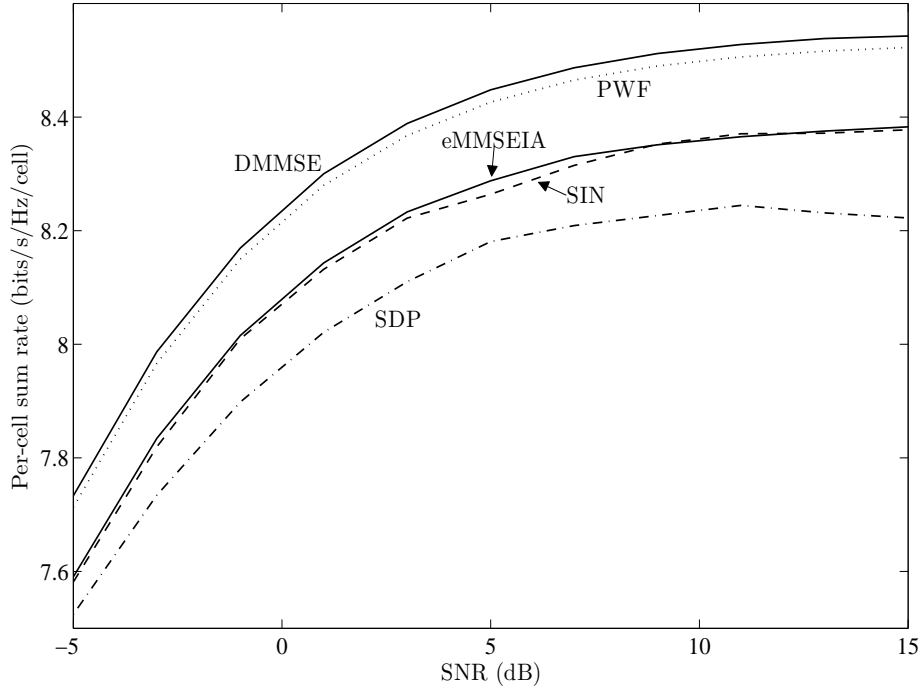


Figure 4.1: Per-cell sum-rate for a MIMO-IFC-GC with  $M = 3$  and  $\kappa = 2$ .

algorithms are updated at each iteration as  $\mathbf{W}_k = \mathbf{E}_k^{-1}$  using the current MSE-matrix  $\mathbf{E}_k$ . Fig. 4.1 compares the per-cell sum-rate of the algorithms discussed in this chapter for a cluster with  $M = 3$  cells and a cooperation factor  $\kappa = 2$ . The results show that our proposed DMMSE algorithm outperforms other techniques, while the polite water-filling algorithm (PWF) [71,75] has a similar performance. Our proposed eMMSEIA scheme converges to a poorer local optimum value compared to these two schemes. The soft interference nulling (SIN) [56] and SDP relaxation [46] algorithms, which use the approximation of the non-convex terms in the objective function, perform worse in this example.

In Fig. 4.2, we evaluate the effect of partial cooperation for the DMMSE, eMMSEIA, and PWF algorithms in a cluster of size  $M = 5$  where each BS is equipped with  $n_t = 4$  transmit antennas, each user employs  $n_r = 2$  receive antennas, and 2 users are dropped randomly in each cell. Recall that the cooperation factor  $\kappa$  represents the number of BSs cooperating in transmission to each user. It can be seen that as  $\kappa$  increases the performance improves with

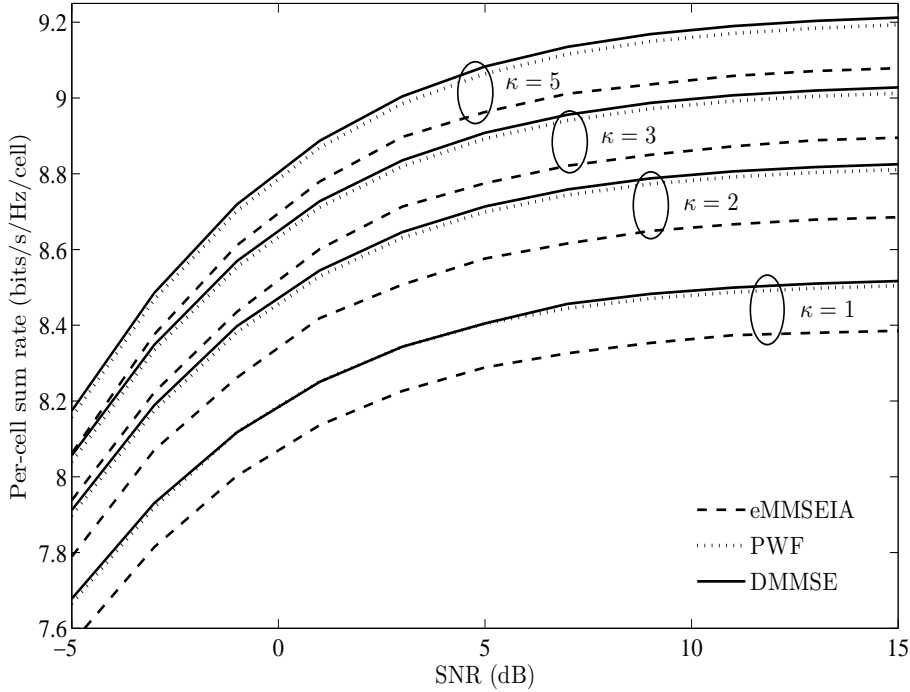


Figure 4.2: Per-cell sum-rate for a MIMO-IFC-GC with  $M = 5$  and  $\kappa = 1, 2, 3, 5$ ,  $n_t = 4$ ,  $n_r = d_k = 2$ , and 2 users per cell.

diminishing returns as  $\kappa$  grows large. Moreover, the relative performance of the algorithms confirms the considerations above.

In Fig. 4.3, we compare again the performance of the schemes considered in Fig. 4.2 but with a stricter requirement on the number of streams, namely  $d_k = 1$ . It can be seen that the proposed DMMSE tends to perform better than PWF, which was not designed to handle rank constraints. We have adopted the PWF algorithm to support  $d_k < \min(m_{t,k}, m_{r,k})$  by using a thin SVD of  $\hat{\mathbf{\Omega}}_k^{-\frac{1}{2}} \mathbf{H}_{k,k}^H \mathbf{\Omega}_k^{-\frac{1}{2}}$  when computing (4.13).

In Fig. 4.4, we vary the size of the cluster  $M$ , showing also the advantages of coordinating transmission over larger clusters, even when the number of cooperating BSs  $\kappa$  is fixed. Recall that  $M$  represents the set of BSs whose transmission is coordinated, but only  $\kappa$  BSs cooperate for transmission to a given user. These  $\kappa$  BSs for each users are selected based on the received signal strength. The  $\kappa$  BSs which has transmit the strongest signals to the user are selected. As an example, for a cluster size of  $M = 7$  a cooperation factor of

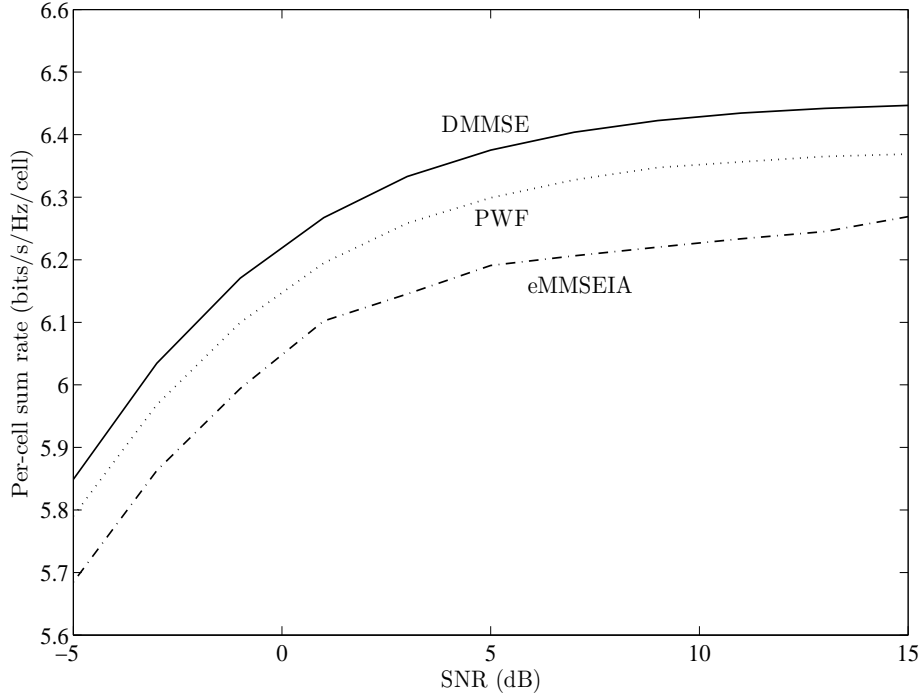


Figure 4.3: Per-cell sum rate of the schemes that can support  $d_k < \min(m_{t,k}, m_{r,k})$  for  $d_k = 1$ ,  $n_t = 4$ ,  $n_r = 2$ ,  $M = 3$  and  $\kappa = 2$ .

$\kappa = 4$  performs almost as well as the full cooperation scenario with  $\kappa = 7$ . This recommends using  $\kappa = 3, 4$  BSs in transmission to each user rather than all  $M = 7$ . Moreover, the performance gains with respect to the non-cooperative case  $\kappa = 1$  are evident. We also show the performance with a cluster containing a single cell, i.e.,  $M = 1$ . This highlights the performance gains attained even in the absence of message sharing among the BSs (i.e.,  $\kappa = 1$ ) due to the coordination of the BSs within the cluster.

Finally, the effect of sectorization is studied in Fig. 4.5 where  $n_t = 6$  transmit antennas at each BS are divided equally into  $S = 1, 3, 6$  sectors. Each cell contains 6 users, each equipped with  $n_r = 2$  receive antennas. The users are randomly located at the distance of  $\frac{2}{3}d_0$  from its BS. For a given channel realization the DMMSE algorithm is used to obtain the per-cell sum rate. The cumulative distribution functions (CDFs) of per-cell sum rates are computed using large number of channel realizations. The gains of sectorization

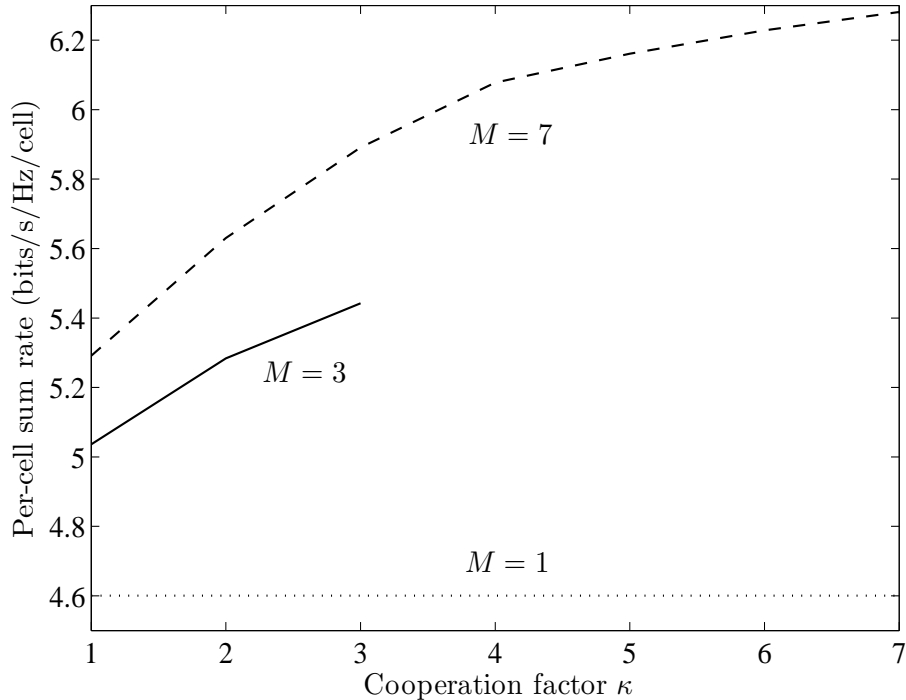


Figure 4.4: Per-cell sum-rate of the proposed DMMSE scheme for cluster sizes  $M = 1, 3, 7$  versus the cooperation factor,  $\kappa$ , with  $n_t = n_r = 2$ , SNR=20 dB, and single-user per cell.

and cooperation are compared. For example, the system with coordination of 7 cells and  $\kappa = 3$  cooperation factor and without sectorization performs better than the sectorized system with  $S = 6$  and without any coordination between the BSs.

## 4.5 Conclusions

In this chapter, we consider a MIMO interference channel with partial cooperation at the BSs and per-BS power constraints. Focusing on linear transmission strategies, we have reviewed some of the available techniques for the maximization of the sum-rate and extended them to the MIMO-IFC-GC when necessary. Moreover, we have proposed two novel strategies for minimization of the weighted mean square error on the data estimates. Specifically, we have proposed an extension of the recently introduced MMSE

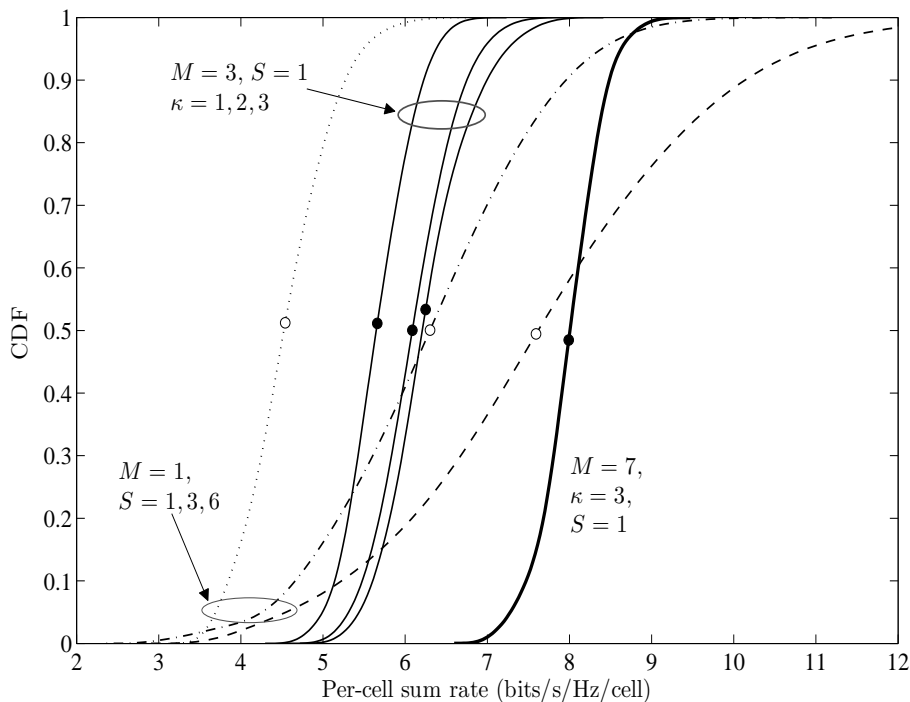


Figure 4.5: CDF of the per-cell sum rates achieved by DMMSE for  $S = 1, 3, 6$  sectors per cell,  $M = 1, 3, 7$  coordinated clusters, and  $\kappa = 1, 2, 3$  cooperation factors with  $\gamma_0 = 20$  dB,  $n_t = 6$ , and  $n_r = 2$ . The circles represent the mean values of the per-cell sum-rates.

interference alignment strategy and a novel strategy termed diagonalized MSE-matrix (DMMSE). Our proposed strategies support transmission of any arbitrary number of data streams per user. Extensive numerical results show that the DMMSE outperforms most previously proposed techniques and performs just as well as the best known strategy. Moreover, our results bring insight into the advantages of partial cooperation and sectorization and the impact of the size of the cooperating cluster of BSs and sectorization.

### Complexity Analysis

We conclude with a brief discussion on the complexity of the algorithms. Due to the difficulty of complete complexity analysis, especially in terms of speed of convergence, we present a discussion based on our simulation experiments. The PWF algorithm converges in almost the same number of

iterations as the DMMSE algorithm. The complexity per iteration of PWF and DMMSE is also almost the same as  $\mathcal{O}(\kappa n_t n_r^2) + \mathcal{O}(n_r^3)$  (required for the thin SVD operation). However, the PWF algorithm contains additional operations (matrix inversion and SVD) to obtain the precoding matrices from the calculated transmit covariance matrices.<sup>6</sup> Also, the PWF algorithm includes a water-filling algorithm within its inner loop, which is not required in the DMMSE algorithm. The eMMSEIA algorithm has lower complexity per iteration (i.e.  $\mathcal{O}(n_r^3)$ ) than the PWF and DMMSE algorithms, since its complexity is due to a matrix inversion per iteration per user. However, eMMSEIA converges in a larger number of iterations than DMMSE and PWF. The complexity per iteration for the SDP relaxation is higher than for the SIN algorithm (this is because of the extra auxiliary positive semi-definite matrix variable,  $\mathbf{Y}$ , introduced in the SDP relaxation algorithm). The SIN algorithm also converges in a smaller number of iterations than the SDP relaxation algorithm.

---

<sup>6</sup>This can be performed together with finding the MMSE receive matrices.

# Chapter 5

## Robust Precoding and Equalization

In the previous chapters, combining precoding at the transmitter and equalization at the receiver is employed to reduce interference in multicell multiuser MIMO systems. Particularly, we focused on linear strategies due to their simplicity and robustness. Although various MIMO linear precoding and equalization techniques have been proposed [29, 31, 74, 114, 122, 123], they mainly assume that the channel state information (CSI) is perfectly known at the transmitter and receiver. In practice, CSI is seldom perfect due to issues such as inaccurate channel estimation process, quantization of CSI, erroneous or limited feedback. In the multicell scenario, the amount of CSI grows with the number of BSs coordinated together. This requires large amount of resources allocated to the channel training, which competes with the resources to be used for the data transmission. Moreover, the length of the channel training sequences are dependent to the coherence time of the channel. One approach is to design the system based on imperfect cross channel information and more accurate local CSI. Consequently, CSI is imperfectly known at the transmitters and the receivers. Inaccurate CSI degrades the performance of the transceivers drastically. This motivates robust linear design of the transmitters and/or receivers [124–138].

Imperfect CSI can be modeled statistically (e.g. if originated by channel estimation process) or deterministically (e.g. when caused by CSI quantization). In these models, the actual channel is assumed to belong to an *uncertainty*

*region*. In the stochastic model, this region is studied probabilistically and it is unbounded. Ideally, the corresponding stochastic robust design optimizes the averaged performance over the entire uncertainty region (see e.g. [134–137]). In this chapter, we consider the *worst-case deterministic* model which assumes that the actual channels lie within a bounded spherical region centered at its estimated value. We are specifically interested in the *worst-case* robust design, because it assures a particular performance level for any channel realization staying in the corresponding uncertainty region and also can characterize instantaneous CSI errors [124–131]. The robust design of linear transceivers based on stochastic CSI will be addressed in the next chapter.

Conventionally, the optimization problem of the worst-case robust linear strategies is approached using semi-definite reformulations (SDR). Although efficient, this approach results in an algorithm with an iterative application of semi-definite programming (SDP). Besides its complexity, SDR approach does not provide a specific structure for the transceivers. Attempts to obtain the structure of the solution for the worst-case robust MMSE precoder assuming pre-fixed equalizer are presented in [129, 131] for the single-user case. However, [131] enforces no power constraint on the system. The result from [129] is further employed in [130] to find the worst-case robust MMSE transceivers. Nonetheless, the proposed algorithm in [130] is based on alternative optimization between precoder and equalizer. Moreover, it involves solving a quintic equation, for which a closed-form solution of the roots is unknown and it must be solved numerically. Nevertheless, [129–131] consider the imperfect knowledge of CSI only in single-user scenario, hence the extension to the multiuser system is not straightforward. An attempt to consider imperfect knowledge of interference plus noise covariance matrix in the single-user case was made in [132] to obtain MMSE equalizers. The results of [132] are only given for the Kullback-Leibler divergence based uncertainty region<sup>1</sup>.

Similar to the case with perfect CSI, the robust design problem in the

---

<sup>1</sup>We consider norm-based uncertainty region, which is more challenging and widely used in related work.

multiuser systems is far more challenging than in the point-to-point scenario. It is even more difficult in the interference channels due to the absence of downlink-uplink duality. The recent trend toward multicell coordinated systems motivates studying the robust transmission strategies in the interference channels [126,139]. Interference channel model emerges in a multicell downlink system, where each base station intends to transmit to its associated users, while the signalling is coordinated across multiple cells. Besides partially cooperative multicell systems can be also modeled as a MIMO interference channel with generalized power constraints [74].

In [126], the problem of robust transceiver design is formulated to maximize the worst-case signal-to-interference-plus-noise-ratio (SINR). First, the SINR expression is approximated with respect to the uncertainty region and therefore the SINR is a function of the bound of error (not the error matrix). Then, a low complexity algorithm is proposed based on alternating optimization of precoders and equalizers. The precoder optimization is performed by SDP using a rank constraint relaxation. [139] investigates the worst-case robust design of precoders in the multicell systems but in single-antenna mobile user case only.

The main contributions of this chapter can be listed as follows:

(i) Our objective is to minimize *weighted sum of mean square errors (WSMSE)* of the estimated symbols. This has been known as a general utility function, which can approximate any performance metric defined as a function of the mean square error (MSE) values (e.g. sum rate, MMSE, see [72,108,109] and the previous chapter for more details).

(ii) The single-user section of this chapter accounts for a wider range of system parameters *all* known inaccurately. In addition to CSI, the imperfect knowledge of interference plus noise covariance matrix, and power shaping matrix are reflected in our design. We first obtain the least favorable interference plus noise covariance and power shaping matrices. Substituting these matrices in the design problem makes it intractable. Hence, we approximate these matrices and derive an upper bound of the worst-case WSMSE objective function. Consequently, we approximate the original problem by minimization

of this upper bound and obtain the exact structures for the precoder and equalizer matrices. Employing these structures, the *joint* precoder and equalizer optimization problem is reduced to a scalar convex problem. Further, the solution to this problem is shown to be characterized by a *depressed quartic equation*, the closed-form expressions for the roots of which are known.

(iii) The results for a single-user case are extended to the multiuser scenario in a MIMO-IFC-GC<sup>2</sup> and using Gauss-Seidel (or Jacobi) algorithm deployed in noncooperative games [141]. Similarly, the structure for a robust precoder and equalizer and worst-case estimation errors are obtained. Finally, we propose a simple iterative algorithm, which is based on our derived structures of the precoders and equalizers and the worst-case channels. Hence, compared to the SDP-based alternating algorithms ([126]) our algorithm performs better while it avoids iterative application of SDP (hence, it is less complex).

The rest of this chapter is organized as follows. Section 5.1 describes the system model, the imperfect CSI model, and introduces the WSMSE minimization problem. We discuss the single-user case in Section 5.2. We first begin with the design of transceivers in the presence of perfect CSI. Then, imperfect knowledge of system matrices is analyzed in Section 5.2.2, where the worst-case error matrices are derived and the robust transceivers are obtained in Section 5.2.3. In Section 5.3, based on the single-user discussion we propose the robust transceiver design for the multiuser scenario. The performance of our algorithms is verified in Section 5.4.

## 5.1 System Model and Problem Formulation

We consider the downlink of a multiuser MIMO system with  $K$  transmitter and receiver pairs, where each transmitter is equipped with  $n_t$  antennas and each receiver employs  $n_r$  antennas. We keep our model which has been introduced in Chapter 2 for the multicell scenario with partial cooperation, i.e. MIMO-IFC-GC. Note that this model can accommodate any type of cooperative

---

<sup>2</sup>We have originally addressed the problem in standard MIMO interference channels in [140]. In this chapter, we have modified it for the model introduced in Chapter 2 for multicell scenario with partial cooperation.

system including MIMO BC and MIMO IFC. The  $k$ th transmitter broadcasts independent data streams denoted by the vector  $\mathbf{u}_k = [u_{k,1}, \dots, u_{k,n_r}]^\top$ , where  $u_{k,j}$  is the  $j$ th data symbol corresponding to the  $k$ th user such that  $\mathbb{E}[|u_{k,j}|^2] = 1$ . For the sake of simplicity, we consider the number of data streams of each user to be equal to the number of receive antennas, i.e.  $n_r$ <sup>3</sup>. The transmitted vector is a result of linear precoding of the symbol vector, i.e.  $\mathbf{x}_k = \mathbf{F}_k \mathbf{u}_k$ , using the precoder matrix  $\mathbf{F}_k \in \mathbb{C}^{n_t \times n_r}$ . For more details of the system model, refer to Section 2.2.1. channel between the  $l$ th transmitter and the  $k$ th receiver is characterized by the matrix  $\mathbf{H}_{k,l} \in \mathbb{C}^{n_r \times n_t}$ . The receiver  $k$  observes the signal

Our objective is to minimize the weighted sum of MSE (WSMSE) values of the estimated data symbols, which can be summarized in the following optimization problem:

$$\begin{aligned} & \underset{\mathbf{F}_k, \mathbf{G}_k, \forall k}{\text{minimize}} && \sum_{k=1}^K \text{tr} \{ \mathbf{W}_k \mathbf{E}_k \} \\ & \text{subject to} && \sum_{k=1}^K \text{tr} \{ \Phi_{k,m} \mathbf{F}_k \mathbf{F}_k^H \} \leq P_m, m = 1, \dots, M \end{aligned} \quad (5.1)$$

where the optimization is over all precoders  $\mathbf{F}_k$  and equalizers  $\mathbf{G}_k \in \mathbb{C}^{n_r \times n_r}$  with given diagonal weight matrices  $\mathbf{W}_k = \text{diag}[w_{k,1}, \dots, w_{k,n_r}]$  with non-negative elements  $w_{k,j} \geq 0$ . This problem is called *weighted sum of MSE minimization (WMMSE)* problem (see [74, 108, 122] for details). It is shown that any performance metric characterized by sum of some particular function of the MSE-matrices  $\mathbf{E}_k$ ,  $f_k(\mathbf{E}_k)$ , can be approximated using the problem (5.1) [72–74, 108, 109, 122]. The approach is that at each iteration, we select  $\mathbf{W}_k = \nabla_{\mathbf{E}_k} f_k(\bar{\mathbf{E}}_k)^\top$  at the operating point  $\bar{\mathbf{E}}_k$ , then solve the optimization problem (5.1). The algorithm iterates until the convergence is achieved. For example, to adopt sum rate maximization one can select  $\mathbf{W}_k = \bar{\mathbf{E}}_k^{-1}$  at each iteration.

The main challenge in our design is to account for imperfect knowledge of channel matrices  $\mathbf{H}_{k,l}$  for all  $1 \leq l, k \leq K$ . The inaccurate channel estimations,  $\hat{\mathbf{H}}_{k,l}$ , are assumed to be available at both transmitters and receivers. The

---

<sup>3</sup>The number of data streams for user  $k$  in the previous chapter could take any value of  $d_k \leq n_r$ .

unknown actual channels must belong to some uncertainty regions around the estimated value. Here, we consider a class of *uncertainty regions*, for which the Frobenius norms of the channel estimation errors are bounded. The actual channel matrix between the  $k$ th receiver and the  $l$ th transmitter is a sum of an estimated value and an error, and therefore the corresponding uncertainty region can be defined as a ball with a specified radius  $\varepsilon_{H_{k,l}}$  centered at the estimated value  $\widehat{\mathbf{H}}_{k,l}$

$$\mathcal{B}_{k,l} = \left\{ \mathbf{H}_{k,l} : \mathbf{H}_{k,l} = \widehat{\mathbf{H}}_{k,l} + \Delta_{H_{k,l}}, \|\Delta_{H_{k,l}}\| \leq \varepsilon_{H_{k,l}} \right\}. \quad (5.2)$$

The *worst-case robust design* must guarantee a particular performance level for any channel matrix staying in the corresponding uncertainty region. Thus, this problem can be described as

$$\begin{aligned} & \underset{\mathbf{F}_k, \mathbf{G}_k, \forall k}{\text{minimize}} && \max_{\substack{\mathbf{H}_{k,l} \in \mathcal{B}_{k,l} \\ 1 \leq k, l \leq K}} \sum_{k=1}^K \text{tr} \{ \mathbf{W}_k \mathbf{E}_k \} \\ & \text{subject to} && \text{tr} \{ \Phi_{k,m} \mathbf{F}_k \mathbf{F}_k^H \} \leq P_k, k = 1, \dots, K. \end{aligned} \quad (5.3)$$

## 5.2 Single-user Case

We first address the single-user case ( $K = 1$ ). The analysis presented in this section is the basis for that of the multiuser system in Section 5.3. For ease of exposition, we drop the index  $k$  in this section. We also consider that a power constraint  $\text{tr} \{ \Phi \mathbf{F} \mathbf{F}^H \} \leq P$  on the linear precoder is enforced and we refer to the weight matrix  $\Phi$  in the power constraint as *power shaping matrix*. This matrix also characterizes the direction in which the transmitted power can propagate, while reducing the interference in other directions (e.g., to other users in a multiuser case). Moreover, we assume that the matrix  $\Phi$  is full rank and square of size  $n_t$ . This is a practical assumption because if  $\Phi$  is a rank deficient matrix then one can always transmit infinite power in one direction (corresponding to a zero eigenvector of  $\Phi$ ) without violating the power constraint. Please note that when  $\Phi = \mathbf{I}$ , the sum power constraint emerges. Additionally, we assume that the noise at the receiver is correlated and its covariance matrix is  $\Omega = \mathbb{E} [\mathbf{nn}^H]$ . We note that the consideration of power shaping matrix  $\Phi$  and correlation of the noise vector only belongs to the

single-user case discussed in this section. In the multiuser context, we return to the original system definition specified in Section 5.1 and the problem (5.3) with the known per-transmitter power constraints. Hereinafter (in the single-user scenario), we call the matrices  $\mathbf{H}$ ,  $\Phi$ , and  $\Omega$  the *system matrices*. Unlike most of the related work in point-to-point MIMO systems, we account for the inaccurate knowledge of *all* of these system matrices.

*Remark 5.1.* The introduction of the matrices  $\Phi$  and  $\Omega$  and their corresponding uncertainties are limited to the single-user case. In the multiuser scenario, we consider per-transmitter power constraints. The system matrices and their uncertainties are  $\mathbf{H}_{k,l}$  and their uncertainties. When the multiuser problem is mapped to a number of single-user problems, then the introduction of matrices  $\Phi$  and  $\Omega$  serves to find a robust transceiver. In the multiuser problem when we look at a single user  $k$ , matrix  $\mathbf{H}$  represents the individual user channels for each user (i.e.  $\mathbf{H}_{k,k}$ ) and matrices  $\Phi$  and  $\Omega$  are defined from the cross channel matrices (i.e.  $\mathbf{H}_{k,l}, \mathbf{H}_{l,k}, \forall l \neq k$ ).

### 5.2.1 Perfect Knowledge of System Matrices

In this section, we state joint precoder and equalizer optimization problem when the system matrices are perfectly known. This provides a foundation for the worst-case robust design. Joint MMSE transceiver optimization with perfect CSI has been investigated in [114,122,123]. Here, we extend the results given in [114,122] to our system model, which also includes the power shaping matrix. More detailed discussion of this problem with generalized constraints is given in [74] and the previous chapter. Here, we also give a shorter proof with a different approach to a special case of this problem. The transceiver optimization problem can be posed as an optimization problem

$$\begin{aligned} & \underset{\mathbf{G}, \mathbf{F}}{\text{minimize}} && \text{tr} \{ \mathbf{W} \mathbf{E} \} \\ & \text{subject to} && \text{tr} \{ \Phi \mathbf{F} \mathbf{F}^H \} \leq P \end{aligned} \tag{5.4}$$

where  $\mathbf{E}$  is defined from (2.16).

**Lemma 5.1.** [74] *For any channel matrix  $\mathbf{H}$  and given the full rank and square matrices  $\Phi$  and  $\Omega$ , the optimum precoding and equalization matrices of*

the problem (5.4) have the following structure

$$\mathbf{F} = \Phi^{-\frac{1}{2}} \mathbf{V} \Sigma, \quad (5.5)$$

$$\mathbf{G} = \Lambda \mathbf{U}^H \Omega^{-\frac{1}{2}}. \quad (5.6)$$

where  $\Sigma$  and  $\Lambda$  are diagonal matrices with the diagonal elements  $\sigma_i \geq 0$  and  $\lambda_i \geq 0, i = 1, \dots, n_r$ , respectively.  $\mathbf{U} \in \mathbb{C}^{n_r \times n_r}$  and  $\mathbf{V} \in \mathbb{C}^{n_t \times n_r}$  are obtained by performing the singular value decomposition (SVD) of the following matrix

$$\Omega^{-\frac{1}{2}} \mathbf{H} \Phi^{-\frac{1}{2}} = \mathbf{U} [\mathbf{\Gamma} \ \mathbf{0}_{n_r \times n_t - n_r}] \begin{bmatrix} \mathbf{V} & \check{\mathbf{V}} \end{bmatrix}^H, \quad (5.7)$$

in which  $\mathbf{\Gamma}$  contains its  $n_r$  nonzero eigenvalues and  $\check{\mathbf{V}} \in \mathbb{C}^{n_t \times (n_t - n_r)}$  contains the right singular vectors corresponding to the zero eigenvalues<sup>4</sup>.

*Proof.* The proof is given in Section 5.A. □

## 5.2.2 Imperfect Knowledge of System Matrices

Now, we include the imperfect knowledge of system matrices. It is assumed that the estimates,  $\hat{\mathbf{H}}$  and  $\hat{\Omega} \succeq \mathbf{0}$  and  $\hat{\Phi} \succeq \mathbf{0}$ , are available at both ends. Specifically, the actual value of these matrices can be described as the sum of the estimation value and the error matrices. Consequently, the corresponding uncertainty region can be characterized by

$$\begin{aligned} \mathcal{B} = \left\{ (\mathbf{H}, \Omega, \Phi) : \mathbf{H} = \hat{\mathbf{H}} + \Delta_H, \|\Delta_H\| \leq \varepsilon_H, \right. \\ \Omega = \hat{\Omega} + \Delta_\Omega \succeq \mathbf{0}, \|\Delta_\Omega\| \leq \varepsilon_\Omega, \\ \left. \Phi = \hat{\Phi} + \Delta_\Phi \succeq \mathbf{0}, \|\Delta_\Phi\| \leq \varepsilon_\Phi \right\}. \end{aligned} \quad (5.8)$$

The worst-case transceiver design can be expressed as

$$\begin{aligned} & \underset{\mathbf{F}, \mathbf{G}}{\text{minimize}} && \max_{(\mathbf{H}, \Omega, \Phi) \in \mathcal{B}} \text{tr} \{ \mathbf{W} \mathbf{E} \} \\ & \text{subject to} && \text{tr} \{ \Phi \mathbf{F} \mathbf{F}^H \} \leq P. \end{aligned} \quad (5.9)$$

*Remark 5.2.* Our proposed solution for the multiuser scenario is based on a so-called Jacobi (or Gauss-Seidel) algorithm [141], where at every step of

---

<sup>4</sup>The matrix  $\Omega^{-\frac{1}{2}} \mathbf{H} \Phi^{-\frac{1}{2}}$  with probability one has a rank of  $n_r$ , due to the random nature of the channel matrix  $\mathbf{H}$  and the fact that  $n_r \leq n_t$ .

the algorithm we consider a single user (user  $k$ ) problem while other users' transmission strategies ( $\forall l \neq k$ ) are fixed. Hence, we optimize the total performance (e.g. WSMSE) function over the precoder and equalizer of user  $k$  and this iterates until convergence. Each single user problem accounts two types of interference, one is coming from other users and the other is sent out to other users by user  $k$ . These interference covariance matrices are dependent on the cross link channel matrices (i.e.  $\mathbf{H}_{k,l}$  and  $\mathbf{H}_{l,k}, \forall l \neq k$ ) rather than the local channel matrix  $\mathbf{H}_{k,k}$ . The two matrices  $\mathbf{\Omega}$  and  $\mathbf{\Phi}$  and their corresponding uncertainties represent these two types of interference and their uncertainties, and they are separated from the local channel uncertainty of  $\mathbf{H}_{k,k}$ .

**Least Favorable Matrices  $\mathbf{\Delta}_\Omega$  and  $\mathbf{\Delta}_\Phi$ :** We proceed by finding the worst-case estimation errors for the system matrices. First, we expand the objective function in terms of the estimated system and error matrices and simplify the worst-case problem with some calculations as

$$\begin{aligned} & \underset{\mathbf{\Delta}_H, \mathbf{\Delta}_\Phi, \mathbf{\Delta}_\Omega}{\text{maximize}} \quad \text{tr} \left\{ \mathbf{W}\widehat{\mathbf{E}} \right\} + \text{tr} \left\{ \mathbf{G}^H \mathbf{W} \mathbf{G} \mathbf{\Delta}_\Omega \right\} \\ & \quad \quad \quad + \text{tr} \left\{ \mathbf{A} \mathbf{\Delta}_H \mathbf{B} \mathbf{\Delta}_H^H \right\} + 2\Re \left\{ \text{tr} \left\{ \mathbf{C} \mathbf{\Delta}_H \right\} \right\} \\ & \text{subject to} \quad \text{tr} \left\{ \widehat{\mathbf{\Phi}} \mathbf{F} \mathbf{F}^H \right\} \leq P - \text{tr} \left\{ \mathbf{\Delta}_\Phi \mathbf{F} \mathbf{F}^H \right\} \\ & \quad \quad \quad \|\mathbf{\Delta}_H\| \leq \varepsilon_H, \|\mathbf{\Delta}_\Omega\| \leq \varepsilon_\Omega, \|\mathbf{\Delta}_\Phi\| \leq \varepsilon_\Phi \end{aligned} \quad (5.10)$$

where

$$\begin{aligned} \widehat{\mathbf{E}} = & \mathbf{G} \widehat{\mathbf{H}} \mathbf{F} \mathbf{F}^H \widehat{\mathbf{H}}^H \mathbf{G}^H - \mathbf{G} \widehat{\mathbf{H}} \mathbf{F} \\ & - \mathbf{F}^H \widehat{\mathbf{H}}^H \mathbf{G}^H + \mathbf{G} \widehat{\mathbf{\Omega}} \mathbf{G}^H + \mathbf{I}. \end{aligned} \quad (5.11)$$

and

$$\mathbf{A} = \mathbf{G}^H \mathbf{W} \mathbf{G}, \quad (5.12)$$

$$\mathbf{B} = \mathbf{F} \mathbf{F}^H, \quad (5.13)$$

$$\mathbf{C} = \mathbf{F} \mathbf{F}^H \widehat{\mathbf{H}}^H \mathbf{G}^H \mathbf{W} \mathbf{G} - \mathbf{F} \mathbf{W} \mathbf{G} \quad (5.14)$$

The least favorable interference plus noise covariance matrix is a result of following problem extracted from (5.10)

$$\begin{aligned} & \underset{\|\mathbf{\Delta}_\Omega\| \leq \varepsilon_\Omega}{\text{maximize}} \quad \text{tr} \left\{ \mathbf{G}^H \mathbf{W} \mathbf{G} \mathbf{\Delta}_\Omega \right\} \\ & \text{subject to} \quad \widehat{\mathbf{\Omega}} + \mathbf{\Delta}_\Omega \succeq \mathbf{0}. \end{aligned} \quad (5.15)$$

First, we relax the positive semi-definite condition in (5.15) by ignoring it <sup>5</sup>. Using Cauchy-Schwartz inequality, we obtain

$$\text{tr} \{ \mathbf{G}^H \mathbf{W} \mathbf{G} \Delta_{\Omega} \} \leq \| \mathbf{G}^H \mathbf{W} \mathbf{G} \| \cdot \| \Delta_{\Omega} \| \leq \varepsilon_{\Omega} \| \mathbf{G}^H \mathbf{W} \mathbf{G} \| \quad (5.16)$$

and the upper bound occurs when

$$\Delta_{\Omega}^* = \varepsilon_{\Omega} \frac{\mathbf{G}^H \mathbf{W} \mathbf{G}}{\| \mathbf{G}^H \mathbf{W} \mathbf{G} \|}. \quad (5.17)$$

Note that since  $\widehat{\Omega} \succeq \mathbf{0}$  and  $\Delta_{\Omega}^* \succeq \mathbf{0}$  then  $\widehat{\Omega} + \Delta_{\Omega}^* \succeq \mathbf{0}$ , which means that the relaxed constraint on problem (5.15) is also satisfied.

Trivially, the worst-case estimation error of the interference direction matrix, i.e.  $\Delta_{\Phi}$ , happens when the maximum allowed power is minimized. Consequently, we solve the problem

$$\begin{aligned} & \underset{\| \Delta_{\Phi} \| \leq \varepsilon_{\Phi}}{\text{maximize}} && \text{tr} \{ \Delta_{\Phi} \mathbf{F} \mathbf{F}^H \} \\ & \text{subject to} && \widehat{\Phi} + \Delta_{\Phi} \succeq \mathbf{0} \end{aligned} \quad (5.18)$$

Similarly to the problem (5.15), the worst-case error matrix can be expressed as

$$\Delta_{\Phi}^* = \varepsilon_{\Phi} \frac{\mathbf{F} \mathbf{F}^H}{\| \mathbf{F} \mathbf{F}^H \|}. \quad (5.19)$$

Again, the positive semi-definite condition will be satisfied by this choice of  $\Delta_{\Phi}^*$ .

Substituting these worst-case estimation errors  $\Delta_{\Phi}^*$  and  $\Delta_{\Omega}^*$  into problem (5.9) results in the terms  $\varepsilon_{\Omega} \| \mathbf{G}^H \mathbf{W} \mathbf{G} \|$  and  $\varepsilon_{\Phi} \| \mathbf{B} \mathbf{B}^H \|$ . These exact worst-case values involves the precoder and equalizer in complicated forms, which makes the resulting optimization problem intractable. Therefore, we use approximations of these terms and minimize an upper bound of the worst-case WSMSE.

*Remark 5.3.* Our robust transceiver design is in a form of a min-max problem:

$$\underset{x \in \mathfrak{X}}{\text{minimize}} \quad \max_{y \in \mathfrak{Y}} f(x, y) \quad (5.20)$$

If we have  $f(x, y) \leq g(x, y), \forall x \in \mathfrak{X}, y \in \mathfrak{Y}$ , then  $\max_y f(x, y) \leq \max_y g(x, y)$  and therefore minimizing an upper bound on a function over  $x$  will minimize

---

<sup>5</sup>Nevertheless, this relaxation will give us a solution, which also satisfies the positive semi-definite constraint.

the function over  $x$  as well. Although this does not give the globally optimal solution, it is widely used in design of communication systems (e.g.  $\mathcal{Q}(x) \leq \frac{1}{2} \exp(-x^2/2)$ ).

Aligned with this, we can write inequalities

$$\varepsilon_\Omega \|\mathbf{G}^H \mathbf{W} \mathbf{G}\| \leq \varepsilon_\Omega \|\mathbf{W}^{\frac{1}{2}} \mathbf{G}\|^2 = \varepsilon_\Omega \text{tr} \{ \mathbf{G}^H \mathbf{W} \mathbf{G} \} \quad (5.21)$$

$$\varepsilon_\Phi \|\mathbf{F} \mathbf{F}^H\| \leq \varepsilon_\Phi \|\mathbf{F}\|^2 = \varepsilon_\Phi \text{tr} \{ \mathbf{F} \mathbf{F}^H \}. \quad (5.22)$$

We have used the inequality  $\|\mathbf{X} \mathbf{Y}\| \leq \|\mathbf{X}\| \cdot \|\mathbf{Y}\|$ , which can be proved utilizing the Cauchy-Schwartz inequality [96]. Substituting  $\mathbf{Y} = \mathbf{X}^H$  and taking advantage of the fact that the Frobenius norm is invariant under the Hermitian operation, we get  $\|\mathbf{X} \mathbf{X}^H\| \leq \|\mathbf{X}\|^2$ . Now, we replace the terms  $\text{tr} \{ \mathbf{G}^H \mathbf{W} \mathbf{G} \Delta_\Omega \}$  and  $\text{tr} \{ \mathbf{F} \mathbf{F}^H \Delta_\Phi \}$  in the robust transceiver design problem (5.10) with the upper bounds defined in (5.21) and (5.22) respectively. This is equivalent to setting

$$\mathbf{\Omega}^* = \widehat{\mathbf{\Omega}} + \varepsilon_\Omega \mathbf{I}, \quad (5.23)$$

$$\mathbf{\Phi}^* = \widehat{\mathbf{\Phi}} + \varepsilon_\Phi \mathbf{I}. \quad (5.24)$$

**Least Favorable Channel Error Matrix  $\Delta_H$ :** The optimization problem that can find the worst-case channel estimation error  $\Delta_H$  can be extracted from (5.10) as

$$\underset{\|\Delta_H\| \leq \varepsilon_H}{\text{maximize}} \quad \text{tr} \{ \mathbf{A} \Delta_H \mathbf{B} \Delta_H^H \} + 2\Re \{ \text{tr} \{ \mathbf{C} \Delta_H \} \}. \quad (5.25)$$

**Lemma 5.2.** *The optimal solution of the optimization problem (5.25) has the following structure:*

$$\Delta_H^* = \mathbf{\Omega}^{\frac{1}{2}} \widehat{\mathbf{U}} \bar{\mathbf{\Delta}} \widehat{\mathbf{V}}^H \mathbf{\Phi}^{\frac{1}{2}}, \quad (5.26)$$

where  $\widehat{\mathbf{U}} \in \mathbb{C}^{n_r \times n_r}$  and  $\widehat{\mathbf{V}} \in \mathbb{C}^{n_r \times n_t}$  are defined in the SVD

$$\mathbf{\Omega}^{-\frac{1}{2}} \widehat{\mathbf{H}} \mathbf{\Phi}^{-\frac{1}{2}} = \widehat{\mathbf{U}} \begin{bmatrix} \widehat{\mathbf{\Gamma}} & \mathbf{0}_{n_r \times n_t - n_r} \end{bmatrix} \begin{bmatrix} \widehat{\mathbf{V}} & \check{\mathbf{V}} \end{bmatrix}^H, \quad (5.27)$$

and  $\bar{\mathbf{\Delta}} \in \mathbb{R}^{n_r \times n_r}$  is a diagonal matrix with elements  $\bar{\delta}_i \geq 0$ .

*Proof.* The detailed proof can be found in the Section 5.B. □

In order to explain our proposed transceiver optimization algorithm, here we only summarize the approach and results of this proof. The problem (5.25) can be categorized as a *trust-region subproblem* [142, 143]. The matrix-form restatement of this problem is given in [129]. It has been shown that the solution to this problem can be found by minimization over an auxiliary variable  $\vartheta \geq \lambda_{\max}(\mathbf{A})\lambda_{\max}(\mathbf{B})$  [142, 143]. The worst-case channel matrices coincide with a structure of the precoding and equalization matrices given in (5.5) and (5.6) using the worst-case interference plus noise and power shaping matrices defined in (5.23) and (5.24). As a result,  $\bar{\delta}_i$  is given by

$$\bar{\delta}_i = \frac{w_i \lambda_i \sigma_i (\gamma_i \lambda_i \sigma_i - 1)}{\vartheta - w_i \lambda_i^2 \sigma_i^2}, i = 1, \dots, n_r. \quad (5.28)$$

Note that  $\gamma_i, i = 1, \dots, n_r$  are the diagonal elements of  $\hat{\mathbf{\Gamma}}$  in (5.27) and  $\sigma_i$  and  $\lambda_i$  are diagonal elements of  $\mathbf{\Sigma}$  and  $\mathbf{\Lambda}$  defined in (5.5-5.6) (It is also shown that the precoder and equalizer follow structures given in (5.5-5.6)). Recognizing  $j = \operatorname{argmax}_i (w_i \lambda_i^2 \sigma_i^2)$ , if  $\vartheta > w_j \lambda_j^2 \sigma_j^2$ , then  $\vartheta$  is the root of equation

$$\sum_{i=1}^{n_r} \frac{w_i^2 \lambda_i^2 \sigma_i^2 (\gamma_i \lambda_i \sigma_i - 1)^2}{(\vartheta - w_i \lambda_i^2 \sigma_i^2)^2} = \tilde{\varepsilon}_H^2. \quad (5.29)$$

If  $\vartheta = w_j \lambda_j^2 \sigma_j^2$ ,  $\bar{\delta}_j$  cannot be found from equation (5.28). We define

$$\rho(\vartheta) = \sum_{i \neq j} \frac{w_i^2 \lambda_i^2 \sigma_i^2 (\gamma_i \lambda_i \sigma_i - 1)^2}{(\vartheta - w_i \lambda_i^2 \sigma_i^2)^2}. \quad (5.30)$$

Therefore, if  $\rho(w_j \lambda_j^2 \sigma_j^2) < \tilde{\varepsilon}_H^2$ , then  $\bar{\delta}_j = -\sqrt{\tilde{\varepsilon}_H^2 - \rho(\vartheta)}$ . Otherwise,  $\vartheta > w_j \lambda_j^2 \sigma_j^2$  and it can be uniquely determined by (5.29).

### 5.2.3 Robust Transceiver Design

Now, we can use the worst-case system matrices descriptions (5.23), (5.24), and (5.26)-(5.28) and substitute into the problem (5.9). Note that using the trust-region subproblems [142, 143] the resultant problem of finding worst-case channel estimation errors  $\mathbf{\Delta}$  becomes a minimization problem over an auxiliary variable  $\vartheta$ . This translates the overall problem into a minimization problem over  $\vartheta, \mathbf{F}, \mathbf{G}$ . The following result can be obtained from this discussion:

**Theorem 5.1.** *The robust precoding and equalization matrices have the following structure:*

$$\mathbf{F} = \left( \widehat{\Phi} + \varepsilon_{\Phi} \mathbf{I} \right)^{-\frac{1}{2}} \widehat{\mathbf{V}} \Sigma \quad (5.31)$$

$$\mathbf{G} = \Lambda \widehat{\mathbf{U}}^H (\Omega + \varepsilon_{\Omega} \mathbf{I})^{-\frac{1}{2}} \quad (5.32)$$

where

(i)  $\widehat{\mathbf{U}} \in \mathbb{C}^{n_r \times n_r}$  and  $\widehat{\mathbf{V}} \in \mathbb{C}^{n_t \times n_t}$  are orthonormal matrices defined by the thin SVD

$$\left( \widehat{\Omega} + \varepsilon_{\Omega} \mathbf{I} \right)^{-\frac{1}{2}} \widehat{\mathbf{H}} \left( \widehat{\Phi} + \varepsilon_{\Phi} \mathbf{I} \right)^{-\frac{1}{2}} = \widehat{\mathbf{U}} \widehat{\Gamma} \widehat{\mathbf{V}}^H \quad (5.33)$$

where  $\widehat{\Gamma} \in \mathbb{C}^{n_r \times n_r}$  is a diagonal matrix with diagonal elements of  $\gamma_i \geq 0$ ,

(ii)  $\Lambda$  and  $\Sigma$  are diagonal matrices of size  $n_r$  with the diagonal elements of  $\lambda_i, i = 1, \dots, n_r$  and  $\sigma_i, i = 1, \dots, n_r$ , respectively and they are obtained by solving the scalar optimization problem

$$\begin{aligned} & \underset{\substack{\lambda_i, \sigma_i, \vartheta \\ 1 \leq i \leq n_r}}{\text{minimize}} && \sum_{i=1}^{n_r} \frac{\vartheta w_i (\sigma_i \lambda_i \gamma_i - 1)^2}{\vartheta - w_i \lambda_i^2 \sigma_i^2} + \sum_{i=1}^{n_r} w_i \lambda_i^2 + \vartheta \varepsilon_H^2 \\ & \text{subject to} && \vartheta \geq w_i \lambda_i^2 \sigma_i^2, \quad i = 1, \dots, n_r \\ & && \sum_{i=1}^{n_r} \sigma_i^2 \leq P \end{aligned} \quad (5.34)$$

(iii) The optimum solutions for  $\lambda_i$  and  $\sigma_i$  are given by

$$\lambda_i = \sqrt{r_i \sqrt{\frac{\mu}{w_i}}}, \quad (5.35)$$

$$\sigma_i = \sqrt{r_i \sqrt{\frac{w_i}{\mu}}}, \quad (5.36)$$

where  $r_i$  is a positive real root of the quartic equation

$$\begin{aligned} \varphi_i(r) = & \sqrt{\mu} w_i^2 r^4 - w_i \vartheta (2\sqrt{\mu} + \sqrt{w_i} \gamma_i) r^2 \\ & + (\gamma_i^2 \vartheta + w_i) \sqrt{w_i} \vartheta r + \vartheta^2 (\sqrt{\mu} - \gamma_i \sqrt{w_i}) = 0. \end{aligned} \quad (5.37)$$

$\mu > 0$  is the Lagrangian multiplier corresponding to the power constraint, which satisfies  $\mu (\sum_{i=1}^{n_r} \sigma_i^2 - P) = 0$  and  $\vartheta > \max_i (w_i \lambda_i^2 \sigma_i^2)$  satisfies (5.29). Also, the closed-form solutions for the roots of the quartic equation (5.37) can be obtained using the Ferrari's method [144] and can be found in the proof.

*Proof.* The proof is given in Section 5.C.  $\square$

Our proposed robust precoder and equalizer are functions of the auxiliary variables  $\vartheta$  and  $\mu$ . Using dual decomposition concept from [145], we decompose the problem into subproblems. Hence, we can update the auxiliary variables  $\vartheta$  and  $\mu$  using the subgradient directions [115]. By differentiating the objective function in problem (5.34) with respect to  $\vartheta$ , we can obtain the subgradient direction for  $\vartheta$  as

$$\Delta_{\vartheta} = \begin{cases} \tilde{\varepsilon}_H^2 - \sum_{i=1}^{n_r} \frac{w_i \lambda_i^2 \sigma_i^2 (\lambda_i \sigma_i \gamma_i - 1)^2}{(\vartheta - w_i \lambda_i^2 \sigma_i^2)^2} & \vartheta > w_j \lambda_j^2 \sigma_j^2 \\ \tilde{\varepsilon}_H^2 - \rho(\vartheta) & \vartheta = w_j \lambda_j^2 \sigma_j^2 \end{cases} \quad (5.38)$$

Similarly, by differentiation of the Lagrangian function of (5.34), we can get the subgradient direction for  $\mu$  as  $\Delta_{\mu} = \sum_{i=1}^{n_r} \sigma_i^2 - P$ . The robust transceiver optimization algorithm is summarized in Table 5.1.

Table 5.1: Worst-Case Robust Transceiver Design Algorithm (Single-user)

---

Initialize  $\sigma_i$ s and  $\lambda_i$ s and  $\mu > 0$ ,  $\vartheta > \max_i (w_i \lambda_i^2 \sigma_i^2)$ .

Perform thin SVD (5.33) to obtain  $\gamma_i$ s.

**Repeat** (subgradient loop of  $\vartheta$ )

Update  $\vartheta \leftarrow \vartheta + \delta_{\vartheta} \Delta_{\vartheta}$  using (5.38).

**Repeat** (subgradient loop of  $\mu$ )

Form the quartic equation (5.37) for  $i = 1, \dots, n_r$ .

Find its positive real root.

Find  $\sigma_i$  and  $\lambda_i$  using (5.35) and (5.36).

Update  $\mu \leftarrow \mu + \delta_{\mu} \Delta_{\mu}$ .

**Until**  $|\sum_{i=1}^{n_r} \sigma_i^2 - P| \leq \epsilon_0$

**Until** satisfaction of (5.29)

Substitute  $\lambda_i$ s and  $\sigma_i$ s into (5.31) and (5.32) and find  $\mathbf{F}$  and  $\mathbf{G}$ .

---

*Remark 5.4.* The algorithm explained in Table 5.1 contains of two loops. The inner loop attempts to find the optimal values of  $\lambda_i$  and  $\sigma_i$  by solving the necessary conditions and then update the Lagrangian multiplier  $\mu$ . We use a subgradient algorithm to update  $\mu$  to satisfy the power constraints. The subgradient algorithm is convergent (with proper selection of the step sizes [115]) due to the fact that the dual function  $\inf_{\lambda_i, \sigma_i, \forall i} \mathcal{L}(\lambda_i, \sigma_i; \mu)$  is a concave function with respect to  $\mu$  [50]. The outer loop updates the auxiliary variable  $\vartheta$ . If we calculate the second derivative of the objective function of (5.34) with

respect to  $\vartheta$  (first derivative is shown in (5.38)), it is positive in the domain  $\vartheta > w_j \lambda_j \sigma_j$  and consequently the objective function is convex with respect to  $\vartheta$ . Therefore, the subgradient method is also convergent.

*Remark 5.5.* Special case of the problem (5.9) has been discussed in [130] where  $\mathbf{W} = \mathbf{I}$  and  $\mathbf{\Omega} = \mathbf{I}$  and  $\mathbf{\Phi} = \mathbf{I}$  (and perfectly known at both ends). However, the resulting transceiver design relies on alternating optimization between precoder and equalizer. It also involves solving a quintic equation for each of precoder and equalizer optimization, for which a closed-form solution does not exist and the equation has to be solved numerically. Also, this approach is not easily extendable to the multiuser scenario.

### 5.3 Multiuser Case ( $K > 1$ )

In this section, we use the results established in the single-user case to solve the corresponding multiuser problem. We begin with the case of perfect channel knowledge.

#### 5.3.1 Perfect Channel Knowledge

Consider the WSMSE minimization problem (5.1). This problem is jointly non-convex in terms of all precoding and equalization matrices  $\mathbf{F}_k$  and  $\mathbf{G}_k$ . Hence, we use an iterative approach to optimize the transceivers for each user by fixing other users' transceivers [74]. Since the utility function is minimized at each optimization step, the iterative approach must be convergent. Substituting the MSE-matrix given in (2.16) into problem (5.1), we obtain the WSMSE function, which is a convex quadratic function in terms of each  $\mathbf{F}_k$  and  $\mathbf{G}_k$ . Now, we focus on the transceiver optimization problem for each user  $k$  assuming that other users' transceivers, i.e.  $(\mathbf{G}_l, \mathbf{F}_l), \forall l \neq k$  are fixed. We can use the method of Lagrange duality and Karush-Kuhn-Tucker (KKT) conditions [115] to solve this optimization problem. The Lagrangian function

can be formed as

$$\mathcal{L}(\mathbf{G}_k, \mathbf{F}_k, \boldsymbol{\mu}) = \sum_{k=1}^K \text{tr} \{ \mathbf{W}_k \mathbf{E}_k \} + \sum_{k=1}^K \text{tr} \left\{ \left( \sum_{m=1}^M \mu_m \boldsymbol{\Phi}_{k,m} \right) \mathbf{F}_k \mathbf{F}_k^H \right\} - \sum_{m=1}^M \mu_m P_m \quad (5.39)$$

The corresponding zero gradient KKT conditions for user  $k$ ,  $\nabla_{\mathbf{F}_k} \mathcal{L} = 0$  and  $\nabla_{\mathbf{G}_k} \mathcal{L} = 0$ , can be expanded as

$$\begin{aligned} \mathbf{W}_k \mathbf{G}_k \mathbf{H}_{k,k} &= \mathbf{F}_k^H \mathbf{H}_{k,k}^H \mathbf{G}_k^H \mathbf{W}_k \mathbf{G}_k \mathbf{H}_{k,k} + \mathbf{F}_k^H \boldsymbol{\Phi}_k(\boldsymbol{\mu}) \\ &\quad + \sum_{l \neq k} \mathbf{F}_k^H \mathbf{H}_{l,k}^H \mathbf{G}_l^H \mathbf{W}_l \mathbf{G}_l \mathbf{H}_{l,k} \end{aligned} \quad (5.40)$$

$$\mathbf{H}_{k,k} \mathbf{F}_k = \mathbf{H}_{k,k} \mathbf{F}_k \mathbf{F}_k^H \mathbf{H}_{k,k}^H \mathbf{G}_k^H + \boldsymbol{\Omega}_k \mathbf{G}_k^H \quad (5.41)$$

where  $\boldsymbol{\Phi}_k(\boldsymbol{\mu}) = \sum_{m=1}^M \mu_m \boldsymbol{\Phi}_{k,m}$ . Also, for the simplification of further analysis, we introduce

$$\boldsymbol{\Psi}_k = \sum_{l \neq k} \mathbf{H}_{l,k}^H \mathbf{G}_l^H \mathbf{W}_l \mathbf{G}_l \mathbf{H}_{l,k} \quad (5.42)$$

which is dependent to other users' transmission strategies only and it is a full rank and square matrix with probability one due to the random nature of channel matrices.

**Lemma 5.3.** [74] *For a given Lagrangian multiplier  $\mu_k \geq 0$  and fixed other users' transmission strategies  $(\mathbf{G}_l, \mathbf{F}_l), \forall l \neq k$ , the optimal transceiver for user  $k$  has the following structure:*

$$\mathbf{F}_k = (\boldsymbol{\Phi}_k(\boldsymbol{\mu}) + \boldsymbol{\Psi}_k)^{-\frac{1}{2}} \mathbf{V}_k \boldsymbol{\Sigma}_k \quad (5.43)$$

$$\mathbf{G}_k = \boldsymbol{\Lambda}_k \mathbf{U}_k^H \boldsymbol{\Omega}_k^{-\frac{1}{2}} \quad (5.44)$$

$\mathbf{U}_k \in \mathbb{C}^{n_r \times n_r}$  and  $\mathbf{V}_k \in \mathbb{C}^{n_t \times n_r}$  contain the left and right singular vectors of the equivalent channel matrix  $\tilde{\mathbf{H}}_k = (\boldsymbol{\Phi}_k(\boldsymbol{\mu}) + \boldsymbol{\Psi}_k)^{-\frac{1}{2}} \mathbf{H}_{k,k} \boldsymbol{\Omega}_k^{-\frac{1}{2}}$  corresponding to its non-zero eigenvalues.

*Proof.* Note that the matrices  $\boldsymbol{\Omega}_k$  and  $\boldsymbol{\Psi}_k$  are full rank and square with probability one. We define the equivalent system matrices for the  $k$ th user

similar to the Lemma 5.1 as

$$\tilde{\mathbf{G}}_k = \mathbf{G}_k \boldsymbol{\Omega}_k^{\frac{1}{2}} \quad (5.45)$$

$$\tilde{\mathbf{F}}_k = (\boldsymbol{\Phi}_k(\boldsymbol{\mu}) + \boldsymbol{\Psi}_k)^{\frac{1}{2}} \mathbf{F}_k \quad (5.46)$$

$$\tilde{\mathbf{H}}_k = (\boldsymbol{\Phi}_k(\boldsymbol{\mu}) + \boldsymbol{\Psi}_k)^{-\frac{1}{2}} \mathbf{H}_{k,k} \boldsymbol{\Omega}_k^{-\frac{1}{2}} \quad (5.47)$$

Substituting these equivalent system matrices into (5.40) and (5.41), we find the KKT conditions having the same form as in the single-user case (5.74) and (5.75) (see Section 5.A). The proof follows by Lemma 5.1 instantly.  $\square$

### 5.3.2 Imperfect Channel Knowledge

Now, we move to the case of imperfect channel knowledge in the multiuser system. Assuming fixed  $(\mathbf{G}_l, \mathbf{F}_l), l \neq k$ , the robust transceiver optimization problem for user  $k$  can be expressed by

$$\begin{aligned} & \underset{\mathbf{F}_k, \mathbf{G}_k}{\text{minimize}} && \max_{(\mathbf{H}_{k,k}, \boldsymbol{\Psi}_k, \boldsymbol{\Omega}_k) \in \mathcal{B}_k} \text{tr} \{ \mathbf{W}_k \mathbf{E}_k \} + \text{tr} \{ \boldsymbol{\Psi}_k \mathbf{F}_k \mathbf{F}_k^H \} \\ & \text{subject to} && \sum_{k=1}^K \text{tr} \{ \boldsymbol{\Phi}_{k,m} \mathbf{F}_k \mathbf{F}_k^H \} \leq P_m, \forall m \end{aligned} \quad (5.48)$$

The terms independent of  $\mathbf{F}_k, \mathbf{G}_k$  are removed from the objective function.  $\mathcal{B}_k$  denotes the uncertainty region for user  $k$ .

**Uncertainty regions:** We define the uncertainty region for user  $k$  as

$$\begin{aligned} \mathcal{B}_k = \left\{ (\mathbf{H}_{k,k}, \boldsymbol{\Omega}_k, \boldsymbol{\Psi}_k) : \right. & \|\boldsymbol{\Delta}_{H_{k,k}}\| \leq \varepsilon_{H_{k,k}}, \\ & \widehat{\boldsymbol{\Omega}}_k + \boldsymbol{\Delta}_{\Omega_k} \succeq \mathbf{0}, \|\boldsymbol{\Delta}_{\Omega_k}\| \leq \varepsilon_{\Omega_k}, \\ & \left. \widehat{\boldsymbol{\Psi}}_k + \boldsymbol{\Delta}_{\Psi_k} \succeq \mathbf{0}, \|\boldsymbol{\Delta}_{\Psi_k}\| \leq \varepsilon_{\Psi_k} \right\} \end{aligned} \quad (5.49)$$

Thus, we require to estimate the uncertainty radiuses  $\varepsilon_{\Omega_k}$  and  $\varepsilon_{\Psi_k}$ . Using the triangle inequality, we can obtain that

$$\begin{aligned} \|\boldsymbol{\Omega}_k\|^2 & \leq \|\widehat{\boldsymbol{\Omega}}_k\|^2 + \left\| \sum_{l \neq k} \boldsymbol{\Delta}_{k,l} \mathbf{F}_l \mathbf{F}_l^H \boldsymbol{\Delta}_{k,l}^H \right\|^2 \\ & \leq \|\widehat{\boldsymbol{\Omega}}_k\|^2 + \sum_{l \neq k} \|\mathbf{F}_l \mathbf{F}_l^H\|^2 \varepsilon_{H_{k,l}}^2 \end{aligned} \quad (5.50)$$

and similarly

$$\begin{aligned}\|\Psi_k\|^2 &\leq \|\widehat{\Psi}_k\|^2 + \left\| \sum_{l \neq k} \Delta_{l,k}^H \mathbf{G}_l^H \mathbf{W}_l \mathbf{G}_l \Delta_{l,k} \right\|^2 \\ &\leq \|\widehat{\Psi}_k\|^2 + \sum_{l \neq k} \|\mathbf{G}_l^H \mathbf{W}_l \mathbf{G}_l\|^2 \varepsilon_{H_{l,k}}^2\end{aligned}\quad (5.51)$$

Therefore, the uncertainty (square) radii can be approximated as

$$\varepsilon_{\Omega_k}^2 = \sum_{l \neq k} \|\mathbf{F}_l \mathbf{F}_l^H\|^2 \varepsilon_{H_{k,l}}^2 \quad (5.52)$$

$$\varepsilon_{\Psi_k}^2 = \sum_{l \neq k} \|\mathbf{G}_l^H \mathbf{W}_l \mathbf{G}_l\|^2 \varepsilon_{H_{l,k}}^2. \quad (5.53)$$

*Remark 5.6.* Note that the uncertainty regions of matrices  $\Omega_k$  and  $\Psi_k$  are functions of several spherical uncertainty regions of the cross channel matrices. Hence, these uncertainty regions are not necessarily spherical and will be intractable for the robust transceiver design purposes. In order to find a reduced-complexity robust design, we find a spherical upper bound for these regions to approximate the worst-case scenario. Note that similar to many cases in the design of communication systems, we minimize an upper bound of the performance measure (e.g. worst-case WSMSE) to design the robust transceivers since it is more tractable.

**Worst-case System Matrices:** Expanding the WSMSE objective function in (5.48) with respect to the estimated system matrices of user  $k$ , (i.e.  $\widehat{\mathbf{H}}_{k,k}, \widehat{\Omega}_k, \widehat{\Psi}_k$ ) and the error matrices (i.e.  $\Delta_{H_{k,k}}, \Delta_{\Omega_k}, \Delta_{\Psi_k}$ ), we can simplify its maximization problem as

$$\begin{aligned}\text{maximize}_{(\mathbf{H}_{k,k}, \Psi_k, \Omega_k) \in \mathcal{B}_k} & \text{tr} \left\{ \mathbf{W}_k \widehat{\mathbf{E}}_k \right\} + \text{tr} \left\{ \widehat{\Psi}_k \mathbf{F}_k \mathbf{F}_k^H \right\} \\ & + \text{tr} \left\{ \mathbf{A}_k \Delta_{H_{k,k}} \mathbf{B}_k \Delta_{H_{k,k}}^H \right\} \\ & + 2\Re \left\{ \text{tr} \left\{ \mathbf{C}_k \Delta_{H_{k,k}} \right\} \right\} \\ & + \text{tr} \left\{ \mathbf{G}_k^H \mathbf{W}_k \mathbf{G}_k \Delta_{\Omega_k} \right\} + \text{tr} \left\{ \Delta_{\Psi_k} \mathbf{F}_k \mathbf{F}_k^H \right\}\end{aligned}\quad (5.54)$$

$$\text{subject to} \quad \sum_{k=1}^K \text{tr} \left\{ \Phi_{k,m} \mathbf{F}_k \mathbf{F}_k^H \right\} \leq P_m, \forall m$$

where

$$\begin{aligned}\widehat{\mathbf{E}}_k &= \mathbf{G}_k \widehat{\mathbf{H}}_{k,k} \mathbf{F}_k \mathbf{F}_k^H \widehat{\mathbf{H}}_{k,k}^H \mathbf{G}_k^H - \mathbf{G}_k \widehat{\mathbf{H}}_{k,k} \mathbf{F}_k \\ &\quad - \mathbf{F}_k^H \widehat{\mathbf{H}}_{k,k}^H \mathbf{G}_k^H + \mathbf{G}_k \widehat{\boldsymbol{\Omega}}_k \mathbf{G}_k^H + \mathbf{I}.\end{aligned}\quad (5.55)$$

$$\mathbf{A}_k = \mathbf{G}_k^H \mathbf{W}_k \mathbf{G}_k, \quad (5.56)$$

$$\mathbf{B}_k = \mathbf{F}_k \mathbf{F}_k^H, \quad (5.57)$$

$$\mathbf{C}_k = \mathbf{F}_k \mathbf{F}_k^H \widehat{\mathbf{H}}_{k,k}^H \mathbf{G}_k^H \mathbf{W}_k \mathbf{G}_k - \mathbf{F}_k \mathbf{W}_k \mathbf{G}_k. \quad (5.58)$$

Note that this optimization problem is similar to the corresponding problem in the single-user case (5.10). Similarly from the results of Section 5.2, we can select the worst-case values of

$$\boldsymbol{\Omega}_k^* = \widehat{\boldsymbol{\Omega}}_k + \varepsilon_{\Omega_k} \mathbf{I}, \quad (5.59)$$

$$\boldsymbol{\Psi}_k^* = \widehat{\boldsymbol{\Psi}}_k + \varepsilon_{\Psi_k} \mathbf{I}. \quad (5.60)$$

We can also conclude from Lemma 5.2 that the worst-case channel estimation error must be in a form of

$$\Delta_{H_{k,k}}^* = \boldsymbol{\Omega}_k^{\frac{1}{2}} \widehat{\mathbf{U}}_k \widetilde{\boldsymbol{\Delta}}_k \widehat{\mathbf{V}}_k^H (\boldsymbol{\Phi}_k(\boldsymbol{\mu}) + \boldsymbol{\Psi}_k)^{\frac{1}{2}}, \quad (5.61)$$

where  $\widehat{\mathbf{U}}_k \in \mathbb{C}^{n_r \times n_r}$  and  $\widehat{\mathbf{V}}_k \in \mathbb{C}^{n_r \times n_t}$  are defined in the SVD

$$\boldsymbol{\Omega}_k^{-\frac{1}{2}} \widehat{\mathbf{H}}_{k,k} (\boldsymbol{\Phi}_k(\boldsymbol{\mu}) + \boldsymbol{\Psi}_k)^{-\frac{1}{2}} = \widehat{\mathbf{U}}_k \begin{bmatrix} \widehat{\boldsymbol{\Gamma}}_k & \mathbf{0} \end{bmatrix} \begin{bmatrix} \widehat{\mathbf{V}}_k & \check{\mathbf{V}}_k \end{bmatrix}^H \quad (5.62)$$

and  $\widetilde{\boldsymbol{\Delta}}_k \in \mathbb{R}^{n_r \times n_r}$  is a diagonal matrix with elements  $\bar{\delta}_{k,i} \geq 0$ . The values of  $\bar{\delta}_{k,i}$  can be obtained through the minimization problem over an auxiliary variable  $\vartheta_k$  as discussed in Section 5.B.

**Robust Transceiver Design:** We use dual decomposition method [145] to decompose the problem into subproblems with the Lagrangian variable  $\boldsymbol{\mu}$ . For a given  $\boldsymbol{\mu}$ , we must solve the following problem:

$$\underset{\mathbf{F}_k, \mathbf{G}_k}{\text{minimize}} \quad \max_{\mathcal{B}_k} \sum_{k=1}^K \text{tr} \{ \mathbf{W}_k \mathbf{E}_k \} + \sum_{k=1}^K \text{tr} \{ \boldsymbol{\Phi}_k \mathbf{F}_k \mathbf{F}_k^H \} - \sum_{m=1}^M \mu_m P_m \quad (5.63)$$

with respect to  $\mu_k$ . The outer loop master optimization problem updates  $\mu_m, m = 1, \dots, M$  using subgradient algorithm [115, 145]. We can insert (5.59) and (5.60) into this problem and following Lemma 5.2, the maximization

problem of (5.48) becomes a minimization problem with respect to  $\vartheta_k$  (see Section 5.B). We know from Section 5.3.1 that for any given estimation error matrices the optimal precoding and equalization matrices for user  $k$  assuming other user's transceivers fixed are in a form of (5.43) and (5.44). Note that since maximization preserves convexity, the overall minimization problem is still convex with respect to  $\mathbf{F}_k$  and  $\mathbf{G}_k$ . This problem can be simplified similarly to the single-user case as

$$\begin{aligned} \underset{\substack{\sigma_{k,i}, \lambda_{k,i}, \vartheta_k \\ i=1, \dots, n_r}}{\text{minimize}} \quad & \sum_{i=1}^{n_r} \frac{\vartheta_k w_{k,i} (\sigma_{k,i} \lambda_{k,i} \gamma_{k,i} - 1)^2}{\vartheta_k - w_{k,i} \lambda_{k,i}^2 \sigma_{k,i}^2} + \sum_{i=1}^{n_r} w_i \lambda_{k,i}^2 \\ & + \sum_{i=1}^{n_r} \sigma_{k,i}^2 + \vartheta_k \tilde{\varepsilon}_{H_{k,k}}^2 \end{aligned} \quad (5.64)$$

Following the approach for Lemma 5.3, we equate the derivatives of the Lagrangian function with respect to  $\sigma_{k,i}$  and  $\lambda_{k,i}$  to zero (i.e.  $\partial \mathcal{L} / \partial \sigma_{k,i} = \partial \mathcal{L} / \partial \lambda_{k,i} = 0$ ). Then, by introducing  $X_{k,i} = \lambda_{k,i} \sigma_{k,i}$ , the result can be combined together into a single quartic equation (see Section 5.C)

$$\begin{aligned} \varphi_{k,i}(r) = & w_{k,i}^2 r^4 - w_{k,i} \vartheta_k (2 + \sqrt{w_{k,i} \gamma_{k,i}}) r^2 \\ & + (\gamma_{k,i}^2 \vartheta_k + w_{k,i}) \sqrt{w_{k,i}} \vartheta_k r + \vartheta_k^2 (1 - \gamma_{k,i} \sqrt{w_{k,i}}) = 0. \end{aligned} \quad (5.65)$$

The closed-form expressions for the roots of this equation can be found following the Ferrari's method [144] as discussed in Section 5.C. The values of  $\lambda_{k,i}$  and  $\sigma_{k,i}$  are characterized from the real positive root of this equation as

$$\sigma_{k,i} = \sqrt{r_{k,i} \sqrt{w_{k,i}}} \quad (5.66)$$

$$\lambda_{k,i} = \sqrt{\frac{r_{k,i}}{\sqrt{w_{k,i}}}} \quad (5.67)$$

Therefore, the algorithm to obtain the worst-case transceivers in the multiuser system is as detailed in Table 5.2.

Table 5.2: Worst-Case Robust Transceiver Design Algorithm (Multiuser)

---

Initialize  $\mathbf{F}_k$  and  $\mathbf{G}_k$  for all  $k$  and  $\boldsymbol{\mu} = (\mu_1, \dots, \mu_K) \succeq \mathbf{0}$ .

**Repeat** (subgradient loop of  $\boldsymbol{\mu}$ )

**Repeat** for any user  $k$

        Compute  $\boldsymbol{\Omega}_k$  and  $\boldsymbol{\Psi}_k$  from (2.17) and (5.42)

        Calculate  $\varepsilon_{\Omega_k}$  and  $\varepsilon_{\Psi_k}$  from (5.52) and (5.53).

        Initialize  $\sigma_{k,i}, \lambda_{k,i}, i = 1, \dots, n_r$

        Perform thin SVD

$$\left(\widehat{\boldsymbol{\Omega}}_k + \varepsilon_{\Omega_k} \mathbf{I}\right)^{-\frac{1}{2}} \widehat{\mathbf{H}}_{k,k} \left(\widehat{\boldsymbol{\Psi}}_k + \mu_k \mathbf{I} + \varepsilon_{\Psi_k} \mathbf{I}\right)^{-\frac{1}{2}} = \widehat{\mathbf{U}}_k \widehat{\boldsymbol{\Gamma}}_k \widehat{\mathbf{V}}_k^H$$

$\widehat{\boldsymbol{\Gamma}}_k = \text{diag}(\gamma_{k,1}, \dots, \gamma_{k,n_r})$

**Repeat** (subgradient loop of  $\vartheta_k$ )

$j = \text{argmax}_i (w_{k,i} \lambda_{k,i}^2 \sigma_{k,i}^2)$

**If**  $\vartheta_k = w_{k,j} \lambda_{k,j}^2 \sigma_{k,j}^2$

                Calculate  $\rho(\vartheta_k) = \sum_{i \neq j} \frac{w_{k,i}^2 \lambda_{k,i}^2 \sigma_{k,i}^2 (\gamma_{k,i} \lambda_{k,i} \sigma_{k,i} - 1)^2}{(\vartheta_k - w_{k,i} \lambda_{k,i}^2 \sigma_{k,i}^2)^2}$

**If**  $\rho(\vartheta_k) < \varepsilon_{H_{k,k}}^2$

$$\delta_i = \frac{w_{k,i} \lambda_{k,i} \sigma_{k,i} (\gamma_{k,i} \lambda_{k,i} \sigma_{k,i} - 1)}{\vartheta_k - w_{k,i} \lambda_{k,i}^2 \sigma_{k,i}^2} \quad i \neq j$$

$$\delta_j = -\sqrt{\varepsilon_{H_{k,k}}^2 - \rho(\vartheta_k)}$$

**End**

**Else**

$\vartheta_k \leftarrow \vartheta_k + \delta_{\vartheta_k} \Delta_{\vartheta_k}$

**End**

            Form the quartic equation (5.65) for all  $i = 1, \dots, n_r$ .

            Find the positive real root of this equation,  $r_{k,i}$

            (if any, otherwise  $r_{k,i} = 0$ )

            Set  $\lambda_{k,i} = \sqrt{\frac{r_{k,i}}{w_{k,i}}}, \sigma_{k,i} = \sqrt{r_{k,i} \sqrt{w_{k,i}}}$ .

**Until** Convergence

**Until** Convergence

        Update  $\mu_k \leftarrow \mu_k + \delta_{\mu_k} (\text{tr} \{\mathbf{F}_k \mathbf{F}_k^H\} - P_k), \forall k$

**Until**  $\sum_k \mu_k (\text{tr} \{\mathbf{F}_k \mathbf{F}_k^H\} - P_k) \leq \epsilon_0$ .

    Substitute  $\boldsymbol{\Lambda}_k$  and  $\boldsymbol{\Sigma}_k$  into (5.43)-(5.44) to find  $\mathbf{F}_k$  and  $\mathbf{G}_k$ .

---

## 5.4 Numerical Results

In this section, the performance of robust transceivers is evaluated numerically. The robust design guarantees a performance level for any point within the uncertainty region. Hence, the performance is expressed by the average worst-case sum of MSE values. These values are averaged over different system

realizations. Each system realization is a random generation of the elements of the estimated system matrices (i.e.  $\hat{\mathbf{H}}, \hat{\mathbf{\Omega}}, \hat{\mathbf{\Phi}}$  in single-user case and  $\hat{\mathbf{H}}_{k,k}$  in multiuser scenario), which are i.i.d. Gaussian with zero mean. The uncertainty region is characterized by a parameter  $0 \leq \bar{\varepsilon} \leq 1$ . In our simulations, it is assumed that  $\sqrt{\bar{\varepsilon}}$  is the radius of uncertainty region for each of the system matrices when they are normalized by their Frobenius norms of the estimated value. The non-robust transceivers assume the estimated system matrices as the actual system matrices and are discussed in [74]. The worst-case estimation error matrices are given in Section 5.2.2 and are used in the calculations of the worst-case sum-MSE or sum-rates.

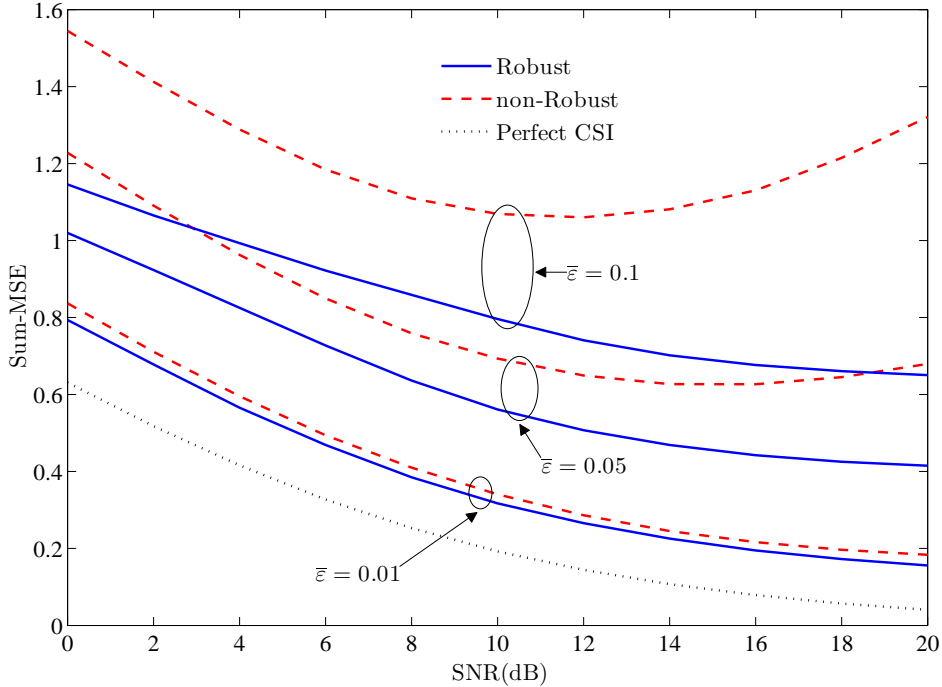


Figure 5.1: Comparison of performance of the proposed robust design, the non-robust design, and the transceiver design when system matrices are perfectly known (perfect CSI) for  $n_t = n_r = 2$ .

Fig. 5.1 shows the comparison of robust and non-robust design [74] for different values of  $\bar{\varepsilon}$ , i.e. the size of uncertainty regions in the single-user case. The performance of the transceivers in the presence of perfect knowledge of the system matrices is also shown as a baseline. Fig. 5.2 explicitly illustrates the

performance of the robust and non-robust design with respect to the size of the uncertainty region for a single-user system. As it is expected, the performance of the robust transceivers deteriorates at a much lower rate with increase of the size of the uncertainty region  $\bar{\epsilon}$  compared to the non-robust transceivers.

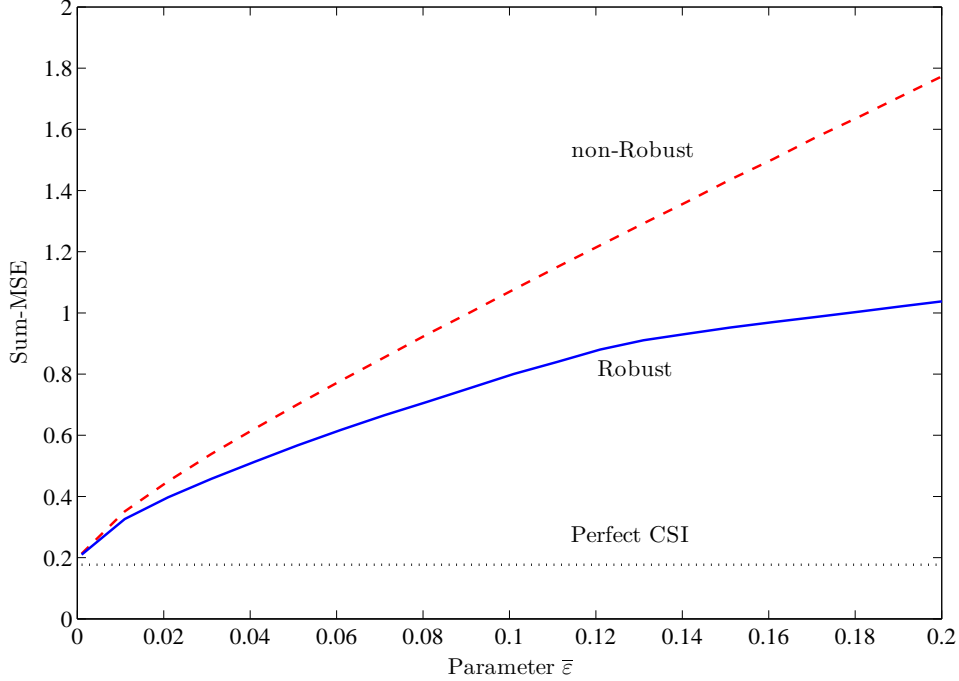


Figure 5.2: Comparison of performance of different transceiver designs with respect to the size of uncertainty region  $\bar{\epsilon}$  for  $n_t = n_r = 2$ .

In the multiuser scenario, we have presented the numerical results for a MIMO interference channel with  $K = 3$  users and  $n_t = n_r = 2$ . The performance of robust and non-robust designs for the worst-case scenario is shown in Fig. 5.3 and Fig. 5.4 for different values of  $\bar{\epsilon}$ . The performance with perfect CSI is also given for comparison. Fig. 5.3 compares the sum-MSE (across all users data symbol estimates) and Fig. 5.4 presents the sum rate results. As SNR increases the performance of the system degrades significantly for higher values of  $\bar{\epsilon}$ , but much less for robust design than for its non-robust counterpart.

Fig. 5.5 shows the comparison of our proposed algorithm with the SDR-based algorithm proposed in [126] for interference channels. As it is

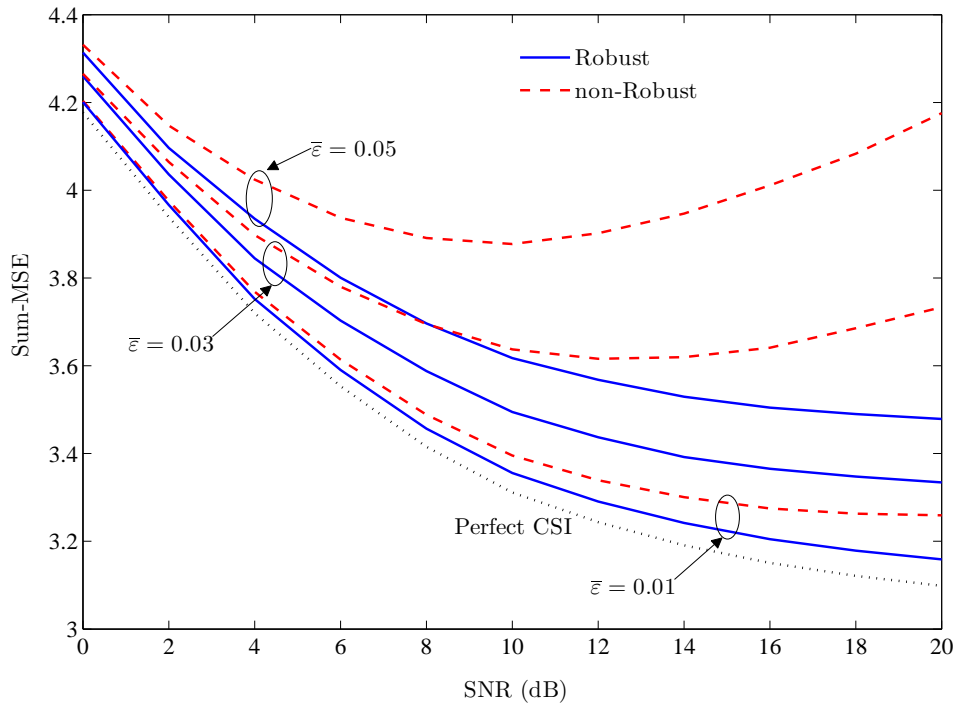


Figure 5.3: Sum-MSE comparison of the proposed robust design, the non-robust design with  $\bar{\epsilon} = 0.01, 0.03, 0.05$ , and with perfect CSI in  $K = 3$  interference channel.  $n_t = n_r = 2$ .

evident, our algorithm outperforms the previous robust design in interference channels. This improvement is a result of employing the Gauss-Seidel algorithm controlling the interference sent out by each user, deriving the structure of the precoders, equalizers, and the worst-case channel matrices. We also use a sub-gradient algorithm to satisfy the per-BS power constraints, while in [126] an iterative scaling of the precoding vectors are deployed to satisfy the power. Sub-gradient algorithm is a convergent algorithm and standard in the optimization problems [145]. Moreover, [126] also applies SDP at each iteration of their algorithm, which compared to our iterative algorithm is more complex. It is known that the complexity<sup>6</sup> of SDP grows as  $\mathcal{O}(n^6)$ , where  $n$  is the number of variables in the optimization problem [70]. Therefore, the complexity per iteration of SDP-based algorithms is  $\mathcal{O}((Kn_t)^6)$ . Each iteration of our proposed

<sup>6</sup>The complexity refers to the time complexity. Time complexity of an algorithm is its running time as a function of the length of the input string. It is described asymptotically by  $\mathcal{O}(n)$  when the input size, i.e.  $n$ , goes to infinity.

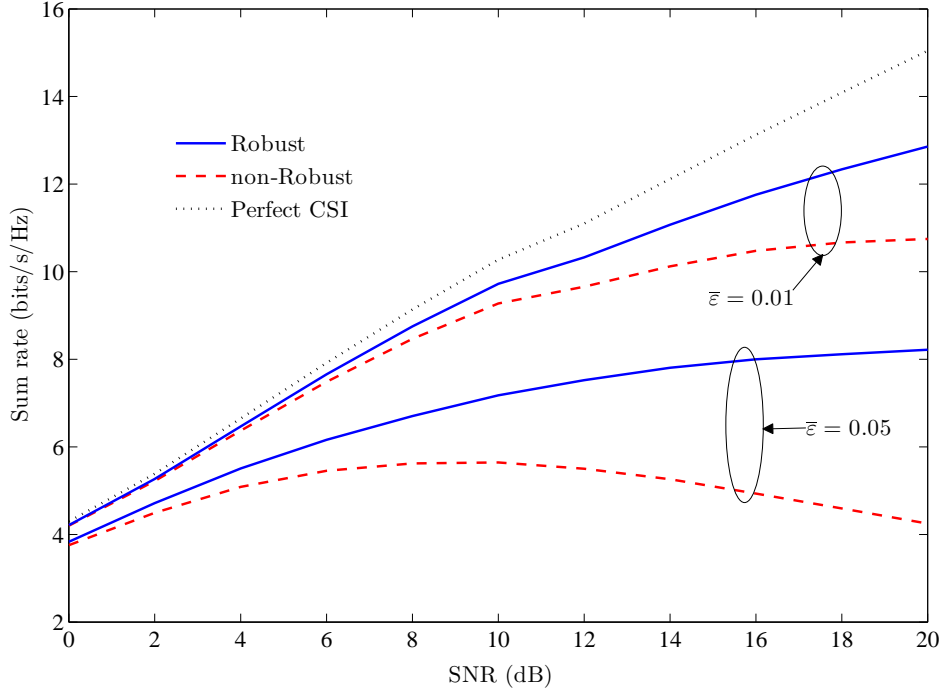


Figure 5.4: Sum rate comparison of the proposed robust design, the non-robust design with  $\bar{\epsilon} = 0.01, 0.05$ , and with perfect CSI in  $K = 3$  interference channel.  $n_t = n_r = 2$ .

algorithm contains matrix operations (inverse and SVD operations), which grows as  $\mathcal{O}(n^3)$  with  $n$  as size of the matrix. Hence, the complexity order per iteration of our algorithm is  $\mathcal{O}(n_t^3) + \mathcal{O}(n_r^3)$ .

## 5.5 Conclusions

We have considered the worst-case robust design of linear precoders and equalizers in MIMO interference channels. We have addressed the problem for the single-user systems first, where the channel matrix, interference plus noise covariance matrix, and power shaping matrix (system matrices) are all imperfectly known to the transmitter and receiver. Using this approach, we have then analyzed the multiuser scenario. We approximate the uncertainty regions to obtain the simplified structures of the precoders and equalizers, which also involves finding the worst-case system matrices. The resulting

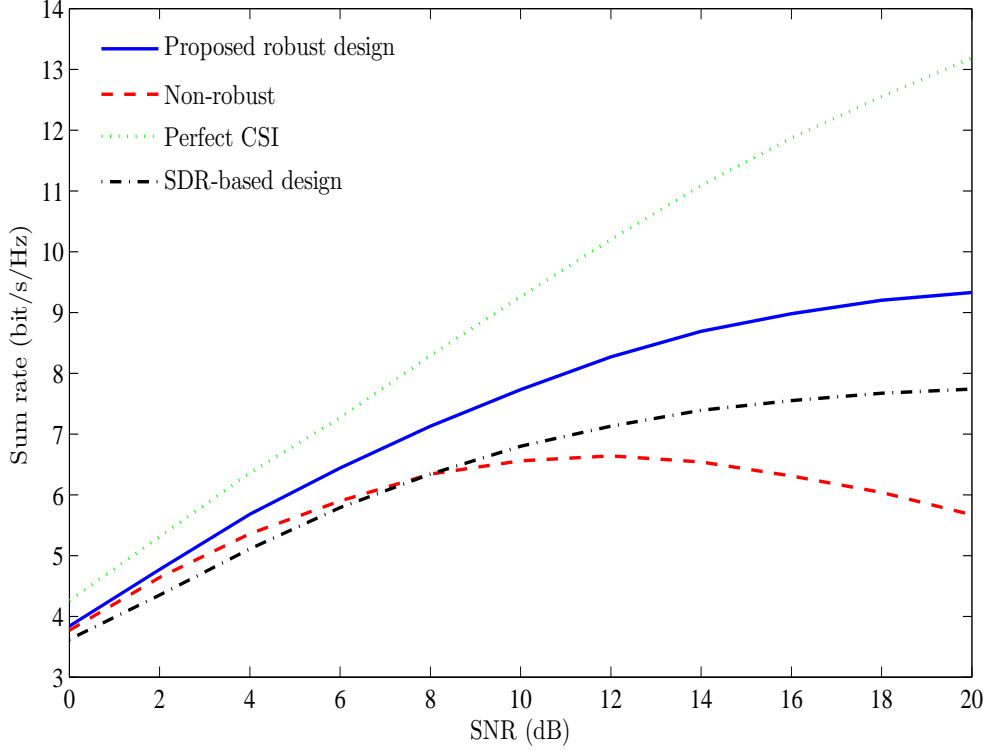


Figure 5.5: Sum rate comparison of the proposed robust design with the semi-definite relaxation based algorithm, with  $\varepsilon_{H_{k,l}} = 0.1, \forall k, l$  in  $K = 3$  interference channel.  $n_t = n_r = 2$ .

problem has been reduced to a scalar convex form. The solution to this optimization problem can be expressed in a form of depressed quartic equation, the closed-form expressions for roots of which are known. Finally, we have proposed an iterative algorithm to obtain a robust transceivers, which is less complex compared to SDP-based alternating optimizations.

## 5.A Proof of Lemma 5.1

We first define the *equivalent channel matrix*  $\tilde{\mathbf{H}}$ , *equivalent precoding matrix*  $\tilde{\mathbf{F}}$  and *equivalent equalization matrix*  $\tilde{\mathbf{G}}$  expressed as

$$\tilde{\mathbf{H}} = \mathbf{\Omega}^{-\frac{1}{2}} \mathbf{H} \mathbf{\Phi}^{-\frac{1}{2}} \quad (5.68)$$

$$\tilde{\mathbf{G}} = \mathbf{G} \mathbf{\Omega}^{\frac{1}{2}} \quad (5.69)$$

$$\tilde{\mathbf{F}} = \mathbf{\Phi}^{\frac{1}{2}} \mathbf{F} \quad (5.70)$$

Since the matrices  $\Phi$  and  $\Omega$  are square and full rank matrices, we can substitute  $\tilde{\mathbf{G}}$ ,  $\tilde{\mathbf{F}}$  and  $\tilde{\mathbf{H}}$  into the problem (5.4) and obtain an equivalent problem

$$\begin{aligned} & \underset{\tilde{\mathbf{F}}, \tilde{\mathbf{G}}}{\text{minimize}} \quad \text{tr} \left\{ \mathbf{W} \tilde{\mathbf{E}} \right\} \\ & \text{subject to} \quad \text{tr} \left\{ \tilde{\mathbf{F}} \tilde{\mathbf{F}}^{\text{H}} \right\} \leq P \end{aligned} \quad (5.71)$$

where the equivalent MSE-matrix  $\tilde{\mathbf{E}}$  in the equivalent system is defined as

$$\begin{aligned} \tilde{\mathbf{E}} = & \tilde{\mathbf{G}} \tilde{\mathbf{H}} \tilde{\mathbf{F}} \tilde{\mathbf{F}}^{\text{H}} \tilde{\mathbf{H}}^{\text{H}} \tilde{\mathbf{G}}^{\text{H}} - \tilde{\mathbf{G}} \tilde{\mathbf{H}} \tilde{\mathbf{F}} \\ & - \tilde{\mathbf{F}}^{\text{H}} \tilde{\mathbf{H}}^{\text{H}} \tilde{\mathbf{G}}^{\text{H}} + \tilde{\mathbf{G}} \tilde{\mathbf{G}}^{\text{H}} + \mathbf{I}. \end{aligned} \quad (5.72)$$

Plugging this into the problem (5.71) we find that the objective function is a convex quadratic function in each of  $\tilde{\mathbf{F}}$  and  $\tilde{\mathbf{G}}$ . Nevertheless, it is not jointly convex. Hence, the KKT conditions [115] are only necessary for optimality, which means that the optimal solution must satisfy them. We first establish the Lagrangian function

$$\mathcal{L}(\mu, \tilde{\mathbf{F}}, \tilde{\mathbf{G}}) = \text{tr} \left\{ \mathbf{W} \tilde{\mathbf{E}} \right\} + \mu \left( \text{tr} \left\{ \tilde{\mathbf{F}} \tilde{\mathbf{F}}^{\text{H}} \right\} - P \right) \quad (5.73)$$

where  $\mu \geq 0$  is the Lagrangian multiplier. Next, the KKT conditions can be listed below<sup>7</sup>:

$$\nabla_{\tilde{\mathbf{F}}} \mathcal{L} = \tilde{\mathbf{F}}^{\text{H}} \tilde{\mathbf{H}}^{\text{H}} \tilde{\mathbf{G}}^{\text{H}} \mathbf{W} \tilde{\mathbf{G}} \tilde{\mathbf{H}} - \mathbf{W} \tilde{\mathbf{G}} \tilde{\mathbf{H}} + \mu \tilde{\mathbf{F}}^{\text{H}} = 0, \quad (5.74)$$

$$\nabla_{\tilde{\mathbf{G}}} \mathcal{L} = \tilde{\mathbf{H}} \tilde{\mathbf{F}} \tilde{\mathbf{F}}^{\text{H}} \tilde{\mathbf{H}}^{\text{H}} \tilde{\mathbf{G}}^{\text{H}} - \tilde{\mathbf{H}} \tilde{\mathbf{F}} + \tilde{\mathbf{G}}^{\text{H}} = 0, \quad (5.75)$$

$$\text{tr} \left\{ \tilde{\mathbf{F}} \tilde{\mathbf{F}}^{\text{H}} \right\} \leq P, \quad (5.76)$$

$$\mu \left( \text{tr} \left\{ \tilde{\mathbf{F}} \tilde{\mathbf{F}}^{\text{H}} \right\} - P \right) = 0. \quad (5.77)$$

Scrutinizing the KKT conditions (5.74) and (5.75), we notice that the precoding matrix  $\tilde{\mathbf{F}}$  is always pre-multiplied by the channel matrix  $\tilde{\mathbf{H}}$  and the equalization matrix  $\tilde{\mathbf{G}}$  is always post-multiplied by the channel matrix  $\tilde{\mathbf{H}}$ . Since  $\mathbf{U}$  contains the left singular vectors of  $\tilde{\mathbf{H}}$  and  $\mathbf{V}$  contains the right singular vectors of the channel matrix, both create the basis for the range

---

<sup>7</sup>We use differentiation rules  $\nabla_{\mathbf{X}} \text{tr} \{ \mathbf{G} \mathbf{X} \mathbf{F} \} = \mathbf{F} \mathbf{G}$  and  $\nabla_{\mathbf{X}} \text{tr} \{ \mathbf{Y}^{-1} \} = -\mathbf{Y}^{-1} (\nabla_{\mathbf{X}} \mathbf{Y}) \mathbf{Y}^{-1}$ . For the complex gradient operator each matrix and its conjugate transpose are treated as independent variables [116].

space of  $\tilde{\mathbf{H}}$ . We first employ the most general form for the matrices  $\tilde{\mathbf{F}}$  and  $\tilde{\mathbf{G}}$  and decompose them into the range space and null space of  $\tilde{\mathbf{H}}$ :

$$\tilde{\mathbf{F}} = \mathbf{V}\boldsymbol{\Sigma} + \check{\mathbf{V}}\check{\boldsymbol{\Sigma}} = \mathbf{F}_{\parallel} + \mathbf{F}_{\perp}, \quad (5.78)$$

$$\tilde{\mathbf{G}} = \boldsymbol{\Lambda}\mathbf{V}^{\mathbf{H}}\tilde{\mathbf{H}}^{\mathbf{H}} + \check{\boldsymbol{\Lambda}}\check{\mathbf{V}}^{\mathbf{H}}\tilde{\mathbf{H}}^{\mathbf{H}} = \mathbf{G}_{\parallel} + \mathbf{G}_{\perp}, \quad (5.79)$$

where  $\mathbf{F}_{\parallel}$  and  $\mathbf{G}_{\parallel}$  are each in the range space of  $\tilde{\mathbf{H}}$ , and  $\mathbf{F}_{\perp}$  and  $\mathbf{G}_{\perp}$  are each in its null space;  $\check{\boldsymbol{\Sigma}} \in \mathbb{C}^{(n_t-n_r) \times n_r}$  and  $\check{\boldsymbol{\Lambda}} \in \mathbb{C}^{n_r \times (n_t-n_r)}$  are arbitrary matrices.

We have

$$\mathbf{F}_{\perp}^{\mathbf{H}}\mathbf{F}_{\parallel} = \mathbf{0}, \quad \mathbf{F}_{\parallel}^{\mathbf{H}}\mathbf{F}_{\perp} = \mathbf{0}, \quad \tilde{\mathbf{H}}\mathbf{F}_{\perp} = \mathbf{0}, \quad (5.80)$$

$$\mathbf{G}_{\perp}^{\mathbf{H}}\mathbf{G}_{\parallel} = \mathbf{0}, \quad \mathbf{G}_{\parallel}^{\mathbf{H}}\mathbf{G}_{\perp} = \mathbf{0}, \quad \mathbf{G}_{\perp}\tilde{\mathbf{H}} = \mathbf{0}. \quad (5.81)$$

Post-multiplying (5.74) by  $\mathbf{F}_{\perp}$  and using (5.80), we obtain

$$\tilde{\mathbf{F}}^{\mathbf{H}}\mathbf{F}_{\perp} = \mathbf{0} \quad \Rightarrow \quad \mathbf{F}_{\perp}^{\mathbf{H}}\mathbf{F}_{\perp} = \mathbf{0} \quad \Rightarrow \quad \mathbf{F}_{\perp} = \mathbf{0}. \quad (5.82)$$

Pre-multiplying (5.75) by  $\mathbf{G}_{\perp}$  and using (5.81), we get

$$\mathbf{G}_{\perp}\tilde{\mathbf{G}}^{\mathbf{H}} = \mathbf{0} \quad \Rightarrow \quad \mathbf{G}_{\perp}\mathbf{G}_{\perp}^{\mathbf{H}} = \mathbf{0} \quad \Rightarrow \quad \mathbf{G}_{\perp} = \mathbf{0}. \quad (5.83)$$

Consequently, we have  $\tilde{\mathbf{F}} = \mathbf{V}\boldsymbol{\Sigma}$  and  $\tilde{\mathbf{G}} = \boldsymbol{\Lambda}\mathbf{V}^{\mathbf{H}}\tilde{\mathbf{H}}^{\mathbf{H}} = \boldsymbol{\Lambda}\boldsymbol{\Gamma}\mathbf{U}^{\mathbf{H}}$ . Now, we need to prove that  $\boldsymbol{\Sigma}$  and  $\boldsymbol{\Lambda}$  must be diagonal matrices. From (5.75), we can obtain the receiver structure as

$$\tilde{\mathbf{G}} = \tilde{\mathbf{F}}^{\mathbf{H}}\tilde{\mathbf{H}}^{\mathbf{H}} \left( \mathbf{I} + \tilde{\mathbf{H}}\tilde{\mathbf{F}}\tilde{\mathbf{F}}^{\mathbf{H}}\tilde{\mathbf{H}}^{\mathbf{H}} \right)^{-1} \quad (5.84)$$

which is the known MMSE receiver (e.g. see [114]). Substituting this into (5.72), we obtain the equivalent MSE-matrix as

$$\tilde{\mathbf{E}} = \left( \mathbf{I} + \tilde{\mathbf{F}}^{\mathbf{H}}\tilde{\mathbf{H}}^{\mathbf{H}}\tilde{\mathbf{H}}\tilde{\mathbf{F}} \right)^{-1} \quad (5.85)$$

We first prove that the minimum of the Lagrangian function is reached where the corresponding  $\tilde{\mathbf{E}}$  is diagonal. Assume that the minimum of the Lagrangian function is reached at where the corresponding  $\tilde{\mathbf{E}}$  is not diagonal. Then, one can always find a unitary matrix  $\mathbf{Q} \in \mathbb{C}^{n_r \times n_r}$  such that the matrix  $\bar{\mathbf{F}} = \tilde{\mathbf{F}}\mathbf{Q}$  diagonalizes  $\tilde{\mathbf{E}}$  since with  $\bar{\mathbf{F}}$  we have  $\tilde{\mathbf{E}} = \mathbf{Q}^{\mathbf{H}} \left( \mathbf{I} + \bar{\mathbf{F}}^{\mathbf{H}}\tilde{\mathbf{H}}^{\mathbf{H}}\tilde{\mathbf{H}}\bar{\mathbf{F}} \right)^{-1} \mathbf{Q}$  [114]. The

function  $\text{tr} \{ \mathbf{W} \tilde{\mathbf{E}} \}$  is Schur concave, and therefore the matrix  $\bar{\mathbf{F}}$  does not decrease the function with respect to  $\tilde{\mathbf{F}}$ , while  $\bar{\mathbf{F}}\bar{\mathbf{F}}^H = \tilde{\mathbf{F}}\tilde{\mathbf{F}}^H$  is subject to the constraint of (5.71). Now, if we substitute the equivalent MSE-matrix (5.85) into the Lagrangian function (5.73) and rewrite the first gradient condition in (5.74), we have

$$\nabla_{\tilde{\mathbf{F}}} \mathcal{L} = -\tilde{\mathbf{E}}\mathbf{W}\tilde{\mathbf{E}}\tilde{\mathbf{F}}^H\tilde{\mathbf{H}}^H\tilde{\mathbf{H}} + \mu\tilde{\mathbf{F}}^H = 0 \quad (5.86)$$

Right-multiplying (5.86) by  $\tilde{\mathbf{F}}$  gives us

$$\tilde{\mathbf{E}}\mathbf{W}\tilde{\mathbf{E}}\tilde{\mathbf{F}}^H\tilde{\mathbf{H}}^H\tilde{\mathbf{H}}\tilde{\mathbf{F}} = \mu\tilde{\mathbf{F}}^H\tilde{\mathbf{F}} \quad (5.87)$$

Since  $\tilde{\mathbf{E}}$ , and consequently  $\tilde{\mathbf{F}}^H\tilde{\mathbf{H}}^H\tilde{\mathbf{H}}\tilde{\mathbf{F}}$  are diagonal, the right side of the above equation must be diagonal as well. This is equivalent to  $\Sigma^H\Sigma$  being diagonal, which results in  $\Sigma$  being also diagonal. Now, Replacing this structure of  $\tilde{\mathbf{F}}$  results that the matrix  $\Lambda$  is also diagonal. Now, from (5.84) we have

$$\tilde{\mathbf{G}} = \Lambda\Gamma\mathbf{U}^H = \Sigma^H\Gamma\mathbf{U}^H\mathbf{U} (\mathbf{I} + \Gamma\Sigma\Sigma^H\Gamma)^{-1} \mathbf{U}^H \quad (5.88)$$

By post-multiplying the above equation by  $\mathbf{U}$  and using the fact that  $\mathbf{U}^H\mathbf{U} = \mathbf{I}$ , we have  $\Lambda = \Sigma^H (\mathbf{I} + \Gamma\Sigma\Sigma^H\Gamma)^{-1}$ . This immediately results in diagonality of  $\Lambda$ .

## 5.B Proof of Lemma 5.2

First we introduce a lemma:

**Lemma 5.4** (The trust-region subproblem [142,143,146]). *Let  $q(\mathbf{x}) = \mathbf{x}^H\mathbf{Q}\mathbf{x} - 2\Re\{\mathbf{p}^H\mathbf{x}\}$  where  $\mathbf{Q} \in \mathbb{C}^{n \times n}$  is a Hermitian matrix and  $\mathbf{x}, \mathbf{p} \in \mathbb{C}^n$ . The trust region subproblem is defined as the quadratic minimization problem:*

$$\begin{aligned} & \text{minimize } q(\mathbf{x}) \\ & \text{subject to } \mathbf{x}^H\mathbf{x} = r^2 \end{aligned} \quad (5.89)$$

where  $r > 0$ . Then, (i)  $\mathbf{x}$  is a global minimum if and only if there exists  $\vartheta$  such that

$$(\mathbf{Q} + \vartheta\mathbf{I})\mathbf{x} = \mathbf{p}, \quad (5.90)$$

$$\mathbf{Q} + \vartheta\mathbf{I} \succeq \mathbf{0}, \quad (5.91)$$

$$\mathbf{x}^H\mathbf{x} = r^2, \quad (5.92)$$

and (ii) strong duality holds for the trust-region subproblem and its dual problem with zero duality gap is

$$\begin{aligned} & \underset{\vartheta}{\text{maximize}} && h(\vartheta) \\ & \text{subject to} && \mathbf{Q} + \vartheta \mathbf{I} \succeq \mathbf{0} \end{aligned} \quad (5.93)$$

where  $h(\vartheta) = -\vartheta r^2 - \mathbf{p}^H (\mathbf{Q} + \vartheta \mathbf{I})^\dagger \mathbf{p}$  and  $\dagger$  denotes the Moore-Penrose pseudo-inverse.

The matrix-form of this lemma is restated in [129] and it is useful for our proof.

**Corollary 5.1.** [129] *The optimal solution of problem (5.25) must satisfy the sufficient and necessary conditions*

$$\mathbf{A} \Delta_H \mathbf{B} + \mathbf{C}^H - \vartheta \Delta_H = 0, \quad (5.94)$$

$$\vartheta \geq \lambda_{\max}(\mathbf{A}) \lambda_{\max}(\mathbf{B}), \quad (5.95)$$

$$\text{tr} \{ \Delta_H^H \Delta_H \} = \varepsilon_H^2. \quad (5.96)$$

for some auxiliary variable  $\vartheta$ .

Consider the optimization problem (5.25). Since the objective function is convex, its maximum is acquired at the boundary  $\text{tr} \{ \Delta_H^H \Delta_H \} = \varepsilon_H^2$ . Therefore, we can replace the inequality constraint in problem (5.25) by an equality. Now, keeping these facts in mind, we proceed the proof of Lemma 5.2.

For any matrix  $\Delta_H$ , the optimal forms of the precoding and equalization matrices are given as in Lemma 5.1, which is dependent on the orthonormal matrices  $\mathbf{U}$  and  $\mathbf{V}$  obtained from the following SVD

$$\Omega^{-\frac{1}{2}} \mathbf{H} \Phi^{-\frac{1}{2}} = \Omega^{-\frac{1}{2}} \left( \widehat{\mathbf{H}} + \Delta_H \right) \Phi^{-\frac{1}{2}} \quad (5.97)$$

$$= \mathbf{U} \mathbf{\Gamma} \mathbf{V}^H \quad (5.98)$$

Now Lemma 5.1 clearly states that the optimal precoding and equalization matrices must be in a form of

$$\mathbf{F} = \Phi^{-\frac{1}{2}} \mathbf{V} \mathbf{\Sigma}, \quad (5.99)$$

$$\mathbf{G} = \mathbf{\Lambda} \mathbf{U}^H \Omega^{-\frac{1}{2}}. \quad (5.100)$$

In order to prove the Lemma, first we need to prove that  $\mathbf{U} = \widehat{\mathbf{U}}$  and  $\mathbf{V} = \widehat{\mathbf{V}}$ . Substituting these structures of the precoder and the equalizer into (5.101) and (5.102), we have

$$\mathbf{A} = \mathbf{\Omega}^{-\frac{1}{2}} \mathbf{U} \mathbf{\Lambda}^H \mathbf{W} \mathbf{\Lambda} \mathbf{U}^H \mathbf{\Omega}^{-\frac{1}{2}}, \quad (5.101)$$

$$\mathbf{B} = \mathbf{\Phi}^{-\frac{1}{2}} \mathbf{V} \mathbf{\Sigma} \mathbf{\Sigma}^H \mathbf{V}^H \mathbf{\Phi}^{-\frac{1}{2}}, \quad (5.102)$$

$$\begin{aligned} \mathbf{C} &= \mathbf{\Phi}^{-\frac{1}{2}} \mathbf{V} \mathbf{\Sigma} \mathbf{\Sigma}^H \mathbf{V}^H \widehat{\mathbf{H}}^H \mathbf{U} \mathbf{\Lambda} \mathbf{W} \mathbf{\Lambda}^H \mathbf{U}^H \mathbf{\Omega}^{-\frac{1}{2}} \\ &\quad - \mathbf{\Phi}^{-\frac{1}{2}} \mathbf{V} \mathbf{\Sigma} \mathbf{W} \mathbf{\Lambda} \mathbf{U}^H \mathbf{\Omega}^{-\frac{1}{2}} \\ &= \mathbf{\Phi}^{-\frac{1}{2}} \mathbf{V} \mathbf{\Sigma}^2 \mathbf{\Gamma} \mathbf{\Lambda}^2 \mathbf{W} \mathbf{U}^H \mathbf{\Omega}^{-\frac{1}{2}} - \mathbf{\Phi}^{-\frac{1}{2}} \mathbf{V} \mathbf{\Sigma} \mathbf{W} \mathbf{\Lambda} \mathbf{U}^H \mathbf{\Omega}^{-\frac{1}{2}}, \end{aligned} \quad (5.103)$$

Now, we substitute these into (5.94) then pre-multiply the equation by  $\mathbf{\Phi}^{\frac{1}{2}}$  and post-multiply it by  $\mathbf{\Omega}^{\frac{1}{2}}$  and substituting  $\widetilde{\mathbf{\Delta}}_H = \mathbf{\Omega}^{-\frac{1}{2}} \mathbf{\Delta}_H \mathbf{\Phi}^{-\frac{1}{2}}$ , we have

$$\begin{aligned} &\mathbf{U} \mathbf{\Lambda}^2 \mathbf{W} \mathbf{U}^H \widetilde{\mathbf{\Delta}}_H \mathbf{V} \mathbf{\Sigma}^2 \mathbf{V}^H + \mathbf{U} \mathbf{W} \mathbf{\Lambda}^2 \mathbf{\Gamma} \mathbf{\Sigma}^2 \mathbf{V}^H \\ &\quad - \mathbf{U} \mathbf{\Lambda} \mathbf{W} \mathbf{\Sigma} \mathbf{V}^H - \vartheta \widetilde{\mathbf{\Delta}}_H = \mathbf{0} \end{aligned} \quad (5.104)$$

Reformulating this problem in a vector-form using tensor (Kronecker) product<sup>8</sup>, we obtain

$$\begin{aligned} &(\mathbf{V} \mathbf{\Sigma}^2 \mathbf{V}^H \otimes \mathbf{U} \mathbf{\Lambda}^2 \mathbf{W} \mathbf{U}^H) \widetilde{\mathbf{\delta}}_H \\ &\quad + (\mathbf{V} \otimes \mathbf{U}) \text{vec}(\mathbf{\Sigma}^2 \mathbf{\Gamma} \mathbf{\Lambda}^2 - \mathbf{\Lambda} \mathbf{W} \mathbf{\Sigma}) - \vartheta \widetilde{\mathbf{\delta}}_H = \mathbf{0} \end{aligned} \quad (5.105)$$

Therefore,  $\widetilde{\mathbf{\delta}}_H$  can be uniquely identified as

$$\widetilde{\mathbf{\delta}}_H = (\mathbf{V} \otimes \mathbf{U}) [\vartheta \mathbf{I} - \mathbf{\Sigma}^2 \otimes (\mathbf{\Lambda}^2 \mathbf{W})]^{-1} \quad (5.106)$$

$$\times \text{vec}(\mathbf{\Sigma}^2 \mathbf{\Gamma} \mathbf{\Lambda}^2 \mathbf{W} - \mathbf{\Sigma} \mathbf{W} \mathbf{\Lambda}) \quad (5.107)$$

It can be verified simply that

$$[\vartheta \mathbf{I} - \mathbf{\Sigma}^2 \otimes (\mathbf{\Lambda}^2 \mathbf{W})]^{-1} \text{vec}(\mathbf{\Sigma}^2 \mathbf{\Gamma} \mathbf{\Lambda}^2 \mathbf{W} - \mathbf{\Sigma} \mathbf{W} \mathbf{\Lambda}) \quad (5.108)$$

has the structure, which is a vector-form of a diagonal matrix. Hence, we can conclude that  $\widetilde{\mathbf{\Delta}}_H$  can be described as

$$\widetilde{\mathbf{\Delta}}_H = \mathbf{U} \bar{\mathbf{\Delta}} \mathbf{V}^H \quad (5.109)$$

---

<sup>8</sup>We use tensor product properties  $\text{vec}(\mathbf{A} \mathbf{X} \mathbf{B}) = (\mathbf{B}^H \otimes \mathbf{A}) \text{vec}(\mathbf{X})$  and  $(\mathbf{U}_X \mathbf{\Lambda}_X \mathbf{V}_X^H) \otimes (\mathbf{U}_Y \mathbf{\Lambda}_Y \mathbf{V}_Y^H) = (\mathbf{U}_X \otimes \mathbf{U}_Y) (\mathbf{\Lambda}_X \otimes \mathbf{\Lambda}_Y) (\mathbf{V}_X^H \otimes \mathbf{V}_Y^H)$  where  $\mathbf{U}_X \mathbf{\Lambda}_X \mathbf{V}_X^H$  and  $\mathbf{U}_Y \mathbf{\Lambda}_Y \mathbf{V}_Y^H$  are SVDs of the matrices  $\mathbf{X}$  and  $\mathbf{Y}$ , respectively. We also use the tensor operator rule  $\text{tr}\{\mathbf{W} \mathbf{X} \mathbf{Y} \mathbf{Z}\} = (\text{vec}(\mathbf{Z}))^H (\mathbf{W} \otimes \mathbf{Y}^H) \text{vec}(\mathbf{X}^H)$  and  $\text{tr}\{\mathbf{X}^H \mathbf{Y}\} = (\text{vec}(\mathbf{X}))^H \text{vec}(\mathbf{Y})$

where  $\bar{\Delta}$  must be a diagonal matrix. Since  $\mathbf{H} = \hat{\mathbf{H}} + \Delta_H$ , we can immediately conclude that  $\hat{\mathbf{U}} = \mathbf{U}$  and  $\hat{\mathbf{V}} = \mathbf{V}$ . This is equivalent to the structure of (5.26) which can be determined from the channel estimate matrix  $\hat{\mathbf{H}}$ . Following this result, we can find the diagonal elements of  $\bar{\Delta}$  as

$$w_i \lambda_i^2 \sigma_i^2 \bar{\delta}_i + w_i \lambda_i^2 \sigma_i^2 \gamma_i = w_i \lambda_i \sigma_i + \vartheta \bar{\delta}_i, \quad i = 1, \dots, n_r \quad (5.110)$$

$$\vartheta \geq w_i \lambda_i^2 \sigma_i^2, \quad i = 1, \dots, n_r \quad (5.111)$$

$$\sum_{i=1}^{n_r} \bar{\delta}_i^2 = \tilde{\varepsilon}_H^2 \quad (5.112)$$

Solving the first equation, we have (5.28) and

plugging it into the third equation, we obtain (5.29). Note that the left side of the equation above is a decreasing function in the region of  $\vartheta \in [\max_i(w_i \lambda_i^2 \sigma_i^2), \infty]$  with the values ranging from  $+\infty$  to zero correspondingly. Therefore, there exists a  $\vartheta \in [\max_i(w_i \lambda_i^2 \sigma_i^2), \infty)$  such that the equation (5.29) is satisfied. The proof follows immediately.

## 5.C Proof of Theorem 5.1

When we substitute (5.23), (5.24), and (5.26) into the original problem (5.9), the problem simplifies to a minimization problem with respect to  $\mathbf{F}$ ,  $\mathbf{G}$  and the auxiliary variable  $\vartheta$  (using the dual problem of the trust region subproblems stated in Lemma 5.3). Now, using Lemma 5.1, the optimal precoding and equalization matrices must have the structure given in (5.5) and (5.6) for any values of error matrices. Substituting expressions for  $\mathbf{F}$  and  $\mathbf{G}$  and approximate worst-case system matrices (5.23), (5.24), and (5.26) into (5.9), we can convert the problem into a scalar optimization problem, which is simplified as (5.34). Notice that the maximization preserves the convexity, therefore this problem is a convex optimization problem with respect to each of  $\mathbf{G}$  and  $\mathbf{F}$  (but still jointly non-convex). Consequently, the reduced scalar optimization problem is convex in terms of each of  $\lambda_i$ s or  $\sigma_i$ s,  $i = 1, \dots, n_r$ . Fixing  $\vartheta$ , we can establish the Lagrangian function and equate its derivatives with respect to  $\lambda_i$  and  $\sigma_i$  to zero. These give us necessary conditions for the optimal values of  $\lambda_i$  and  $\sigma_i$ .

Thus, optimal values of these variables must satisfy the following equations:

$$-\frac{\vartheta w_i \sigma_i (\sigma_i \lambda_i \gamma_i - 1) (w_i \sigma_i \lambda_i - \vartheta \gamma_i)}{(\vartheta - w_i \lambda_i^2 \sigma_i^2)^2} + w_i \lambda_i = 0 \quad (5.113)$$

$$-\frac{\vartheta w_i \lambda_i (\sigma_i \lambda_i \gamma_i - 1) (w_i \sigma_i \lambda_i - \vartheta \gamma_i)}{(\vartheta - w_i \lambda_i^2 \sigma_i^2)^2} + \mu \sigma_i = 0 \quad (5.114)$$

where  $\mu \geq 0$  is a Lagrangian multiplier corresponding to the transmit power constraint  $\sum_i \sigma_i^2 \leq P$ . Note that unlike related work (e.g. [130]) we *jointly* optimize the precoder and equalizer (or  $\sigma_i$ s and  $\lambda_i$ s) rather than in an alternating manner optimize the precoder and equalizer.

We denote

$$Z_i = \frac{\vartheta w_i (\sigma_i \lambda_i \gamma_i - 1) (w_i \sigma_i \lambda_i - \vartheta \gamma_i)}{(\vartheta - w_i \lambda_i^2 \sigma_i^2)^2}, \quad (5.115)$$

to simplify (5.113) and (5.114) as

$$-Z_i \sigma_i + w_i \lambda_i = 0, \quad (5.116)$$

$$-Z_i \lambda_i + \mu \sigma_i = 0. \quad (5.117)$$

We can simply conclude that  $Z_i = \sqrt{\mu w_i}$  if  $\sigma_i, \lambda_i > 0$ , which is equivalent to the following equation:

$$\frac{\vartheta w_i (\sigma_i \lambda_i \gamma_i - 1) (w_i \sigma_i \lambda_i - \vartheta \gamma_i)}{(\vartheta - w_i \lambda_i^2 \sigma_i^2)^2} - \sqrt{\mu w_i} = 0 \quad (5.118)$$

Replacing  $r = \lambda_i \sigma_i$  and simplifying (5.118) results in the quartic equation (5.37).

Please note that the quartic equation is the highest-order of polynomial equation, for which the closed-form solutions are available (e.g. Ferrari's method) [144]. The solutions to equation  $\varphi_i(r) = 0$  are given as [144]

$$r_i = \frac{\pm_s \sqrt{a_i + 2y_i} \pm_t \sqrt{-\left(3a_i + 2y_i \pm_s \frac{2b_i}{\sqrt{a_i + 2y_i}}\right)}}{2} \quad (5.119)$$

where two signs of  $\pm_s$  must match, while the sign of  $\pm_t$  is independent of that.

The parameters used in the expression can be defined as

$$a_i = -\frac{2\vartheta}{w_i} - \frac{\gamma_i\vartheta}{\sqrt{\mu w_i}} \quad (5.120)$$

$$b_i = \frac{\gamma_i^2\vartheta^2}{w_i\sqrt{\mu w_i}} + \frac{\vartheta}{\sqrt{w_i\mu}} \quad (5.121)$$

$$c_i = \frac{\vartheta^2}{w_i^2} - \frac{\vartheta^2\gamma_i}{w_i\sqrt{\mu w_i}} \quad (5.122)$$

$$U_i = \sqrt[3]{-\frac{Q_i}{2} + \sqrt{\frac{Q_i^2}{4} + \left(\frac{P_i}{3}\right)^3}} \quad (5.123)$$

$$P_i = -\frac{a_i^2}{12} - c_i \quad (5.124)$$

$$Q_i = -\frac{a_i^3}{108} + \frac{a_i c_i}{3} - \frac{b_i^2}{8} \quad (5.125)$$

$$y_i = -\frac{5}{6}a_i + U_i - \frac{P_i}{3U_i} \quad (5.126)$$

From (5.116) and (5.117), the optimal values of  $\lambda_i$  and  $\sigma_i$  must be in the form of (5.35)-(5.36) result. This close-form structure for the optimal values of  $\lambda_i$  and  $\sigma_i$  produce a reduced-complexity algorithm to design the precoder and equalizer jointly.

# Chapter 6

## Summary of Contributions and Future Work

### 6.1 Summary of Contributions

In this thesis, we have considered a general form of multi-node cooperation by studying partial user message sharing between the nodes (base stations). This scenario is referred to as network MIMO with partial cooperation. Different power limitations have been enforced in the system with emphasis on individual power constraints at the base stations (BSs). First, we have shown that this system is equivalent to a MIMO interference channel with generalized linear constraints (MIMO-IFC-GC). Then, we have investigated linear transmission and reception strategies in this channel model. This has been performed in two scenarios depending on the availability of channel state information (CSI) at both ends of the system: perfect and imperfect CSI. We first review the completed work in case of perfect CSI.

#### 6.1.1 Block diagonalization (multiple-antenna user zero-forcing)

The optimality of the conventional block diagonalization (BD) in multiuser MIMO systems under the total power constraint has been proven rigorously [97]. Sub-optimality of the conventional BD technique under individual power constraints has been shown and it has motivated the search for the optimal BD scheme. The optimal BD scheme for multi-cell cooperative network under

per-antenna/per-BS power constraints has been proposed by fixing the search domain to be any linear combination of the null space of other user's channels. We have proposed a simple iterative descent gradient algorithm, which obtains the optimal precoders for multi-cell BD [62, 63]. Extensive numerical results in realistic cellular model are given to study different benefits delivered by employment of cooperation between multiple BSs.

### 6.1.2 MMSE Linear Precoding and Equalization

In the next step, we consider MMSE precoding and equalization and include linear processing at the receiver. The problems of maximizing the sum-rate (SR) and minimizing the weighted sum mean square error (WSMSE) of the data estimates are non-convex, and suboptimal solutions with reasonable complexity need to be devised. First the suboptimal techniques that aim at maximizing the sum-rate for the MIMO-IFC-GC are reviewed from recent literature and are extended to the MIMO-IFC-GC where necessary. Then, two novel designs that aim at minimizing the WSMSE are proposed [73, 74]. Specifically, we have proposed an extension of the recently introduced MMSE interference alignment strategy and a novel strategy termed diagonalized MSE-matrix (DMMSE). Our proposed strategies support transmission of any arbitrary number of data streams per user. Extensive numerical results show that the DMMSE outperforms most previously proposed techniques and performs just as well as the best known strategy. We have provided numerical results to compare the performance of the investigated schemes for realistic cellular systems considering path loss, lognormal shadowing, small-scale fading and sectorization. With respect to complexity, the extended MMSE interference alignment technique is less complex than the previously discussed techniques. Our DMMSE is slightly less complex than the polite water-filling algorithm, which is known as best algorithm prior to our DMMSE algorithm proposal.

### **6.1.3 Network MIMO User Scheduling**

It is shown that allowing the cell clusters to overlap increases the signal-to-interference-plus-noise-ratio (SINR) dramatically. The general problem of network-level user scheduling is formulated, where there are no pre-defined clusters, but the cooperation and data sharing are constrained. A simple algorithm has been proposed for multi-cell user scheduling and a revised form of BD has been introduced for it [55].

### **6.1.4 Semi-orthogonal User Selection Algorithm for Multiple-antenna Users**

In order to employ BD in the multi-cell systems with mobile users equipped with multiple antennas, we need to extend the user selection algorithm for the single-antenna case. A semi-orthogonal user selection has been extended to the multiple-antenna user case [62].

In the second part of this dissertation, we have considered imperfect CSI.

### **6.1.5 Robust Linear Precoding and Equalization**

Joint design of robust linear precoders and equalizers for MIMO-IFC-GC has been investigated. The inaccurate knowledge of channel state information (CSI) has been assumed to follow the worst-case deterministic model, where the actual channel between each transmitter and receiver is guaranteed to fit within a sphere centered at its estimated value. Our objective is to minimize weighted sum of mean square errors of the estimated symbols, which is a general utility function. We have started with the single-user system, where we account for inaccurate awareness of the interference plus noise covariance matrix and the power shaping matrix in addition to the imperfect knowledge of channel matrix. We derive the worst-case values of these system matrices and transform the joint precoder and equalizer optimization problem into a scalar convex optimization problem. Further, the solution to this problem is simplified to a depressed quartic equation, the closed-form expressions for roots of which are known. Next, we propose an iterative algorithm to obtain the

worst-case robust transceivers based on the derived structures of precoder and equalizer. This design approach is further employed in the multiuser scenario (MIMO-IFC-GC), where it does not require semi-definite reformulation.

## **6.2 Future Work**

Practical issues of implementing multi-cell cooperative systems play the key role in future works in this research area. Hence, in the following we discuss a number of these problems and possible direction of work towards their solutions.

### **6.2.1 Decentralized solution to the optimization problems**

As it is expected in the research work, we started from ideal assumptions in the multi-cell scenario, but stepped further with partial cooperation. Employing fully centralized optimization of downlink transmissions is highly unlikely in the future multi-cell cooperative systems. Therefore, we need to propose a scheme to distribute the optimization problem over the network, so that much of the processing can be done locally with limited exchange of information between the BSs. The decentralized multi-cell cooperation is vital for the network-level user scheduling scheme where the signalling is highly distributed and coupled over the entire network. Our proposed approach involves decoupling the power constraints in the network to enable local optimizations and then control the power allocations through an outer loop.

### **6.2.2 Robust linear strategies**

The external factors such as complexity and backhaul capacity are not the only limitations in multi-cell cooperative systems. Indeed, the amount of spectral resources allocated for training (CSI estimation) is determined by the time and frequency variability of the fading channels [78]. Therefore, CSI estimation error must be accounted for in the design of network MIMO. Hence, we need to track the robustness of the transmission strategies under the statistical CSI.

We have considered the worst-case CSI estimation error in this dissertation, but a future direction may be to consider the errors stochastically distributed. We will follow the MMSE precoding structure using the weighted sum-MSE minimization. Robust MMSE precoding was recently studied in [129] for MIMO systems, which stimulated ideas for further extensions to the multiuser case.

### 6.2.3 Multi-cell user scheduling

As it has been mentioned, the multi-cell user scheduling problem [55] is open, but it is promising. We may start by studying the cellular network analytically. In order to analyze a realistic cellular model, we can consider that the nodal arrangement is almost a stationary Poisson point process, where known mobile (users) and fixed nodes (BSs) are distributed independently within a region. There are interesting results characterizing the distribution of the Euclidean distance between the nodes in this more-realistic model given in [147]. Since this result is available by ordered statistics of the distances, it is more relevant to the multi-cell user scheduling algorithm proposed in our work rather than conventional clustering. Further performance analysis can be carried out. This has been recently studied in [148–150]. With this proposed direction, we may obtain the capacity results of the multi-cell cooperative systems in more-realistic cellular models than quite simplistic Wyner-type models.

### 6.2.4 MMSE interference alignment

The optimization of MMSE transceivers can be extended to complete cancellation of interference (interference alignment) in a more efficient way than the current methods. Computational complexity of the closed-form interference alignment is known to be high (NP-hard) and its performance is poor in low SNR regime. With the MMSE concepts established we expect to obtain a simple iterative approach to this problem.

### **6.2.5 Synchronization**

Multicell downlink cooperation needs tight synchronization with ideally no carrier frequency offset (CFO) between local oscillators at the base stations. This synchronization can be achieved by global positioning system (GPS) receivers. However, there are still challenges for GPS receivers for indoor base stations. Indoor base stations may benefit from the timing signal sent from the outdoor GPS receiver using a precise timed network protocol.

# Appendices

# Appendix A

## Convex Optimization Theory

This chapter contains some preliminaries of the convex optimization theory widely used throughout this dissertation.

### A.1 Basic Optimization Concepts

**Definition A.1** (Convex Set). A set  $\mathcal{C} \in \mathfrak{R}^n$  is convex if for any two points  $x, y \in \mathcal{C}$ , the line segment connecting  $x$  and  $y$  also belongs to  $\mathcal{C}$ :

$$\theta x + (1 - \theta)y \in \mathcal{C}, \quad \forall x, y \in \mathcal{C} \text{ and } \theta \in [0, 1]. \quad (\text{A.1})$$

Examples of convex sets are balls, ellipsoids, hypercubes, polyhedral sets. The intersection of any number of convex sets is also convex. However, the union of two convex sets is typically nonconvex.

**Definition A.2** (Convex Cone). A convex cone  $\mathcal{K}$  is a convex set which is closed under positive scaling:  $\forall x \in \mathcal{K}, \alpha \geq 0, \alpha x \in \mathcal{K}$ .

Examples of convex cones are non-negative orthant  $\mathfrak{R}_+^n$ , second order cone:  $\text{SOC}(n) = \{(t, \mathbf{x}) \mid t \geq \|\mathbf{x}\|\}$ , and the most common convex cone in this dissertation, which is positive semidefinite matrix cone:

$$\mathcal{S}_+^n = \{\mathbf{X} \mid \mathbf{X} \text{ is symmetric and } \mathbf{X} \succeq 0\}. \quad (\text{A.2})$$

**Definition A.3** (Convex functions). A function  $f(\mathbf{x}) : \mathfrak{R}^n \rightarrow \mathfrak{R}$  is convex if for any two points  $\mathbf{x}, \mathbf{y} \in \mathfrak{R}^n$

$$f(\theta \mathbf{x} + (1 - \theta)\mathbf{y}) \leq \theta f(\mathbf{x}) + (1 - \theta)f(\mathbf{y}), \quad \forall \theta \in [0, 1]. \quad (\text{A.3})$$

If  $f$  is continuously differentiable, then the convexity of  $f$  is equivalent to

$$f(\mathbf{y}) \geq f(\mathbf{x}) + \nabla f(\mathbf{x})^T(\mathbf{y} - \mathbf{x}), \quad \forall \mathbf{x}, \mathbf{y} \in \mathfrak{R}^n. \quad (\text{A.4})$$

Therefore, when  $f$  is convex the first-order Taylor approximation is a global underestimator of  $f$ . If  $f$  is twice continuously differentiable, then its convexity is equivalent to the positive semidefiniteness of its Hessian:  $\nabla^2 f(\mathbf{x}) \succeq 0, \forall \mathbf{x} \in \mathfrak{R}^n$ . For example, a quadratic function  $\mathbf{x}^T \mathbf{P} \mathbf{x} + \mathbf{q}^T \mathbf{x} + r$  is convex if and only if  $\mathbf{P} \succeq 0$ .

The convex functions are closed under summation, positive scaling, and the pointwise maximum operations.

**Definition A.4** (Convex Optimization Problems). Generic optimization problem can be expressed as

$$\begin{aligned} & \underset{x \in \mathcal{C}}{\text{minimize}} && f_0(x) \\ & \text{subject to} && f_i(x) \leq 0, \quad i = 1, \dots, m, \\ & && h_j(x) = 0, \quad j = 1, \dots, r \end{aligned} \quad (\text{A.5})$$

where  $f_0$  is called the objective function (or cost/utility function),  $\{f_i\}_{i=1}^m$  and  $\{h_j\}_{j=1}^r$  are called the inequality and equality constraint functions, respectively, and  $\mathcal{C}$  is called a constraint set. The optimization variable  $x$  is feasible if  $x \in \mathcal{C}$  and it satisfies all the inequality and equality constraints. A feasible solution  $x^*$  is globally optimal if  $f_0(x^*) \leq f_0(x)$  for all feasible  $x$ . A feasible point  $\tilde{x}$  is locally optimal if there exists some  $\epsilon > 0$  such that  $f_0(\tilde{x}) \leq f_0(x)$  for all feasible  $x$  satisfying  $\|x - \tilde{x}\| \leq \epsilon$ .

The optimization problem (A.5) is convex if (i) the functions  $f_i, i = 0, 1, \dots, m$  are convex; (ii)  $h_j(x)$  are affine functions (i.e.,  $h_j$  is of the form  $\mathbf{a}_j^T \mathbf{x} + b_j$  for some  $\mathbf{a}_j \in \mathfrak{R}^n$  and  $b_j \in \mathfrak{R}$ ); and (iii)  $\mathcal{C}$  is also convex. If any one of these conditions is not satisfied, the problem is nonconvex.

Convex optimization problems are the largest subclass of optimization problems which are efficiently solvable, whereas nonconvex optimization problems are generally difficult. High quality softwares are available (many of them free) which can obtain accurate solutions efficiently and reliably. Therefore, when an engineering problem is formulated in a convex form, the

problem is considered solved numerically. For a convex optimization problem, any locally optimal solution is also globally optimal. Moreover, when an optimization problem is convex, there exist efficient interior-point optimization algorithms whose worst-case complexity to find an  $\epsilon$ -optimal solution grows as a polynomial function of the problem data length and  $\log 1/\epsilon$ .

## A.2 Lagrangian Duality

Consider a (not necessarily convex) optimization problem

$$\begin{aligned} & \underset{\mathbf{x} \in \mathcal{C}}{\text{minimize}} && f_0(\mathbf{x}) \\ & \text{subject to} && f_i(\mathbf{x}) \leq 0, \quad i = 1, \dots, m, \\ & && h_j(\mathbf{x}) = 0, \quad j = 1, \dots, r. \end{aligned} \tag{A.6}$$

Let  $p^*$  represent the global minimum value of this problem. Now, we introduce a dual variable  $\boldsymbol{\lambda} \in \Re^m$  and  $\boldsymbol{\mu} \in \Re^r$  and establish the Lagrangian function

$$\mathcal{L}(\mathbf{x}, \boldsymbol{\lambda}, \boldsymbol{\mu}) = f_0(\mathbf{x}) + \sum_{i=1}^m \lambda_i f_i(\mathbf{x}) + \sum_{j=1}^r \mu_j h_j(\mathbf{x}). \tag{A.7}$$

The dual function of this problem is correspondingly defined as

$$g(\boldsymbol{\lambda}, \boldsymbol{\mu}) = \min_{\mathbf{x} \in \mathcal{C}} \mathcal{L}(\mathbf{x}, \boldsymbol{\lambda}, \boldsymbol{\mu}). \tag{A.8}$$

The dual function  $g(\boldsymbol{\lambda}, \boldsymbol{\mu})$  is a pointwise minimum of a family of linear functions with respect to  $(\boldsymbol{\lambda}, \boldsymbol{\mu})$  and therefore it is always concave.  $(\boldsymbol{\lambda}, \boldsymbol{\mu})$  is dual feasible when  $\boldsymbol{\lambda} \geq 0$  and  $g(\boldsymbol{\lambda}, \boldsymbol{\mu})$  is finite. The original problem (A.6) is also referred to as primal problem and  $\mathbf{x}$  is called primal vector.

*Proposition A.1 (Weak Duality).* For any primal feasible vector  $\mathbf{x}$  and the dual feasible vector  $(\boldsymbol{\lambda}, \boldsymbol{\mu})$ , we have

$$f_0(\mathbf{x}) \geq g(\boldsymbol{\lambda}, \boldsymbol{\mu}). \tag{A.9}$$

Equivalently, for any dual feasible vector  $(\boldsymbol{\lambda}, \boldsymbol{\mu})$ , the dual function  $g(\boldsymbol{\lambda}, \boldsymbol{\mu})$  is a lower bound of the primal objective function  $f_0(\mathbf{x})$ . Consequently,  $p^* \geq g(\boldsymbol{\lambda}, \boldsymbol{\mu})$  for all dual feasible variables  $(\boldsymbol{\lambda}, \boldsymbol{\mu})$ . Maximizing  $g(\boldsymbol{\lambda}, \boldsymbol{\mu})$  over all dual

feasible  $(\boldsymbol{\lambda}, \boldsymbol{\mu})$  gives us the largest lower bound of the optimal value of the primal problem. Hence, the dual optimization problem is defined as

$$\begin{aligned} & \text{maximize} && g(\boldsymbol{\lambda}, \boldsymbol{\mu}) \\ & \text{subject to} && \boldsymbol{\lambda} \succeq 0, \boldsymbol{\mu} \in \mathfrak{R}^r. \end{aligned} \quad (\text{A.10})$$

The dual problem (A.10) is always convex regardless of the convexity of the primal problem. Let  $d^*$  denote the optimal value of the dual problem (A.10). Therefore, we have  $p^* \geq d^*$ . The non-negative number  $p^* - d^*$  is called *duality gap*. We say that *strong duality* holds for the above problem if the duality gap is zero, i.e.  $d^* = p^*$ . Strong duality holds for most of convex optimization problems (satisfying Slater's conditions [50, 115]). Generally, strong duality holds under a set of conditions known as *constraint qualifications* (for more details refer to [115]). Now, we present the local optimality conditions for the optimization problem (A.6).

*Proposition A.2* (Karush-Kuhn-Tucker Conditions). The necessary condition for  $\mathbf{x}^*$  to be locally optimal solution of (A.6) is that there exists a  $(\boldsymbol{\lambda}^*, \boldsymbol{\mu}^*)$  such that the following conditions are all satisfied:

$$f_i(\mathbf{x}^*) \leq 0, i = 1, \dots, m \quad (\text{A.11})$$

$$h_j(\mathbf{x}^*) = 0, j = 1, \dots, r \quad (\text{A.12})$$

$$\boldsymbol{\lambda}^* \succeq 0, \quad (\text{A.13})$$

$$\lambda_i^* f_i(\mathbf{x}^*) = 0, i = 1, \dots, m \quad (\text{A.14})$$

and

$$\nabla f_0(\mathbf{x}^*) + \sum_{i=1}^m \lambda_i^* \nabla f_i(\mathbf{x}^*) + \sum_{j=1}^r \mu_j^* \nabla h_j(\mathbf{x}^*) = 0. \quad (\text{A.15})$$

The conditions (A.11)-(A.15) are referred to as *Karush-Kuhn-Tucker (KKT) conditions* for optimality. First two conditions (A.11) and (A.12) are primal feasibility conditions of  $\mathbf{x}^*$ , (A.13) is dual feasibility condition, (A.14) represents the complementary slackness condition for the primal and dual inequality constraint pairs:  $f_i(\mathbf{x}^*) \leq 0$  and  $\lambda_i^* \geq 0$ . The last condition is the zero gradient condition  $\nabla_{\mathbf{x}} \mathcal{L}(\mathbf{x}^*, \boldsymbol{\lambda}^*, \boldsymbol{\mu}^*) = 0$ .

### A.3 Semidefinite Programming

The downlink beamforming, precoding, and/or resource allocation problems can be categorized as *linear conic programming*. In this section, we review this class of optimization problem.

**Definition A.5** (Linear Conic Programming). Consider a primal and dual optimization problems

$$\begin{aligned} & \text{minimize} \quad \text{tr}\{\mathbf{C}\mathbf{X}\} \\ & \text{subject to} \quad \mathcal{A}\mathbf{X} = \mathbf{b}, \mathbf{X} \in \mathcal{K} \end{aligned} \quad (\text{A.16})$$

and

$$\begin{aligned} & \text{maximize} \quad \mathbf{b}^\top \mathbf{y} \\ & \text{subject to} \quad \mathcal{A}^* \mathbf{y} + \mathbf{S} = \mathbf{C}, \mathbf{S} \in \mathcal{K}^* \end{aligned} \quad (\text{A.17})$$

where  $\mathcal{A}$  is a linear operator mapping an Euclidean space onto another Euclidean space, and  $\mathcal{A}^*$  is its adjoint.  $\mathcal{K}$  and  $\mathcal{K}^*$  denote a closed convex cone and its dual, respectively. The problems (A.16) and (A.17) are called *linear conic programming*.

Some of the special cases of this problem are reviewed as follows:

**Definition A.6** (Linear Programming (LP)  $\mathcal{K} = \mathfrak{R}_+^n$ ). Linear programming problem is defined as

$$\begin{aligned} & \text{minimize} \quad \mathbf{c}^\top \mathbf{x} \\ & \text{subject to} \quad \mathbf{A}\mathbf{x} = \mathbf{b}, \mathbf{x} \succeq 0 \end{aligned} \quad (\text{A.18})$$

and its dual is given by

$$\begin{aligned} & \text{maximize} \quad \mathbf{b}^\top \mathbf{y} \\ & \text{subject to} \quad \mathbf{A}^\top \mathbf{y} + \mathbf{s} = \mathbf{c}, \mathbf{s} \succeq 0. \end{aligned} \quad (\text{A.19})$$

The optimality condition of the LP is given by

$$\mathbf{A}\mathbf{x} = \mathbf{b}, \mathbf{x} \succeq 0, \mathbf{A}^\top \mathbf{y} + \mathbf{s} = \mathbf{c}, \mathbf{s} \succ 0, \mathbf{x}^\top \mathbf{s} = 0. \quad (\text{A.20})$$

**Definition A.7** (Second-Order Cone Programming (SOCP)  $\mathcal{K} = \prod_{i=1}^m \text{SOC}(n_i)$ ).

$$\begin{aligned} & \text{minimize} \quad \mathbf{c}^\top \mathbf{x} \\ & \text{subject to} \quad \|\mathbf{A}_i \mathbf{x} + \mathbf{b}_i\| \leq t_i, \forall i \end{aligned} \quad (\text{A.21})$$

The SOCP is equivalent to quadratically constrained quadratic program (QCQP).

**Definition A.8** (Semidefinite Programming (SDP)). The SDP can be expressed as

$$\begin{aligned} & \text{minimize} && \text{tr}\{\mathbf{C}\mathbf{X}\} \\ & \text{subject to} && \text{tr}\{\mathbf{A}_i\mathbf{X}\} = b_i, \quad i = 1, \dots, m, \quad \mathbf{X} \succeq 0 \end{aligned} \quad (\text{A.22})$$

and its dual is

$$\begin{aligned} & \text{maximize} && \mathbf{b}^\top \mathbf{y} \\ & \text{subject to} && \sum_{i=1}^m \mathbf{A}_i^\top y_i + \mathbf{S} = \mathbf{C}, \quad \mathbf{S} \succeq 0 \end{aligned} \quad (\text{A.23})$$

The optimality conditions for this problem are given by

$$\text{tr}\{\mathbf{A}_i\mathbf{X}\} = b_i, \quad \mathbf{X} \succeq 0 \quad (\text{A.24})$$

$$\sum_{i=1}^m \mathbf{A}_i^\top y_i + \mathbf{S} = \mathbf{C}, \quad \mathbf{S} \succeq 0, \quad \text{tr}\{\mathbf{X}\mathbf{S}\} = 0. \quad (\text{A.25})$$

Linear conic optimization problems can be solved efficiently using interior-point methods. The worst-case complexity of a general SDP is  $\mathcal{O}(n^{6.5})$ . If the constraint have diagonal structure, then its complexity can be reduced to  $\mathcal{O}(n^{3.5})$ .

## A.4 Gradient and Sub-gradient Algorithms

The gradient and sub-gradient methods are simple algorithms to find the local optimal solution of an optimization problem with differentiable and non-differentiable objective functions. They have little requirements of memory usage and tractable for parallel implementation [115].

Consider a general minimization problem over a convex set defined as

$$\text{minimize}_{\mathbf{x}} \quad f_0(\mathbf{x}) \quad (\text{A.26})$$

$$\text{subject to} \quad \mathbf{x} \in \mathcal{C}. \quad (\text{A.27})$$

The gradient and sub-gradient projection method produce a set of iteratively defined feasible points as

$$\mathbf{x}(t+1) = [\mathbf{x}(t) - \alpha(t)\mathbf{s}(t)]_{\mathcal{C}} \quad (\text{A.28})$$

where  $\mathbf{s}(t)$  is a gradient or sub-gradient of  $f_0$  evaluated at the operating point  $x(t)$  for differentiable or non-differentiable function  $f_0$ , respectively.

$[\cdot]_{\mathcal{C}}$  denotes the projection onto the feasible set  $\mathcal{C}$ , and  $\alpha(t)$  is a positive step-size. For efficiently small step-size, the distance of the current solution  $\mathbf{x}(t)$  and the optimal solution  $\mathbf{x}^*$  decreases. Hence, these algorithms are convergent. The convergence behavior of the gradient/sub-gradient methods with respect to different choices of the step-sizes have been investigated extensively [115, 151, 152]. A decreasing step-size can be defined as  $\alpha(t) = \frac{1+a}{t+a}$ , where  $a$  is a fixed non-negative number. For this type of step-size, the algorithm is guaranteed to converge to the optimal value when the gradient/sub-gradients are bounded [115]. Constant step-sizes are useful in the distributed algorithms and the gradient/sub-gradient algorithms are convergent for the bounded gradient/sub-gradient values [115, 152]. The gradient of an optimization problem can be defined as  $\nabla \mathcal{L}(\mathbf{x}, \boldsymbol{\lambda})$ , where  $\mathcal{L}(\cdot)$  is the Lagrangian function of the problem.  $\mathbf{s}$  is a *sub-gradient* of function  $f_0$  (not necessarily convex) at  $\mathbf{x}$  if

$$f_0(\mathbf{y}) \geq f_0(\mathbf{x}) + \mathbf{s}^\top(\mathbf{y} - \mathbf{x}), \quad \forall \mathbf{y} \quad (\text{A.29})$$

Sub-gradient gives an affine global underestimator of  $f_0$ . If  $f_0$  is convex, it has at least one sub-gradient at every point  $\mathbf{x}$ . If  $f_0$  is convex and differentiable,  $\nabla f_0(\mathbf{x})$  is a sub-gradient (and gradient) of  $f_0$ .

## A.5 Gauss-Seidel Algorithms

Consider the following multivariable minimization problem:

$$\begin{aligned} & \underset{\mathbf{x}_1, \dots, \mathbf{x}_n}{\text{minimize}} && f(\mathbf{x}_1, \dots, \mathbf{x}_n) \\ & \text{subject to} && \mathbf{x}_i \in \mathcal{C}_i \end{aligned} \quad (\text{A.30})$$

over the closed convex sets  $\mathcal{C}_1, \dots, \mathcal{C}_n$ . This problem may arise in cooperative games where multiple players must obtain a strategy  $\mathbf{x}_i$  to minimize a general utility function of the game.

**Definition A.9** (Gauss-Seidel Algorithm [153]). The nonlinear *Gauss-Seidel algorithm* contains iterative optimization in a circular fashion with respect to a single variable vector while the remaining variables are fixed. Hence, each iteration of this algorithm is defined as

$$\mathbf{x}_i^{(t+1)} = \arg \min_{\mathbf{x}_i \in \mathcal{C}_i} f \left( \mathbf{x}_1^{(t+1)}, \dots, \mathbf{x}_{i-1}^{(t+1)}, \mathbf{x}_i, \mathbf{x}_{i+1}^{(t)}, \dots, \mathbf{x}_n^{(t)} \right) \quad (\text{A.31})$$

where  $t$  is the outer loop iteration index. For any given  $t$ , the step (A.31) is performed over  $i = 1, \dots, n$ . This algorithm is also called block-coordinate descent algorithm [152].

**Definition A.10** (Jacobi Algorithm [153]). The nonlinear Jacobi algorithm contains iterative optimization in a parallel fashion with respect to a single variable while the remaining variables are fixed. Therefore, each inner-loop iteration is defined as

$$\mathbf{x}_i^{(t+1)} = \arg \min_{\mathbf{x}_i \in \mathcal{C}_i} f \left( \mathbf{x}_1^{(t)}, \dots, \mathbf{x}_{i-1}^{(t)}, \mathbf{x}_i, \mathbf{x}_{i+1}^{(t)}, \dots, \mathbf{x}_n^{(t)} \right) \quad (\text{A.32})$$

If the function  $f$  is continuously differentiable and convex on the set  $\prod_{i=1}^n \mathcal{C}_i$ , and the minimization problem with respect to each single variable  $\mathbf{x}_i$  has a unique solution, then every limit solution of the nonlinear Gauss-Seidel algorithm minimizes  $f$  [152, 153].

## A.6 Dual Decomposition

*Dual decomposition* is a method to decompose the original large optimization problem into a number of subproblems each solvable in a distributive fashion [152–154]. As a result of decomposition, the original problem is decomposed into a two-level structure with a master problem and subproblems. The two levels will communicate with each other and may require a message passing procedure which can introduce some overhead in the design.

Consider the following problem which contains coupled constraints:

$$\begin{aligned} & \underset{\mathbf{x}_1, \dots, \mathbf{x}_n}{\text{minimize}} && \sum_{i=1}^n f_i(\mathbf{x}_i) \\ & \text{subject to} && \mathbf{x}_i \in \mathcal{C}_i, \forall i \\ & && \sum_{i=1}^n \mathbf{h}_i(\mathbf{x}_i) \leq \mathbf{p}. \end{aligned} \quad (\text{A.33})$$

Note that without the constraint  $\sum_{i=1}^n \mathbf{h}_i(\mathbf{x}_i) \leq \mathbf{p}$  the problem was decoupled and can be solved individually for each single variable  $\mathbf{x}_i$ . Now, we establish the Lagrangian function and relax the coupling constraints as

$$\begin{aligned} & \underset{\mathbf{x}_1, \dots, \mathbf{x}_n}{\text{minimize}} && \sum_{i=1}^n f_i(\mathbf{x}_i) + \boldsymbol{\lambda}^\top \left( \sum_{i=1}^n \mathbf{h}_i(\mathbf{x}_i) - \mathbf{p} \right) \\ & \text{subject to} && \mathbf{x}_i \in \mathcal{C}_i, \forall i. \end{aligned} \quad (\text{A.34})$$

Now, we can establish subproblems

$$\begin{aligned} & \underset{\mathbf{x}_i}{\text{minimize}} && f_i(\mathbf{x}_i) + \boldsymbol{\lambda}^\top \mathbf{h}_i(\mathbf{x}_i) \\ & \text{subject to} && \mathbf{x}_i \in \mathcal{C}_i \end{aligned} \tag{A.35}$$

for each  $i$ . These subproblems can be solved given the Lagrangian variable  $\boldsymbol{\lambda}$ . Therefore, these subproblems form the inner-loop stage and an outer-loop stage updates the Lagrangian variable. The outer-loop problem is also called the master dual problem and can be defined as

$$\begin{aligned} & \underset{\boldsymbol{\lambda}}{\text{maximize}} && g(\boldsymbol{\lambda}) = \sum_{i=1}^n g_i(\boldsymbol{\lambda}) - \boldsymbol{\lambda}^\top \mathbf{p} \\ & \text{subject to} && \boldsymbol{\lambda} \geq 0 \end{aligned} \tag{A.36}$$

where  $g_i(\boldsymbol{\lambda})$  is the dual function obtained as the minimum value of the problem (A.35) for a given  $\boldsymbol{\lambda}$ . With this method, the dual problem will be solved and therefore the solution is only globally optimal for the original problem if strong duality holds. For differentiable dual functions  $g(\boldsymbol{\lambda})$  the master problem can be solved by the gradient method. When it is not differentiable, then sub-gradient algorithm can be employed. In this case, a sub-gradient of each  $g_i(\boldsymbol{\lambda})$  is known as

$$\mathbf{s}_i(\boldsymbol{\lambda}) = \mathbf{h}_i(\mathbf{x}_i^*(\boldsymbol{\lambda})) \tag{A.37}$$

where  $\mathbf{x}_i^*(\boldsymbol{\lambda})$  is the optimal solution of problem (A.35) with respect to  $\boldsymbol{\lambda}$ . Consequently, the global sub-gradient is also given by  $\mathbf{s}(\boldsymbol{\lambda}) = \sum_i \mathbf{s}_i(\boldsymbol{\lambda}) = \sum_i \mathbf{h}_i(\mathbf{x}_i^*(\boldsymbol{\lambda})) - \mathbf{p}$ .

# Bibliography

- [1] G. J. Foschini and M. J. Gans, “On limits of wireless communications in a fading environment when using multiple antennas,” *Wirel. Pers. Commun.*, vol. 6, no. 3, pp. 311 – 335, Mar. 1998.
- [2] E. Telatar, “Capacity of multi-antenna Gaussian channels,” *Euro. Trans. Telecommun.*, vol. 10, no. 6, pp. 585–595, Nov. 1999.
- [3] D. Gesbert, M. Kountouris, J. Heath, R. W., C.-B. Chae, and T. Salzer, “Shifting the MIMO paradigm,” *IEEE Signal Processing Mag.*, vol. 24, no. 5, pp. 36 – 46, Sep. 2007.
- [4] R. Blum, “MIMO capacity with interference,” *IEEE J. Select. Areas Commun.*, vol. 21, no. 5, pp. 793 – 801, Jun. 2003.
- [5] H. Dai, A. F. Molisch, and H. V. Poor, “Downlink capacity of interference-limited MIMO systems with joint detection,” *IEEE Trans. Wireless Commun.*, vol. 3, no. 2, pp. 442 – 53, Mar. 2004.
- [6] D. Gesbert, S. Hanly, H. Huang, S. Shamai, O. Simeone, and W. Yu, “Multi-cell MIMO cooperative networks: A new look at interference,” *IEEE J. Select. Areas Commun.*, vol. 28, no. 9, pp. 1 – 29, Dec. 2010.
- [7] S. Venkatesan, “Coordinating base stations for greater uplink spectral efficiency in a cellular network,” in *Proc. IEEE Int. Symposium on Personal, Indoor and Mobile Radio Commun. (PIMRC)*, Sep. 2007.
- [8] J. Zhang, R. Chen, J. Andrews, A. Ghosh, and R. Heath, “Networked MIMO with clustered linear precoding,” *IEEE Trans. Wireless Commun.*, vol. 8, no. 4, pp. 1910 – 1921, Apr. 2009.

- [9] H. Huang, M. Trivellato, A. Hottinen, M. Shafi, P. J. Smith, and R. Valenzuela, “Increasing downlink cellular throughput with limited network MIMO coordination,” *IEEE Trans. Wireless Commun.*, vol. 8, no. 6, pp. 2983 – 2989, Jun. 2009.
- [10] D. Lee, H. Seo, B. Clerckx, E. Hardouin, D. Mazzaresse, S. Nagata, and K. Sayana, “Coordinated multipoint transmission and reception in LTE-advanced: deployment scenarios and operational challenges,” *IEEE Commun. Mag.*, vol. 50, no. 2, pp. 148 –155, Feb. 2012.
- [11] M. Sawahashi, Y. Kishiyama, A. Morimoto, D. Nishikawa, and M. Tanno, “Coordinated multipoint transmission/reception techniques for LTE-advanced,” *IEEE Wireless Commun. Mag.*, Jun. 2010.
- [12] T. M. Cover and J. A. Thomas, *Elements of Information Theory*. New York: Wiley, 1991.
- [13] A. Gjendemsjø, D. Gesbert, G. E. Øien, and S. G. Kiani, “Binary power control for sum rate maximization over multiple interfering links,” *IEEE Trans. Wireless Commun.*, vol. 7, no. 8, pp. 3164 –3173, Aug. 2008.
- [14] D. Gesbert, S. G. Kiani, A. Gjendemsjø, and G. E. Oien, “Adaptation, coordination, and distributed resource allocation in interference-limited wireless networks,” *Proc. of the IEEE*, vol. 95, no. 12, pp. 2393 –2409, Dec. 2007.
- [15] S. G. Kiani and D. Gesbert, “Optimal and distributed scheduling for multicell capacity maximization,” *IEEE Trans. Wireless Commun.*, vol. 7, no. 1, pp. 288 –297, 2008.
- [16] L. Venturino, N. Prasad, and X. Wang, “Coordinated scheduling and power allocation in downlink multicell OFDMA networks,” *IEEE Trans. Veh. Technol.*, vol. 58, no. 6, pp. 2835 –2848, Jul. 2009.

- [17] M. Chiang, P. Hande, T. Lan, and C. W. Tan, "Power control in wireless cellular networks," *Foundations and Trends in Networking*, vol. 2, no. 4, pp. 381 – 533, Jul. 2008.
- [18] Z.-Q. Luo and S. Zhang, "Dynamic spectrum management: Complexity and duality," *IEEE J. Sel. Topics Signal Process.*, vol. 2, no. 1, pp. 57 –73, Feb. 2008.
- [19] Z. Han, Z. Ji, and K. J. R. Liu, "Non-cooperative resource competition game by virtual referee in multi-cell OFDMA networks," *IEEE J. Select. Areas Commun.*, vol. 25, no. 6, pp. 1079 –1090, Aug. 2007.
- [20] T. Alpcan, T. Basar, and S. Dey, "A power control game based on outage probabilities for multicell wireless data networks," *IEEE Trans. Wireless Commun.*, vol. 5, no. 4, pp. 890 – 899, Apr. 2006.
- [21] C. U. Saraydar, N. B. Mandayam, and D. J. Goodman, "Pricing and power control in a multicell wireless data network," *IEEE J. Select. Areas Commun.*, vol. 19, no. 10, Oct. 2001.
- [22] J. Huang, R. A. Berry, and M. L. Honig, "Distributed interference compensation for wireless networks," *IEEE J. Select. Areas Commun.*, vol. 24, no. 5, pp. 1074 – 1084, May 2006.
- [23] J. Yuan and W. Yu, "Distributed cross-layer optimization of wireless sensor networks: A game theoretic approach," in *Proc. IEEE Global Telecommun. Conf. (GLOBECOM)*, Dec. 2006.
- [24] W. Yu, T. Kwon, and C. Shin, "Joint scheduling and dynamic power spectrum optimization for wireless multicell networks," in *Proc. 44th Conf. Info. Science Sys. (CISS)*, Mar. 2010.
- [25] H. Dahrouj and W. Yu, "Coordinated beamforming for the multicell multi-antenna wireless system," *IEEE Trans. Wireless Commun.*, vol. 9, no. 5, pp. 1748 –1759, May 2010.

- [26] R. Zakhour, Z. Ho, and D. Gesbert, “Distributed beamforming coordination in multicell MIMO channels,” in *Proc. IEEE Veh. Tech. Conf. (VTC-Spring)*, Apr. 2009.
- [27] R. Zakhour and S. V. Hanly, “Base station cooperation on the downlink: Large system analysis,” *IEEE Trans. Inform. Theory*, vol. 58, no. 4, pp. 2079–2106, Apr. 2012.
- [28] H. Huh, H. C. Papadopoulos, and G. Caire, “Multiuser MISO transmitter optimization for intercell interference mitigation,” *IEEE Trans. Signal Processing*, vol. 58, no. 8, pp. 4272–4285, Aug. 2010.
- [29] F. Rashid-Farrokhi, K. J. R. Liu, and L. Tassiulas, “Transmit beamforming and power control for cellular wireless systems,” *IEEE J. Select. Areas Commun.*, vol. 16, no. 8, pp. 1437–1450, Oct. 1998.
- [30] W. Yu and T. Lan, “Transmitter optimization for the multi-antenna downlink with per-antenna power constraints,” *IEEE Trans. Signal Processing*, vol. 55, no. 6, pp. 2646–2660, Jul. 2007.
- [31] A. Wiesel, Y. C. Eldar, and S. Shamai, “Linear precoding via conic optimization for fixed MIMO receivers,” *IEEE Trans. Signal Processing*, vol. 54, no. 1, pp. 161–176, Jan. 2006.
- [32] B. Song, R. L. Cruz, and B. D. Rao, “Network duality for multiuser MIMO beamforming networks and applications,” *IEEE Trans. Commun.*, vol. 55, no. 3, pp. 618–630, Mar. 2007.
- [33] W. Yu, G. Ginis, and J. M. Cioffi, “Distributed multiuser power control for digital subscriber lines,” *IEEE J. Select. Areas Commun.*, vol. 20, no. 5, pp. 1105–1115, Jun. 2002.
- [34] G. Scutari, D. Palomar, and S. Barbarossa, “Competitive design of multiuser MIMO systems based on game theory: A unified view,” *IEEE J. Select. Areas Commun.*, vol. 26, no. 7, pp. 1089–1103, Sep. 2008.

- [35] E. Larsson and E. Jorswieck, “Competition versus cooperation on the MISO interference channel,” *IEEE J. Select. Areas Commun.*, vol. 26, no. 7, pp. 1059–1069, Sep. 2008.
- [36] E. Björnson, R. Zakhour, D. Gesbert, and B. Ottersten, “Cooperative multicell precoding: Rate region characterization and distributed strategies with instantaneous and statistical CSI,” *IEEE Trans. Signal Processing*, vol. 58, no. 8, pp. 4298–4310, Aug. 2010.
- [37] J. Lindblom, E. Karipidis, and E. G. Larsson, “Selfishness and altruism on the MISO interference channel: the case of partial transmitter CSI,” *IEEE Commun. Lett.*, vol. 13, no. 9, pp. 667–669, Sep. 2009.
- [38] G. Caire and S. Shamai, “On achievable rates in a multi-antenna Gaussian broadcast channel,” in *Proc. IEEE Int. Symp. on Infor. Theory (ISIT)*, Jun. 2001, p. 147.
- [39] —, “On the achievable throughput of a multiantenna Gaussian broadcast channel,” *IEEE Trans. Inform. Theory*, vol. 49, no. 7, pp. 1691–706, Jul. 2003.
- [40] M. Costa, “Writing on dirty paper,” *IEEE Trans. Commun.*, vol. 29, no. 3, pp. 439–441, May 1983.
- [41] T. Han and K. Kobayashi, “A new achievable rate region for the interference channel,” *IEEE Trans. Inform. Theory*, vol. 27, no. 1, pp. 49–60, Jan. 1981.
- [42] R. H. Etkin, D. N. C. Tse, and H. Wang, “Gaussian interference channel capacity to within one bit,” *IEEE Trans. Inform. Theory*, vol. 54, no. 12, pp. 5534–5562, Dec. 2008.
- [43] H. Dahrouj and W. Yu, “Interference mitigation with joint beamforming and common message decoding in multicell systems,” in *Proc. IEEE Int. Symp. on Infor. Theory (ISIT)*, Jun. 2010.

- [44] V. Cadambe and S. A. Jafar, “Interference alignment and degrees of freedom of the K-user interference channel,” *IEEE Trans. Inform. Theory*, vol. 54, no. 8, pp. 3425–3441, Aug. 2008.
- [45] M. Maddah-Ali, A. Motahari, and A. Khandani, “Communication over MIMO X channels: Interference alignment, decomposition, and performance analysis,” *IEEE Trans. Inform. Theory*, vol. 54, no. 8, pp. 3457–3470, Aug. 2008.
- [46] M. Razaviyayn, M. Sanjabi, and Z.-Q. Luo, “Linear transceiver design for interference alignment: Complexity and computation,” *IEEE Trans. Signal Processing*, vol. 58, no. 5, pp. 2896–2910, May 2012.
- [47] P. Viswanath and D. Tse, “Sum capacity of the vector Gaussian broadcast channel and uplink-downlink duality,” *IEEE Trans. Inform. Theory*, vol. 49, no. 8, pp. 1912–1921, Aug. 2003.
- [48] W. Yu and J. Cioffi, “Sum capacity of Gaussian vector broadcast channels,” *IEEE Trans. Inform. Theory*, vol. 50, no. 9, pp. 1875–1892, Sep. 2004.
- [49] W. Yu, “Uplink-downlink duality via minimax duality,” *IEEE Trans. Inform. Theory*, vol. 52, no. 2, pp. 361–374, Feb. 2006.
- [50] S. Boyd and L. Vandenberghe, *Convex Optimization*. Cambridge Univ. Press, 2004.
- [51] O. Somekh, B. M. Zaidel, and S. Shamai (Shitz), “Sum rate characterization of joint multiple cell-site processing,” *IEEE Trans. Inform. Theory*, vol. 53, pp. 4473–4497, Dec. 2007.
- [52] S. Jing, D. N. C. Tse, J. B. Soriaga, J. Hou, J. E. Smee, and R. Padovani, “Multicell downlink capacity with coordinated processing,” *EURASIP J. Wireless Commun. Netw.*, vol. 2008, 2008.

- [53] H. Weingarten, Y. Steinberg, and S. Shamai, “The capacity region of the Gaussian multiple-input multiple-output broadcast channel,” *IEEE Trans. Inform. Theory*, vol. 52, no. 9, pp. 3936 – 3964, Sep. 2006.
- [54] W. Yu, D. P. Varodayan, and J. M. Cioffi, “Trellis and convolutional precoding for transmitter-based interference presubtraction,” *IEEE Trans. Commun.*, vol. 53, no. 7, pp. 1220 – 1230, Jul. 2005.
- [55] S. Kaviani and W. A. Krzymień, “Multicell scheduling in network MIMO,” in *Proc. IEEE Global Telecommun. Conf. (GLOBECOM)*, Dec. 2010.
- [56] C. Ng and H. Huang, “Linear precoding in cooperative MIMO cellular networks with limited coordination clusters,” *IEEE J. Select. Areas Commun.*, vol. 28, no. 9, pp. 1446 – 1454, Dec. 2010.
- [57] M. K. Karakayali, G. J. Foschini, and R. A. Valenzuela, “Network coordination for spectrally efficient communications in cellular systems,” *IEEE Wireless Commun. Mag.*, vol. 13, no. 4, pp. 56 – 61, Aug. 2006.
- [58] M. K. Karakayali, G. J. Foschini, R. A. Valenzuela, and R. D. Yates, “On the maximum common rate achievable in a coordinated network,” in *Proc. IEEE Int. Conf. Communications (ICC)*, Jun. 2006.
- [59] G. J. Foschini, K. Karakayali, and R. A. Valenzuela, “Coordinating multiple antenna cellular networks to achieve enormous spectral efficiency,” *IEE Proc., Commun.*, vol. 153, pp. 548 – 555, Aug. 2006.
- [60] F. Boccardi and H. Huang, “Zero-forcing precoding for the MIMO broadcast channel under per-antenna power constraints,” *IEEE Workshop on Signal Processing Advances in Wireless Commun.*, Jul. 2006.
- [61] H. Huh, A. M. Tulino, and G. Caire, “Network MIMO with linear zero-forcing beamforming: Large system analysis, impact of channel

- estimation and reduced-complexity scheduling,” *IEEE Trans. Inform. Theory*, vol. 58, no. 5, pp. 2911 – 2934, May 2012.
- [62] S. Kaviani and W. A. Krzymień, “Sum rate maximization of MIMO broadcast channels with coordination of base stations,” in *IEEE Wireless Commun. and Networking Conf.*, Mar.-Apr. 2008, pp. 1079 – 1084.
- [63] —, “Optimal multiuser zero-forcing with per-antenna power constraints for network MIMO coordination,” *EURASIP J. Wireless Commun. Networking*, 2011.
- [64] Q. Spencer, A. Swindlehurst, and M. Haardt, “Zero-forcing methods for downlink spatial multiplexing in multiuser MIMO channels,” *IEEE Trans. Signal Processing*, vol. 52, no. 2, pp. 461 – 471, Feb. 2004.
- [65] K. Karakayali, R. Yates, G. Foschini, and R. Valenzuela, “Optimum zero-forcing beamforming with per-antenna power constraints,” in *Proc. IEEE Int. Symp. on Infor. Theory (ISIT)*, Jun. 2007, pp. 101 – 105.
- [66] Y. Hadisusanto, L. Thiele, and V. Jungnickel, “Distributed base station cooperation via block-diagonalization and dual-decomposition,” in *Proc. IEEE Global Telecommun. Conf. (GLOBECOM)*, Dec. 2008.
- [67] A. Liu, Y. Liu, H. Xiang, and W. Luo, “On the rate duality of MIMO interference channel and its application to sum rate maximization,” in *Proc. IEEE Global Telecommun. Conf. (GLOBECOM)*, Dec. 2009.
- [68] A. Wiesel, Y. C. Eldar, and S. Shamai, “Zero-forcing precoding and generalized inverses,” *IEEE Trans. Signal Processing*, vol. 56, no. 9, pp. 4409 – 4418, 2008.
- [69] H. Huh, H. Papadopoulos, and G. Caire, “MIMO broadcast channel optimization under general linear constraints,” in *Proc. IEEE Int. Symp. on Infor. Theory (ISIT)*, Jul. 2009, pp. 2664 – 2668.

- [70] L. Vandenberghe, S. Boyd, and S.-P. Wu, “Determinant maximization with linear matrix inequality constraints,” *SIAM J. Matrix Anal. Appl. (USA)*, vol. 19, no. 2, pp. 499 – 533, 1998.
- [71] A. Liu, Y. Liu, H. Xiang, and W. Luo, “Polite water-filling for weighted sum-rate maximization in MIMO B-MAC networks under multiple linear constraints,” *IEEE Trans. Signal Processing*, vol. 60, no. 2, pp. 834 –847, Feb. 2012.
- [72] D. A. Schmidt, C. Shi, A. A. Berry, M. L. Honig, and W. Utschick, “Minimum mean squared error interference alignment,” in *Proc. Asilomar Conf. on Signals, Systems and computers*, Nov. 2009.
- [73] S. Kaviani, O. Simeone, W. A. Krzymień, and S. S. (Shitz), “Linear MMSE precoding and equalization for network MIMO with partial cooperation,” in *Proc. IEEE Global Telecommun. Conf. (GLOBECOM)*, Dec. 2011.
- [74] S. Kaviani, O. Simeone, W. A. Krzymień, and S. Shamai, “Linear precoding and equalization for network MIMO with partial cooperation,” *IEEE Trans. Veh. Technol.*, vol. 61, no. 5, pp. 2083–2096, Jun. 2012.
- [75] A. Liu, Y. Liu, V. K. N. Lau, H. Xiang, and W. Luo, “Polite water-filling for weighted sum-rate maximization in MIMO B-MAC networks under multiple linear constraints,” in *Proc. IEEE Int. Symp. on Infor. Theory (ISIT)*, Aug. 2011.
- [76] V. Jungnickel, T. Wirth, M. Schellmann, T. Haustein, and W. Zirwas, “Synchronization of cooperative base stations,” in *International Symposium on Wireless Communication Systems (ISWCS’08)*, Oct. 2008.
- [77] B. W. Zarikoff and J. K. Cavers, “Coordinated multi-cell systems: Carrier frequency offset estimation and correction,” *IEEE J. Select. Areas Commun.*, vol. 28, no. 9, pp. 1490 –1501, Dec. 2010.

- [78] G. Caire, S. A. Ramprasad, and H. C. Papadopoulos, “Rethinking network MIMO: Cost of CSIT, performance analysis, and architecture comparisons,” in *Proc. Information Theory and Application Workshop (ITA 2010)*, Jan.-Feb 2010.
- [79] J. Hoydis, M. Kobayashi, and M. Debbah, “Optimal channel training in uplink network MIMO systems,” *IEEE Trans. Signal Processing*, vol. 59, no. 6, pp. 2824 –2833, Jun. 2011.
- [80] S. Kaviani and W. A. Krzymień, “User selection for multiple-antenna broadcast channel with zero-forcing beamforming,” in *Proc. IEEE Global Telecommun. Conf. (GLOBECOM)*, Nov.-Dec. 2008.
- [81] A. Papadogiannis, D. Gesbert, and E. Hardouin, “A dynamic clustering approach in wireless networks with multi-cell cooperative processing,” in *Proc. IEEE Int. Conf. Communications (ICC)*, May 2008.
- [82] G. L. Stüber, *Principles of Mobile Communications (2nd edition)*. Boston, M.A., USA: Kluwer Academic Publishers, 2002.
- [83] D. P. Palomar and Y. Jiang, “MIMO transceiver design via majorization theory,” *Found. Trends Commun. Inf. Theory (USA)*, vol. 3, no. 4 - 5, pp. 331 – 551, 2006.
- [84] S. Vishwanath, N. Jindal, and A. Goldsmith, “Duality, achievable rates, and sum-rate capacity of Gaussian MIMO broadcast channels,” *IEEE Trans. Inform. Theory*, vol. 49, no. 10, pp. 2658 – 2668, Oct. 2003.
- [85] T. Lan and W. Yu, “Input optimization for multi-antenna broadcast channels with per-antenna power constraints,” *Proc. IEEE Global Telecommun. Conf. (GLOBECOM)*, vol. 1, Nov-Dec 2004.
- [86] P. Viswanath and D. N. C. Tse, “Sum capacity of the vector gaussian broadcast channel and uplink-downlink duality,” *IEEE Trans. Inform. Theory*, vol. 49, no. 8, pp. 1912 – 1921, Aug. 2003.

- [87] M. Schubert and H. Boche, "Solution of the multiuser downlink beamforming problem with individual SINR constraints," *IEEE Trans. Veh. Technol.*, vol. 53, no. 1, pp. 18 – 28, Jan. 2004.
- [88] B. Song, R. L. Cruz, and B. D. Rao, "Network duality and its application to multi-user MIMO wireless networks with SINR constraints," in *Proc. IEEE Int. Conf. Communications (ICC)*, May 2005.
- [89] L. Zhang, R. Zhang, Y.-C. Liang, Y. Xin, and H. V. Poor, "On Gaussian MIMO BC-MAC duality with multiple transmit covariance constraints," <http://arxiv.org/abs/0809.4101v1>.
- [90] T. J. Stieltjes, "Sur les racines de l'équation  $x_n = 0$ ," *Acta Math*, no. 9, pp. 385–400, 1886.
- [91] S. Shi, M. Schubert, and H. Boche, "Downlink MMSE transceiver optimization for multiuser MIMO systems: Duality and sum-MSE minimization," *IEEE Trans. Signal Processing*, vol. 55, no. 11, pp. 5436 –5446, Nov. 2007.
- [92] H. Zhang and H. Dai, "Cochannel interference mitigation and cooperative processing in downlink multicell multiuser MIMO networks," *EURASIP J. Wireless Commun. Netw.*, no. 2, pp. 222 – 235, 2004.
- [93] W. Choi and J. Andrews, "The capacity gain from intercell scheduling in multi-antenna systems," *IEEE Trans. Wireless Commun.*, vol. 7, no. 2, Feb. 2008.
- [94] L.-U. Choi and R. D. Murch, "A transmit preprocessing technique for multiuser MIMO systems using a decomposition approach," *IEEE Trans. Inform. Theory*, vol. 3, no. 1, pp. 20 – 24, Jan. 2004.
- [95] R. Zhang, "Cooperative multi-cell block diagonalization with per-base-station power constraints," *IEEE J. Select. Areas Commun.*, vol. 28, no. 9, pp. 1435 –1445, Dec. 2010.

- [96] R. A. Horn and C. R. Johnson, *Matrix Analysis*. Cambridge, U.K.: Cambridge Univ. Press, 1985.
- [97] S. Kaviani and W. A. Krzymień, “On the optimality of multiuser zero-forcing precoding in MIMO broadcast channels,” in *Proc. IEEE Veh. Tech. Conf. (VTC-Spring)*, Apr. 2009.
- [98] H. Viswanathan, S. Venkatesan, and H. Huang, “Downlink capacity evaluation of cellular networks with known-interference cancellation,” *IEEE J. Select. Areas Commun.*, vol. 21, no. 5, pp. 802 – 811, Jun. 2003.
- [99] S. Sigdel and W. A. Krzymień, “Simplified channel-aware greedy scheduling and antenna selection algorithms for multiuser MIMO systems employing orthogonal space division multiplexing,” Chapter 2 in *Advances in Mobile and Wireless Communications - Views of the 16th IST Mobile and Wireless Communication Summit*. Heidelberg, Germany: Springer 2008, pp. 23 - 51.
- [100] —, “Simplified fair scheduling and antenna selection algorithms for multiuser MIMO orthogonal space-division multiplexing downlink,” *IEEE Trans. Veh. Technol.*, vol. 58, no. 3, pp. 1329 –1344, Mar. 2009.
- [101] T. Yoo and A. Goldsmith, “On the optimality of multiantenna broadcast scheduling using zero-forcing beamforming,” *IEEE J. Select. Areas Commun.*, vol. 24, no. 3, pp. 528 – 541, Mar. 2006.
- [102] R. C. Elliott and W. A. Krzymień, “Downlink scheduling via genetic algorithms for multiuser single-carrier and multicarrier MIMO systems with dirty paper coding,” *IEEE Trans. Veh. Technol.*, vol. 58, no. 7, pp. 3247 –3262, Sep. 2009.
- [103] G. Dimic and N. D. Sidiropoulos, “On downlink beamforming with greedy user selection: performance analysis and a simple new algorithm,” *IEEE Trans. Signal Processing*, vol. 53, no. 10, pp. 3857 – 3868, Oct. 2005.

- [104] Z. Shen, R. Chen, J. G. Andrews, R. W. Heath Jr., and B. L. Evans, “Low complexity user selection algorithms for multiuser MIMO systems with block diagonalization,” *IEEE Trans. Signal Processing*, vol. 54, no. 9, pp. 3658 – 3663, Sep. 2006.
- [105] D. Tse and S. V. Hanly, “Multiaccess fading channels. I. Polymatroid structure, optimal resource allocation and throughput capacities,” *IEEE Trans. Inform. Theory*, vol. 44, no. 7, pp. 2796 – 2815, Nov. 1998.
- [106] C. B. Peel, B. M. Hochwald, and A. L. Swindlehurst, “A vector-perturbation technique for near-capacity multiantenna multiuser communication-part I: channel inversion and regularization,” *IEEE Trans. Commun.*, vol. 53, no. 1, pp. 195 – 202, Jan. 2005.
- [107] R. R. Müller, D. Guo, and A. L. Moustakas, “Vector precoding for wireless MIMO systems and its replica analysis,” *IEEE J. Select. Areas Commun.*, vol. 26, no. 3, pp. 530 – 540, Apr. 2008.
- [108] S. S. Christensen, R. Agarwal, E. Carvalho, and J. Cioffi, “Weighted sum-rate maximization using weighted MMSE for MIMO-BC beamforming design,” *IEEE Trans. Wireless Commun.*, vol. 7, no. 12, pp. 4792 – 4799, Dec. 2008.
- [109] Q. Shi, M. Razaviyayn, Z.-Q. Luo, and C. He, “An iteratively weighted MMSE approach to distributed sum-utility maximization for a MIMO interfering broadcast channel,” *IEEE Trans. Signal Processing*, vol. 59, no. 9, pp. 4331 – 4340, Sep. 2011.
- [110] Z.-Q. Luo and S. Zhang, “Dynamic spectrum management: Complexity and duality,” *IEEE J. Select. Areas Commun.*, vol. 2, no. 1, pp. 57 – 73, Feb. 2008.
- [111] K. Gomadam, V. Cadambe, and S. A. Jafar, “Approaching the capacity of wireless networks through distributed interference alignment,” Nov. 2008.

- [112] S. W. Peters and R. W. Heath, “Cooperative algorithms for MIMO interference channels,” *IEEE Trans. Veh. Technol.*, vol. 60, no. 1, pp. 206 –218, Jan. 2011.
- [113] H. Yu and V. K. N. Lau, “Rank-constrained schur-convex optimization with multiple trace/log-det constraints,” *IEEE Trans. Signal Processing*, vol. 59, no. 1, pp. 304 – 314, Jan. 2011.
- [114] D. P. Palomar, J. M. Cioffi, and M. A. Lagunas, “Joint Tx-Rx beamforming design for multicarrier MIMO channels: a unified framework for convex optimization,” *IEEE Trans. Signal Processing*, vol. 51, no. 9, pp. 2381 – 2401, Sep. 2003.
- [115] D. P. Bertsekas, A. Nedić, and A. E. Ozdaglar, *Convex analysis and optimization*. Belmont, M.A., USA: Athena Scientific, 2003.
- [116] A. Hjörungnes and D. Gesbert, “Complex-valued matrix differentiation: techniques and key results,” *IEEE Trans. Inform. Theory*, vol. 55, no. 6, pp. 2740 – 2746, Jun. 2007.
- [117] H. Huh, S.-H. Moon, Y.-T. Kim, I. Lee, and G. Caire, “Multi-cell MIMO downlink with cell cooperation and fair scheduling: A large-system limit analysis,” *IEEE Trans. Inform. Theory*, vol. 57, no. 12, pp. 7771 –7786, Dec. 2011.
- [118] C. Shi, R. Berry, and M. Honig, “Adaptive beamforming in interference networks via bi-directional training,” in *Proc. 44th Annual Conference on Information Sciences and Systems (CISS)*, Mar. 2010.
- [119] S. Ye and R. S. Blum, “Some properties of the capacity of MIMO systems with co-channel interference,” in *Proc. IEEE Int. Conf. Acoustics, Speech, and Signal Processing (ICASSP)*, vol. III, Mar. 2005, pp. III–1153 – III–1156.
- [120] W. L. Stutzman and G. A. Thiele, *Antenna theory and design (2nd edition)*. John Wiley & Sons, 1998.

- [121] H. Huang, O. Alrabadi, J. Daly, D. Samardzija, C. Tran, R. Valenzuela, and S. Walker, "Increasing throughput in cellular networks with higher-order sectorization," in *Proc. Asilomar Conf. on Signals, Systems and computers*, Nov. 2010.
- [122] H. Sampath, P. Stoica, and A. Paulraj, "Generalized linear precoder and decoder design for MIMO channels using the weighted MMSE criterion," *IEEE Trans. Commun.*, vol. 49, no. 12, pp. 2198 –2206, Dec. 2001.
- [123] A. Scaglione, P. Stoica, S. Barbarossa, G. Giannakis, and H. Sampath, "Optimal designs for space-time linear precoders and decoders," *IEEE Trans. Signal Processing*, vol. 50, no. 5, pp. 1051 –1064, May 2002.
- [124] S. A. Vorobyov, A. B. Gershman, and Z.-Q. Luo, "Robust adaptive beamforming using worst-case performance optimization: a solution to the signal mismatch problem," *IEEE Trans. Signal Processing*, vol. 51, no. 2, pp. 313 – 324, Feb. 2003.
- [125] Y. C. Eldar and N. Merhav, "A competitive minimax approach to robust estimation of random parameters," *IEEE Trans. Signal Processing*, vol. 52, no. 7, pp. 1931 – 1946, Jul. 2004.
- [126] E. Chiu, V. K. N. Lau, H. Huang, T. Wu, and S. Liu, "Robust transceiver design for K-pairs quasi-static MIMO interference channels via semi-definite relaxation," *IEEE Trans. Wireless Commun.*, vol. 9, no. 12, pp. 3762 – 3769, Dec. 2010.
- [127] N. Vucic, H. Boche, and S. Shi, "Robust transceiver optimization in downlink multiuser MIMO systems," *IEEE Trans. Signal Processing*, vol. 57, no. 9, pp. 3576 –3587, Sep. 2009.
- [128] J. Wang and D. P. Palomar, "Worst-case robust MIMO transmission with imperfect channel knowledge," *IEEE Trans. Signal Processing*, vol. 57, no. 8, pp. 3086 –3100, Aug. 2009.

- [129] —, “Robust MMSE precoding in MIMO channels with pre-fixed receivers,” *IEEE Trans. Signal Processing*, vol. 58, no. 11, pp. 5802 – 5818, Nov. 2010.
- [130] J. Wang and M. Bengtsson, “Joint optimization of the worst-case robust MMSE MIMO transceiver,” *IEEE Signal Processing Lett.*, vol. 18, no. 5, pp. 295 –298, May 2011.
- [131] Y. Guo and B. C. Levy, “Worst-case MSE precoder design for imperfectly known MIMO communications channels,” *IEEE Trans. Signal Processing*, vol. 53, no. 8, pp. 2918 – 2930, Aug. 2005.
- [132] M. D. Nisar and W. Utschick, “Minimax robust a priori information aware channel equalization,” *IEEE Trans. Signal Processing*, vol. 59, no. 4, pp. 1734 –1745, Apr. 2011.
- [133] Y. Guo and B. C. Levy, “Robust MSE equalizer design for MIMO communication systems in the presence of model uncertainties,” *IEEE Trans. Signal Processing*, vol. 54, no. 5, pp. 1840 – 1852, May 2006.
- [134] M. Joham, P. M. Castro, L. Castedo, and W. Utschick, “Robust precoding with bayesian error modeling for limited feedback MU-MISO systems,” *IEEE Trans. Signal Processing*, vol. 58, no. 9, pp. 4954 –4960, Sep. 2010.
- [135] A. Gründndinger, M. Joham, and W. Utschick, “Stochastic transceiver design in point-to-point MIMO channels with imperfect CSI,” in *Smart Antennas (WSA), 2011 International ITG Workshop on*, Feb. 2011.
- [136] A. Gründinger, M. Joham, and W. Utschick, “Stochastic transceiver design in multi-antenna channels with statistical channel state information,” in *Proc. IEEE Int. Conf. Acoustics, Speech, and Signal Processing (ICASSP)*, May 2011.

- [137] X. Zhang, D. P. Palomar, and B. Ottersten, “Statistically robust design of linear MIMO transceivers,” *IEEE Trans. Signal Processing*, vol. 56, no. 8, pp. 3678–3689, Aug. 2008.
- [138] T. E. Bogale, B. K. Chalise, and L. Vandendorpe, “Robust transceiver optimization for downlink multiuser MIMO systems,” *IEEE Trans. Signal Processing*, vol. 59, no. 1, pp. 446–453, Jan. 2011.
- [139] A. Tajer, N. Prasad, and X. Wang, “Robust linear precoder design for multi-cell downlink transmission,” *IEEE Trans. Signal Processing*, vol. 59, no. 1, pp. 235–251, Jan. 2011.
- [140] S. Kaviani and W. A. Krzymień, “Worst-case robust design of linear transceivers in MIMO interference channels,” submitted to *IEEE Trans. Veh. Tech.*, 2012.
- [141] T. Başar and G. J. Olsder, *Dynamic noncooperative game theory*, 2nd ed. SIAM, 1995.
- [142] R. J. Stern and H. Wolkowicz, “Indefinite trust region subproblems and nonsymmetric eigenvalue perturbations,” *SIAM J. Optim.*, vol. 5, pp. 286–313, May 1995.
- [143] P. D. Tao and L. T. H. An, “Difference of convex functions optimization algorithms (DCA) for globally minimizing nonconvex quadratic forms on euclidean balls and spheres,” *Operations Research Letters*, vol. 19, no. 5, pp. 207–216, 1996.
- [144] M. Spiegel, S. Lipschutz, and J. Liu, *Mathematical Handbook of Formulas and Tables*, 3rd ed. McGraw-Hill, Aug. 2008.
- [145] D. P. Palomar and M. Chiang, “A tutorial on decomposition methods for network utility maximization,” *IEEE J. Select. Areas Commun.*, vol. 24, no. 8, pp. 1439–1451, Aug. 2006.

- [146] F. Rendl and H. Wolkowicz, “A semidefinite framework for trust region subproblems with applications to large scale minimization,” *Mathematical Programming*, vol. 77, no. 1, pp. 273–299, 1997.
- [147] S. Srinivasa and M. Haenggi, “Distance distributions in finite uniformly random networks: Theory and applications,” *IEEE Trans. Veh. Technol.*, vol. 59, no. 2, pp. 940–949, Feb. 2010.
- [148] H. S. Dhillon, R. K. Ganti, F. Baccelli, and J. G. Andrews, “Modeling and analysis of K-tier downlink heterogeneous cellular networks,” *IEEE J. Select. Areas Commun.*, vol. 30, no. 3, pp. 550–560, Apr. 2012.
- [149] J. G. Andrews, R. K. Ganti, M. Haenggi, N. Jindal, and S. Weber, “A primer on spatial modeling and analysis in wireless networks,” *IEEE Commun. Mag.*, vol. 48, no. 11, pp. 156–163, Nov. 2010.
- [150] S. Mukherjee, “Distribution of downlink SINR in heterogeneous cellular networks,” *IEEE J. Select. Areas Commun.*, vol. 30, no. 3, pp. 575–585, Apr. 2012.
- [151] N. Z. Shor, *Minimization methods for non-differentiable functions*. Springer-Verlag, 1985.
- [152] D. P. Bertsekas, *Nonlinear Programming*. 2nd ed. Belmont, MA, USA: Athena Scientific, 2003.
- [153] D. P. Bertsekas and J. N. Tsitsiklis, *Parallel and Distributed Computation: Numerical Methods*. Englewood Cliffs, NJ, USA: Prentice Hall, 1989.
- [154] L. S. Lasdon, *Optimization Theory for Large Systems*. New York: Macmillan, 1970.